On the Origin of Secosterols upon Oxidation of Cholesterol

By

Nadia Zopyrus

Thesis submitted to the Department of Chemistry and Biomolecular Sciences

in conformity with the requirements for the

Degree of Master of Science

University of Ottawa

Ottawa, Ontario, Canada

Abstract

Cholesterol is one of the most abundant lipids in the body, and like all unsaturated lipids, it can be oxidized by a variety of reactive oxygen species (ROS). Lipid peroxidation is one of the main pathways by which ROS induce oxidative damage, and has been linked to neurodegenerative and cardiovascular diseases. In 2003, Wentworth *et al.* detected both 3β-hydroxy-5-oxo-5,6-secocholestan-6-al (secosterol-A) and its intramolecular aldolization product 3β-hydroxy-5β-hydroxy-B-norcholestane-6β-carboxaldehyde (secosterol-B) in human atherosclerotic plaques – compounds which, at the time, were only known to be formed by cholesterol ozonolysis.

However, our group has shown that cholesterol 5α-hydroperoxide, which is the product of the reaction of cholesterol with singlet oxygen, can undergo acid-catalyzed Hock fragmentation to generate secosterol-A and -B as well. Nevertheless, cholesterol 5α-hydroperoxide readily rearranges to a more thermodynamically stable cholesterol 7-hydroperoxide. Herein we show that cholesterol 7-hydroperoxide, the main product of cholesterol autoxidation, can also undergo acid-catalyzed Hock fragmentation that gives rise to electrophilic species with similar chromatographic characteristics to those that were allegedly identified as secosterol-A and -B.

We also proposed to prepare authentic products of the Hock fragmentation of cholesterol 7-hydroperoxide by subjecting $\Delta^{6'7}$-cholesterol to ozonolysis. Herein, we explore the limitations and complications of $\Delta^{6'7}$-cholesterol ozonolysis as well as cholesterol 7-OOH Hock fragmentation which both resulted in unexpected (unprecedented) products.

Acknowledgements

First and foremost, I would like to express my heartfelt gratitude to Dr. Derek Pratt for providing me with the opportunity to do this project. The success and final outcome of this project required a lot of guidance and assistance and I was extremely fortunate to have his support. Your patience, generous attitude, enthusiasm for teaching and admirable knowledge for chemistry is exceptional. Thank you so much for all your help and support, Dr. Pratt.

Others who helped me along the way include my greatly supportive colleagues: J.P. Chauvin, Evan Haidasz, Ron Shah, Omkar Zilka, Bo Li and Emily Schaefer. Special thanks to Zosia Zielinski for her help and support and taking the painful task of editing my works throughout my masters. Thanks for understanding my English and making sure that others will understand it too.

I would also like to thank my committee members, Dr. Christopher Body and Dr. Adam Shuhendler, for their time and support; NMR facility manager, Dr. Glenn Facey; and MS facility manager, Dr. Sharon Curtis for their much appreciated assistance and the University of Ottawa's Chemistry Department.

I cannot possibly thank my dearest Ibrahim enough for his endless support and kindness. You comforted me when doubts filled my mind and spoiled me with your care whenever I failed. My love, without you this would not have been possible.

Last but not least, I would like to also thank my family. Many thanks to my lovely parents; Guiti and Aarshum for their constant encouragements; my brother, Mehrdod, for the countless laughs; my dear sweet grandfather, Rajab-ali, for his support through thick and thin; and my friends and extended family for their constant love and warmth.

Nadia Zopyrus

Statement of Originality

I hereby certify that all of the work described within this thesis is the original work of the author. Any published (or unpublished) ideas from the work of others are fully acknowledged in accordance with the referencing practices.

Nadia Zopyrus

February, 2017

Table of Content

List of Figures

List of Tables

List of Schemes

-1-

Introduction

1.1 Autoxidation

Autoxidation is the spontaneous oxidation of a compound in the presence of oxygen (air) at normal temperature and pressure. It is an autocatalytic free radical chain reaction which generates peroxides and/or hydroperoxides as the primary products. Extensive research by Bolland, Lundberg and colleagues at the British Rubber Producers Research Association established the role of free radicals in the autoxidation process.[1, 2] Their work was followed by Ingold's remarkable research where the mechanism of hydrocarbon autoxidation was further clarified.[3, 4] The accepted mechanism is shown in Scheme 1.1.

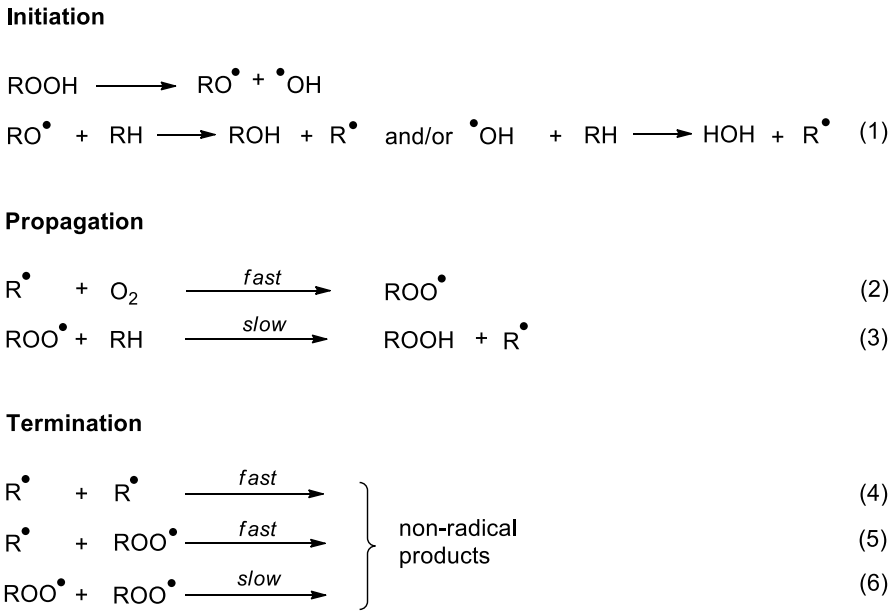

Scheme 1.1. Radical chain mechanism of hydrocarbon autoxidation.

Hydrocarbon autoxidation, just like all other radical chain reactions, consists of three steps: initiation, propagation and termination. The first step, initiation, begins with autocatalytic decomposition of ROOH to RO• and •OH, either of which can abstract a H-atom from a substrate (RH) to generate a substrate-derived carbon-centred radical (R•) (Scheme 1.1-reaction 1). However, in practice, any reaction which generates an alkyl radical (e.g. decomposition of an azo-compound) can be an initiation step. At the first propagation step, R• reacts with oxygen near the diffusion-controlled rate to yield peroxyl radicals (ROO•) (reaction 2).[5] For the next propagation step, ROO• abstracts a H-atom from the substrate to form another carbon-centered radical, R• (reaction 3). The chain propagation continues by alternative repetition of these two steps until a spontaneous or induced (aided) termination step breaks the chain reaction. Termination occurs when two radicals react to form non-radical products (reactions 4-6). The so-called Russell termination reaction where two peroxyl radicals react to form non-radical products (reaction 6) is the primary termination reaction under most conditions. This is mainly due to the rapid reaction of R• and O_2 that keeps the R• concentration very low for the other two termination reactions to be competitive.

Termination can be aided by the addition of so-called 'antioxidants'. Chain breaking antioxidants such as substituted phenols can effectively terminate propagation by capturing chain-carrying radicals. They first transfer their phenolic H-atom to the ROO• to generate ROOH and the corresponding antioxidant-derived radical. Under most conditions, the antioxidant-derived radicals do not carry on the chain reaction as they do not react with oxygen or abstract H-atom from RH or ROOH. They however can couple with a second peroxyl radical to form non-

radical products (Scheme 1.2). In general, a good antioxidant reacts much faster with peroxyl radicals than the substrate because the bond dissociation enthalpy (BDE) of an antioxidant-H (ArO-H) is significantly lower than the BDE of ROO-H. Nature's best antioxidant is α-tocopherol whose BDE is ca. 10 kcal/mol weaker than that in a hydroperoxide and whose inhibition rate constant, k_{inh}, of 10^6 $M^{-1}s^{-1}$ is greater than the propagation rate constant, k_p, of polyunsaturated lipids which is between 10 to 100 $M^{-1}s^{-1}$. [6, 7, 8]

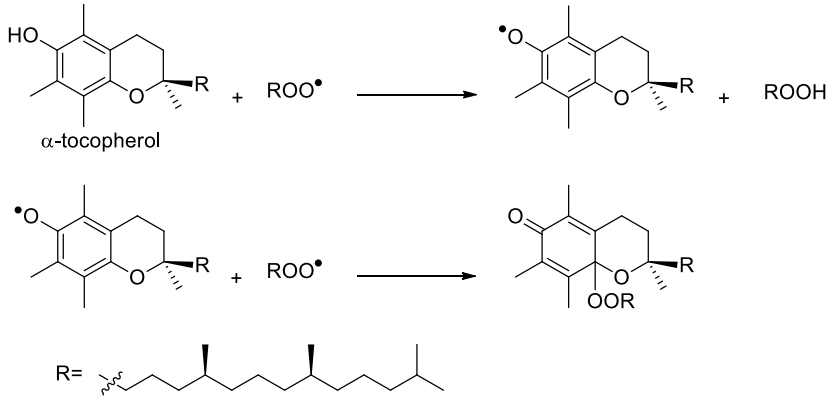

Scheme 1.2. Inhibition of hydrocarbon autoxidation by α-tocopherol, an effective phenolic radical-trapping antioxidant.

1.2 Lipid Peroxidation

Lipid peroxidation, the term that is generally used to describe the autoxidation of unsaturated fatty acids esters and sterols has been implicated in the pathophysiology of many progressive diseases including atherosclerosis,[9, 10] asthma,[11,12] and neurodegenerative disorders such as Alzheimer's disease and Parkinson disease.[13, 14]

Studies of the autoxidation of oleic acid, a monounsaturated lipid, dates back to 1943 when Farmer and Sutton studied methyl oleate autoxidation.[15] They suggested that oleate autoxidation yields a mixture of C8 and C11 oleate hydroperoxides. Farmer *et al*. later proposed a more complete free radical chain mechanism by including both C9 and C10 oleate hydroperoxides to the product mixture of methyl oleate autoxidation.[16] They proposed that oxygen can attack equally at positions 8, 9, 10 and 11, therefore, the olefin can also be equally located at $\Delta^{8,9}$, $\Delta^{9,10}$ and $\Delta^{10,11}$ (Scheme 1.3).[17]

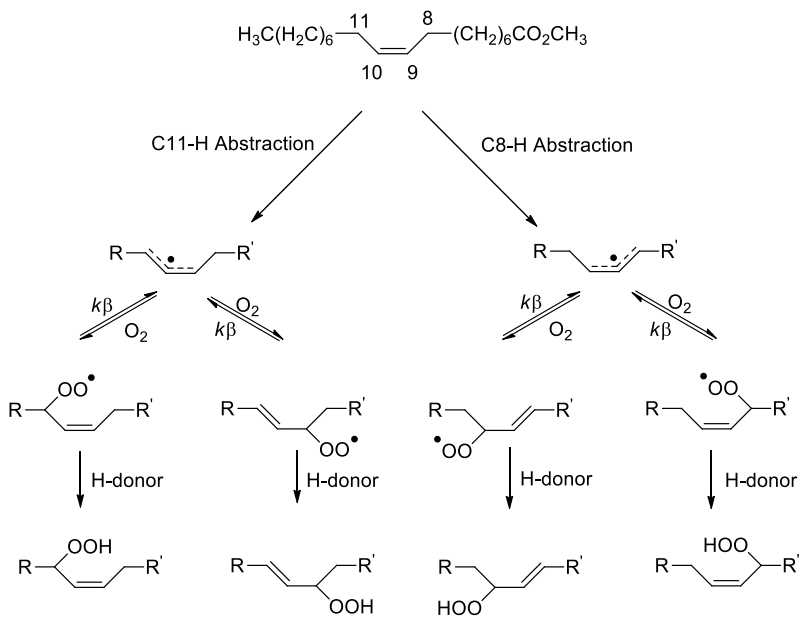

Scheme 1.3. Proposed methyl oleate symmetrical autoxidation mechanism (1984).

Two decades later, Porter *et al.* showed that the mechanism is not as symmetrical as it seemed.[18, 19] For example, upon abstracting hydrogen from C11, 45% of products are derived from O_2 addition to position 11 to form 11-*cis* oleate peroxyl while 55% of products are derived from O_2 addition to position 9 to form 9-*trans* oleate peroxyl. They proposed that this is mainly because O_2 prefers to attack the allyl terminus with higher spin density (Scheme 1.4).

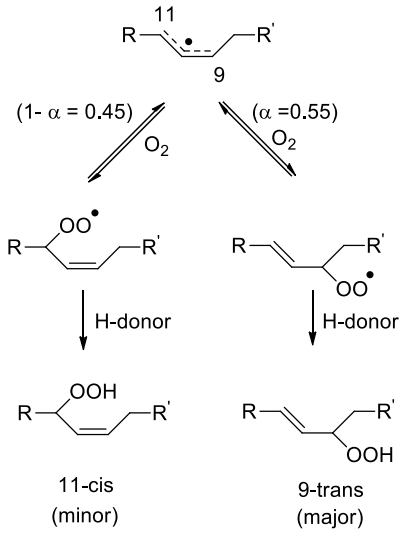

Scheme 1.4. Partition of oxygen addition to the oleate radical.

Furthermore, Porter *et al.* proposed that 11-*trans* and 8-*trans* oleate hydroperoxide can also be generated via methyl oleate autoxidation (Scheme 1.5).[18] The intermediate peroxyl radicals undergo β-fragmentation after bond rotation, resulting in 11-*trans* and 8-*trans* hydroperoxide configurations after re-addition of oxygen and H-atom abstraction.

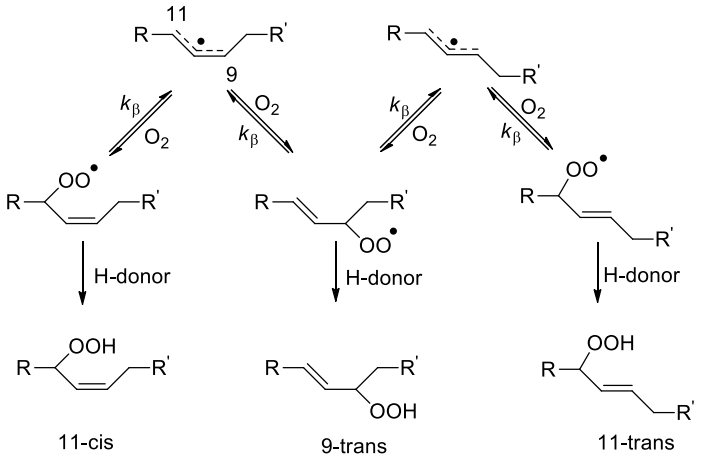

Scheme 1.5. Proposed oleate autoxidation including the rearrangement. Synthesis of 8-*trans* is not shown for simplicity.

Polyunsaturated lipids such as linoleate are substantially more prone to oxidation than monounsaturated lipids such as oleate. The rate of lipid peroxidation is affected by the bond dissociation enthalpy (BDE) of the C-H, which is governed largely by the stability of the produced alkyl radicals. [19, 20] The allylic C-H BDE of monounsaturated lipids are higher than the C-H BDE of bis-allylic centres on polyunsaturated lipids due to greater spin delocalization via the greater conjugation in the pentadienyl radical as compared to an allylic radical. Therefore, polyunsaturated fatty acids (PUFAs) such as linoleic acid, (Scheme 1.6-**1**), or arachidonic acid, **2**, are particularly more prone to autoxidation compared to monounsaturated lipids such as oleic acid, **3**, and cholesterol, **4.**

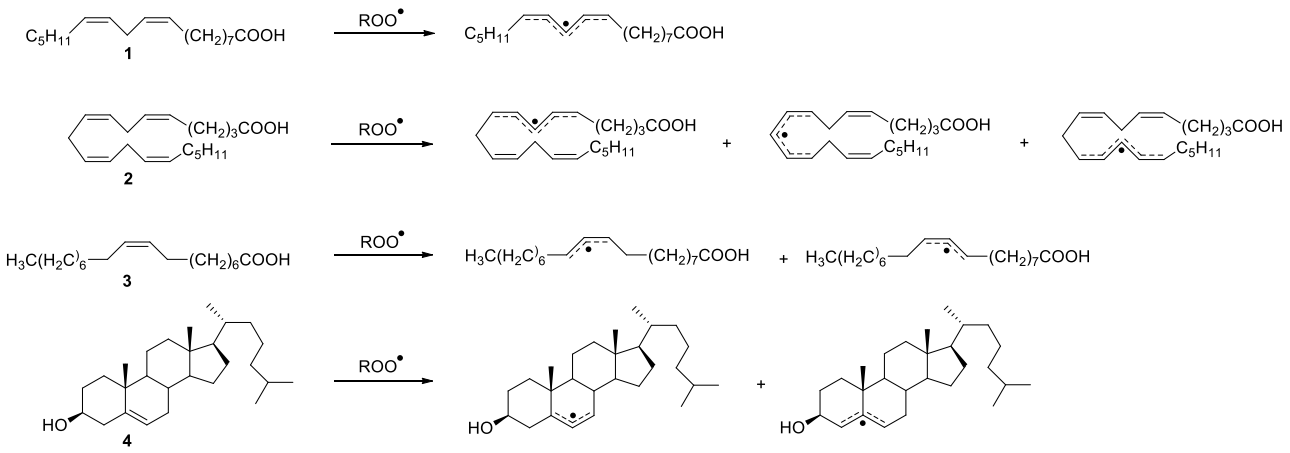

Scheme 1.6. Carbon-centered radicals resulting from H-atom abstraction from the most reactive positions of linoleic acid (**1**), arachidonic acid (**2**), oleic acid (**3**) and cholesterol (**4**).

The mechanism of linoleic acid autoxidation is illustrated in Scheme 1.7. The first step is H-atom abstraction from the bis-allylic position. The unpaired electron spin density at C9, C11 and C13 enables O_2 to add to each of these positions. The peroxides formed from the addition of oxygen to the alkyl radical can be trapped by an antioxidant, a good H-atom donor or another lipid molecule, to produce the corresponding hydroperoxides in *cis-cis* and *cis-trans* conformations. However, upon β-fragmentation to regain the peroxyl radical, bond rotation is possible, giving the *trans-trans* configuration after addition of oxygen and H-atom abstraction.

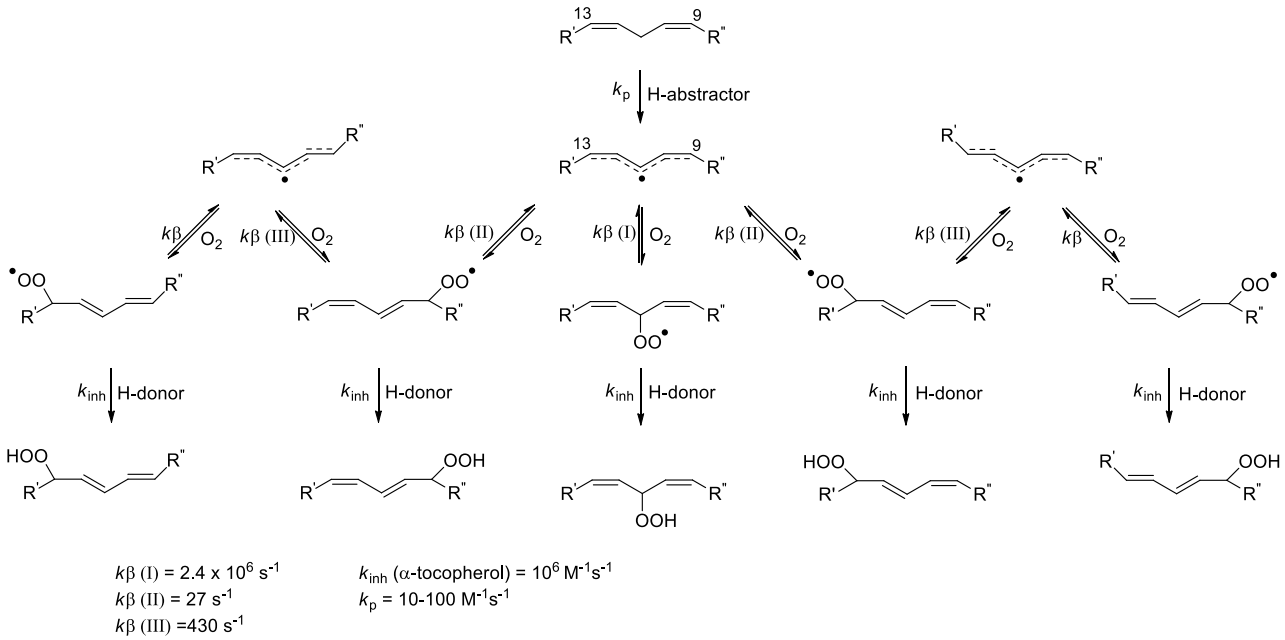

Scheme 1.7. Proposed mechanism of the autoxidation of linoleic acid.

The product distribution is dictated by the rate constants that control the competing processes. One is the magnitude of the β-fragmentation rate constant (k_β) to form pentadienyl radical and oxygen. The other is the rate of inhibition (k_{inh}) to trap peroxyl radicals as hydroperoxides, which is dictated by the concentration and reactivity of H-atom donors in the medium. A good H-atom donor can trap the peroxyl radicals upon their formation hence in the presence of a good H-atom donor *cis-trans* configurations are the major products. In the absence of a good H-atom donor, *trans-trans* configurations are formed via β-fragmentation and consecutive rearrangement of the intermediate peroxyl radicals.

Lipid oxidation can also occur by singlet oxygen via a non-radical mechanism. Singlet oxygen ($^1O_2$) is the electronically excited state of triplet oxygen in which all of its electrons are paired. Singlet oxygen is 22 kcal/mol higher in energy than triplet oxygen[21] and can be generated in *vivo* via pathways such as myeloperoxidase using hydroperoxides (H_2O_2) (Scheme 1.8).[22, 23]

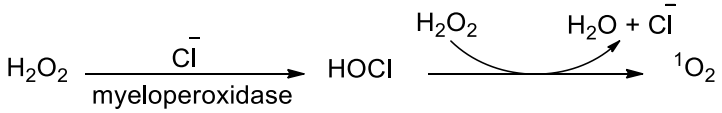

Scheme 1.8. Singlet oxygen formation from hydrogen peroxide by myeloperoxidase.

As an oxidant, $^1O_2$ displays significant reactivity toward electron-rich organic molecules such as lipids, proteins and nucleic acids. Like many other reactive species, $^1O_2$ is toxic at high concentrations, but at a very low concentration it plays an essential role in cell signaling pathways associated with apoptosis.[24, 25] $^1O_2$ addition to an unsaturated lipid proceeds via a so-called ene-reaction. Singlet oxygen addition and double bond migration result in the corresponding hydroperoxides, illustrated in Scheme 1.9. [26, 27]

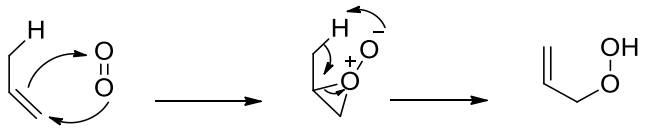

Scheme 1.9. Single oxygen oxidation of an olefin (the ene-reaction).

Lipid peroxidation is not the only mechanism to produce lipid hydroperoxides, they can also be formed by enzymatic reactions that are key to immunity, pain and inflammation, as well as cell growth and differentiation. For instance, arachidonic acid is oxidized by the enzyme 5-lipoxygenase to form the corresponding hydroperoxides (5-HPETE) (Scheme 1.10).[28] The hydroperoxides produced are key intermediates in the biosynthesis of compounds such as leukotrienes and lipoxines which are involved in immune responses.[29] Another example of an enzymatic reaction is arachidonic acid oxidation by the cyclooxygenase enzyme to generate prostaglandin endoperoxides PGG_2 and PGH_2 (Scheme 1.10). These are key intermediates toward prostaglandins and thromboxanes which mediate pain and inflammation.[30]

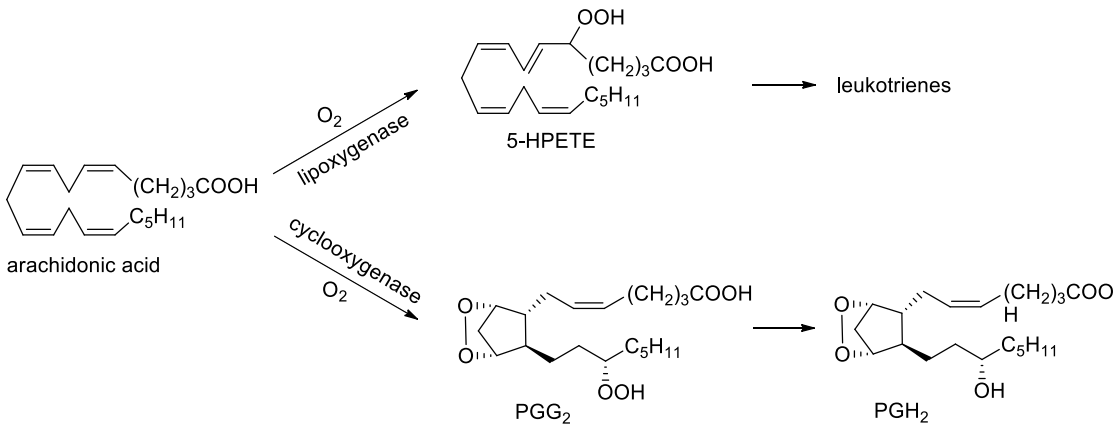

Scheme 1.10. Examples of enzymatic oxidation of arachidonic acid.

Lipid hydroperoxides can also be extremely harmful. For instance, oxidized acyl chains located in the cell membrane move out of the lipid phase and into the aqueous phase. It is believed that this lipid displacement upon oxidation can reduce bilayer thickness, which can affect membrane permeability, can cause ion leakage and can alter the membrane fluidity. [31,32]

Free oxidized lipids can interact with proteins and interfere with protein folding and function.[33] Furthermore, hydroperoxides, the primary products of lipid peroxidation, can give rise to reactive electrophilic species (i.e. aldehydes) that can covalently modify nucleophilic protein side chains and DNA bases. Humans, like any other aerobic organism, have evolved to live with the consequences of lipid peroxidation and to minimize them by the use of antioxidants. However, the urge to reveal the nature of biological and chemical processes involved in lipid peroxidation has never subsided since their strong link with chronic diseases was discovered.

1.3 Cholesterol Oxidation

Cholesterol is one of the most abundant lipids in our body and has a vital role as a regulator for flexibility, permeability and selectivity of the plasma membrane. In addition to its vital role within the cell, cholesterol is also the precursor for steroid hormones, bile acid and vitamin D.[34, 35]

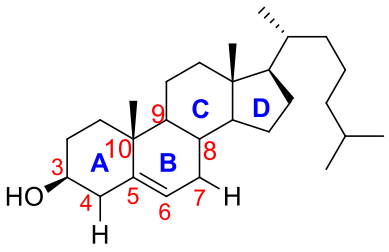

cholesterol

Cholesterol is autoxidized by O_2 slowly as compared to polyunsaturated fatty acids (PUFAs). Cholesterol lacks the bis-allylic hydrogen which can readily be abstracted to form a more stable bis-allylic carbon-centered radical. However, in biological systems, the concentration of cholesterol hydroperoxides (cholesterol oxidation products) are as high as some PUFA oxidation products.[36] Firstly, cholesterol is a trisubstituted endocylic monoalkene, hence it is more prone to oxidative attack by peroxyl radicals in comparison to disubstituted monoalkenes such as oleate.[37] Secondly, cholesterol hydroperoxides are known to be more resistant to glutathione-dependent enzymatic detoxification compared to PUFA hydroperoxides, causing them to accumulate in biological systems for a longer time.[38] Therefore, understanding the chemical and biological pathways in which cholesterol can oxidize to generate cholesterol hydroperoxides and other oxysterols has become a topic of interest to many research groups in recent years.[39, 40, 41]

For many years, researchers have inferred the identity of ROS in biological or chemical systems from the oxidation products they form. Smith, one of the pioneers in this field, used cholesterol as a biomarker for lipid peroxidation and reactive oxygen species.[42] This is mainly because until very recently, it was believed that cholesterol oxidation products are reagent specific. For instance, the epimers of cholesterol 7-OOH were believed to be the only primary products of the reaction of cholesterol with molecular oxygen (Scheme 1.11.a). On the other hand, cholesterol 5α-OOH was believed to arise solely from the reaction of cholesterol with singlet oxygen (Scheme 1.11.b) and secosterols were generally accepted to only arise from the reaction of cholesterol with ozone (Scheme 1.11.c). The traditional reagent-product specificity of cholesterol oxidation is illustrated in Scheme 1.11.

Therefore, cholesterol was deemed to be a good biomarker for oxidative stress by specific ROS since it lacks the complexity of polyunsaturated lipids, oxidizes more readily than monounsaturated lipids, and seemed to impose an ideal reagent-product specificity.

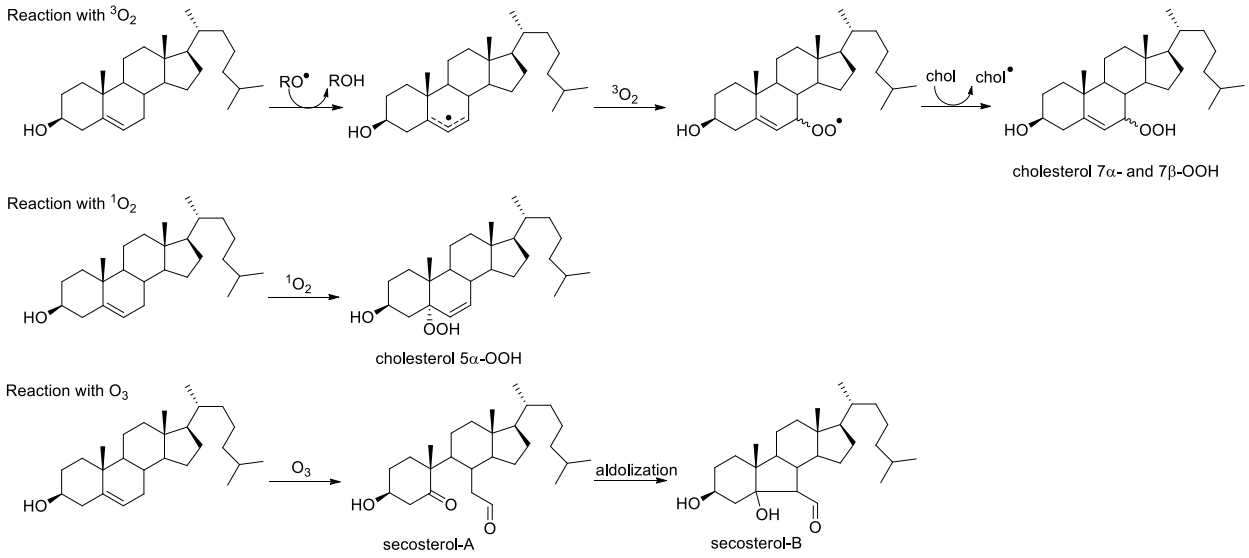

Scheme 1.11. Cholesterol oxidation with three different reactive oxygen species demonstrating the general belief of ROS-specific product formation.

Nonetheless, until very recently, it was unclear as to why only the epimers of cholesterol 7-OOH were formed from the reaction of cholesterol with O_2 in particular, since autoxidation of oleate yields all four isomers of corresponding hydroperoxides. Therefore, Zielinski and Pratt revisited the product distribution arising in the autoxidation of cholesterol where they proposed that just like oleate, cholesterol autoxidation should result in four products and their stereoisomers (Scheme 1.12). They initially performed the reaction in aerated chlorobenzene (0.5 M) at 37 ˚C for 16 hours. The resultant product mixtures were treated with PPh_3 to reduce hydroperoxides to alcohols for better stability. They were able to detect three of the expected products and their stereoisomers (cholesterol 4α-OH, 4β-OH, 6α-OH, 6β-OH, 7α-OH and 7β-OH) in the absence of an antioxidant. In the presence of a good H-atom donor (such as 2,6-dimethyl-

4-tert-butylphenol), cholesterol 5α-OOH was also formed since the β-fragmentation of cholesterol 5α-OO• to form cholesterol 7α-OO• was inhibited.

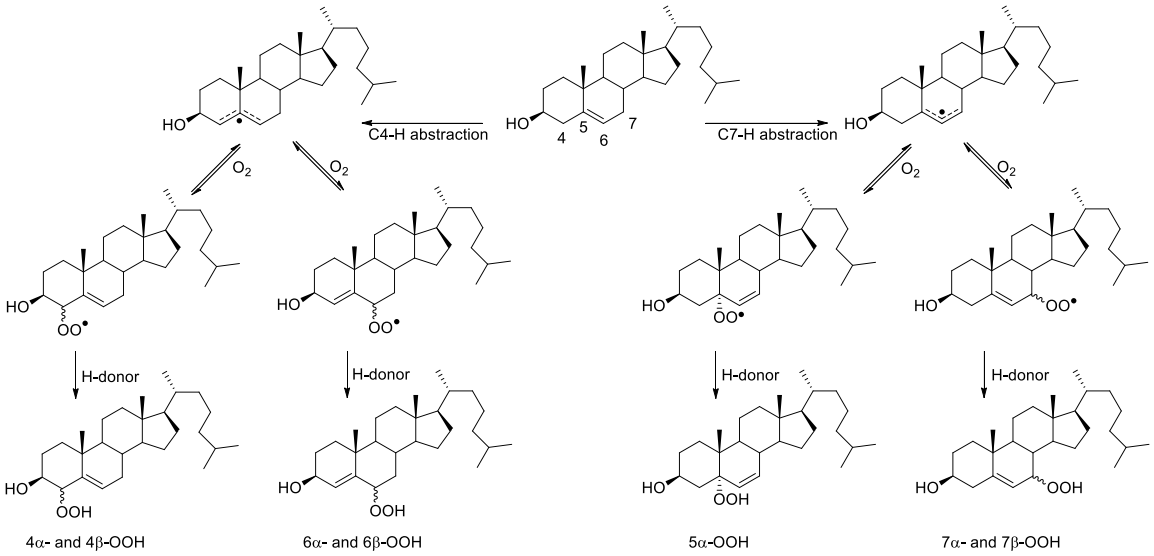

Scheme 1.12. Proposed mechanism of cholesterol autoxidation.

Thus, the epimers of cholesterol 7-OOH are not the only primary products of cholesterol autoxidation. They also showed that cholesterol 5α-OOH is not unique to the reaction of cholesterol with $^1O_2$ and can also be produced by cholesterol autoxidation in the presence of a good H-atom donor. Moreover, they were able to show that cholesterol 6-OOH can lead to secosterols, as will be discussed below. Thus, cholesterol oxidation products are not good indicators of specific ROS formation.

1.4 Antibody Catalyzed Water Oxidation

In 2003, Wentworth *et al.* detected cholesterol-derived secosterol-A and secosterol-B (also called atheronal-A and -B) derivatives in human atherosclerotic plaques and brain tissues of patients with Alzheimer disease.[43] The physiological sites where these bioptical samples were taken eliminates the chance of the involvement of atmospheric ozone in production of these secosterols. Wentworth and co-workers, relying on the literature of the time, concluded that these secosterols unambiguously prove endogenous ozone production in biological systems (Scheme 1.13). Up to then, secosterols were believed to derive only from the reaction of cholesterol with ozone.[44, 45, 46] The first *in vivo* detection of these secosterols was in the lung tissues of rats exposed to ozone gas by Pryor *et al.*, one of the pioneers who studied the ozonolysis of cholesterol extensively.[47]

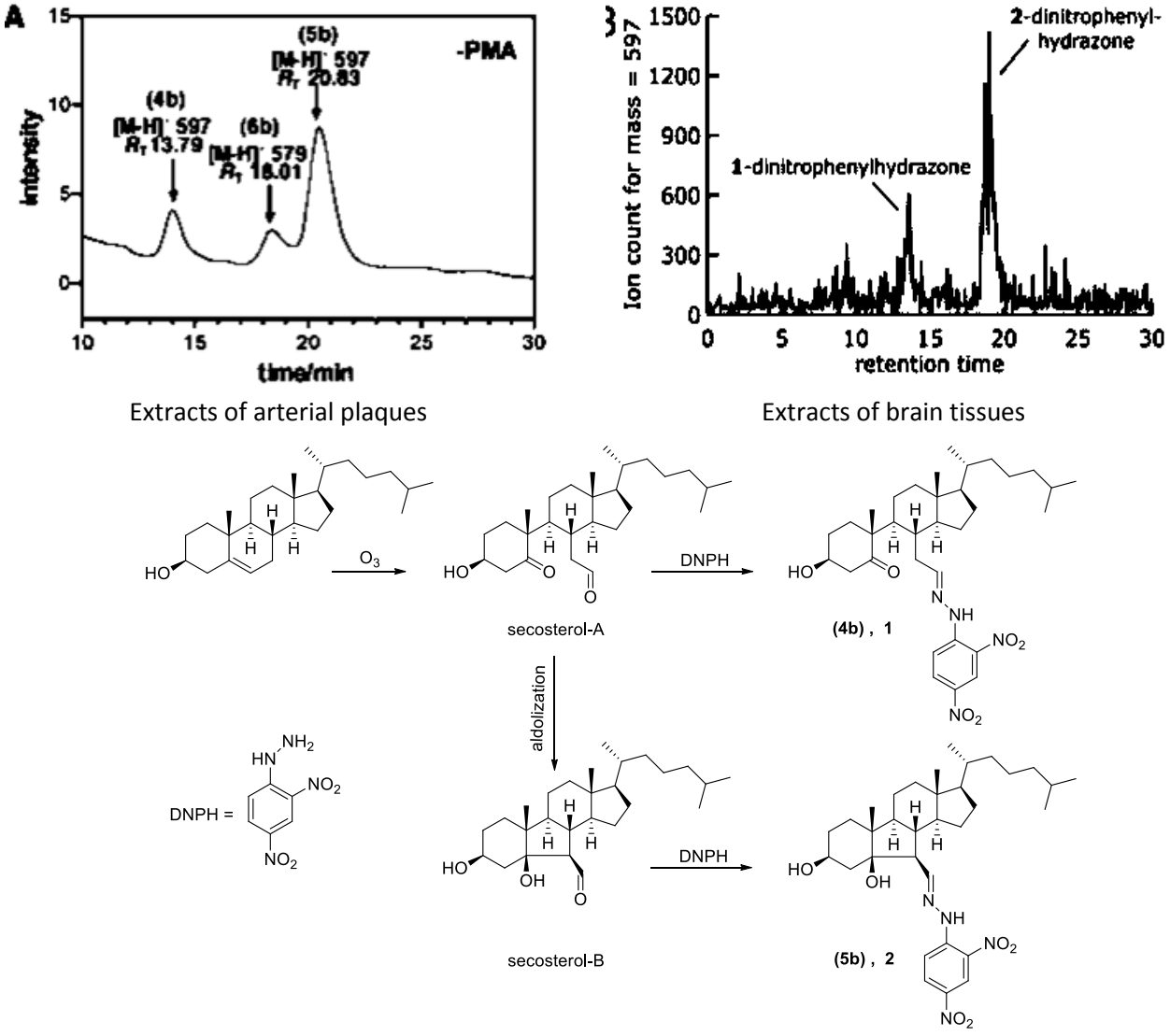

Scheme 1.13. Chromatograms of extracts of arterial plaques and brain tissues obtained by Wentworth and co-workers.[43] Generation of DNPH derivatized secosterol-A and secosterol-B via cholesterol ozonolysis.

In the early 2000s, Wentworth and co-workers proposed that a trioxidic species with the chemical signature of ozone is generated during the antibody-catalyzed water-oxidation pathway at the inflammation site as the first line of defence to attack and destroy antigens (Scheme 1.14).

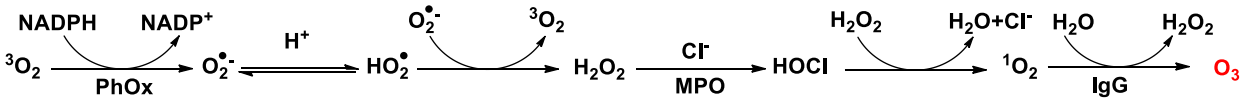

Scheme 1.14. Proposed mechanism of antibody catalyzed water oxidation and generation of ozone in biological systems.

It was proposed that electron transfer converts ground state triplet oxygen ($^3O_2$) to a superoxide radical anion ($O_2^{\bullet -}$) via NADPH oxidase, a transmembrane phagocytes system that was originally proposed by Allen *et al.* in 1972.[48] Dismutation of superoxide is done by the superoxide dismutase enzyme (SOD) by converting it to triplet oxygen ($^3O_2$) and hydrogen peroxide (H_2O_2). Hypochlorous acid can form by the reaction of H_2O_2 and the heme enzyme myeloperoxidase (MPO).[49] Remarkably, MPO is the only mammalian enzyme that oxidizes Cl^- to HOCl at plasma concentration of the halide. [50] Singlet molecular oxygen ($^1O_2$), a key component of this oxygen-scavenging cascade, is proposed to be originated from the reaction of hypochlorous acid with H_2O_2.[51] Antibodies are then proposed to catalyze the generation of hydroperoxides (H_2O_2) from $^1O_2$ and water via the postulated intermediate of dihydrogen trioxide (H_2O_3), which can eventually lead to ozone (O_3).[52, 53]

Oxygen-18 isotopic incorporation into H_2O_2 is one of the few mechanistic studies that was performed by Wentworth and co-workers. The isotopic content of H_2O_2 was assayed indirectly by reducing it with tris(carboxyethyl) phosphine (TCEP) and the resultant phosphine oxide was monitored by mass spectroscopy. When horse IgG was irradiated under air in $H_2{}^{18}O$, the ratio of TCEP-^{18}O to TCEP-^{16}O was 1:2. Likewise, when the same experiment was carried out, but using $^{18}O_2$ and $H_2{}^{16}O$, a ratio of 2:1 of TCEP-^{18}O to TCEP-^{16}O was obtained. These striking results were rationalized by a mechanism in which a trioxidic intermediate is generated via water oxidation by $^1O_2$. During this process, Wentworth *et al*. postulated that oxidants such as dihydrogen trioxide (HOOOH), hydrotrioxy radical (HOOO•),[54] and even ozone (O_3)[55] are formed endogenously in biological systems. The formation of these oxidants was further supported by quantum calculations performed by Datta *et al.* in 2002.[56]

1.5 Debunking Endogenous Ozone

In 2008, our laboratory showed that cholesterol 5α-hydroperoxide, the major product of $^1O_2$ oxidation of cholesterol can undergo acid-catalyzed Hock fragmentation to produce secosterol-A and secosterol-B.[57] The proposed mechanism is illustrated in Scheme 1.15.

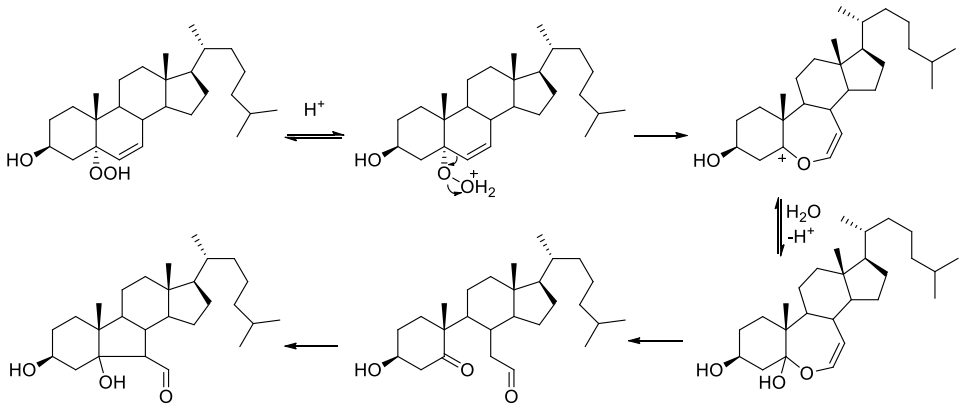

Scheme 1.15. The proposed mechanism of Hock fragmentation of cholesterol 5α-OOH.

Various protic acids (e.g., HCl, p-TsOH, TFA) and different solvents (e.g., EtOH, THF, $CHCl_3$) were investigated. Under all conditions, Hock fragmentation was found to proceed readily where it was monitored by ^{1}H NMR, ^{13}C NMR and HRMS. However, the distribution of the products was affected by the solvent. Acid-catalyzed Hock fragmentation of cholesterol 5α-OOH in non-alcoholic solvents led to the quantitative formation of aldolized product (secosterol-B). Whereas, in alcoholic solvents non-aldolized product (secosterol-A) was also observed. The effect of alcoholic solvents on the product distribution was explained by the ability of solvent to attack the oxocarbenium ion to yield the hemiacetal structure which slows down any further aldolization.

Brinkhorst *et al.* also subjected cholesterol 5α-OOH to acid-catalyzed Hock fragmentation under DNPH derivatization conditions, the same derivatization conditions used for the identification of secosterols in atherosclerotic plaques. Not surprisingly, the same DNPH derivatized secosterols as those obtained from cholesterol ozonolysis were formed. These findings clearly demonstrate that secosterol-A and secosterol-B are not unique to ozonolysis. The same procedure was performed by Zielinski and Pratt using cholesterol 6β-OOH instead.[58] They also found that Hock fragmentation of cholesterol 6β-OOH, a minor product of cholesterol autoxidation, leads to secosterols as well.

1.6 Hock Fragmentation of Hydroperoxides

The acid-catalyzed decomposition of peroxides, commonly known as Hock fragmentation, (named after its discoverer Heinrich Hock) is a very important synthetic process. In 1936 Hock reported that cyclohexene hydroperoxide, upon treating with sulfuric acid, generates cyclopentene carboxaldehyde (Scheme 1.16). [59]

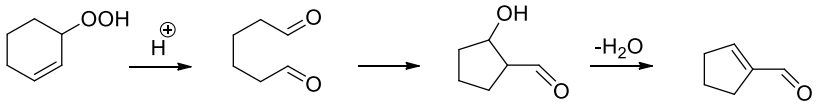

Scheme 1.16. Acid-catalyzed Hock fragmentation of cyclohexene hydroperoxide.

Hock fragmentation is best known for its involvement in commercial preparation of phenol where acid-catalyzed decomposition of cumene hydroperoxide provides acetone and phenol in quantitative amounts (Scheme 1.17). The Hock fragmentation of cumene hydroperoxide was first reported by Hock and Lang.[60] The reaction starts with the protonation of the β-oxygen, which leads to an irreversible O-O heterolysis and carbon-to-oxygen rearrangement. Vinyl and aryl groups, especially those with electron donating substituents, have greater migratory aptitude for this kind of rearrangement.

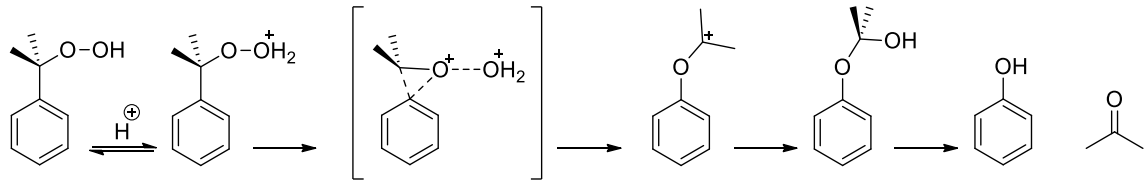

Scheme 1.17. Proposed mechanism for cumene hydroperoxide Hock fragmentation.

Hock fragmentation is not unique to industrial synthesis and is very much related to biological systems. For example, 4-hydroxynonenal (4-HNE), an α,β-unsaturated hydroxyalkenal linked to the pathology of neurodegenerative and cardiovascular diseases, is suggested to be produced by lipid peroxidation followed by Hock fragmentation.[61] The proposed mechanism for formation of 4-HNE from linoleate is shown in Scheme 1.18.

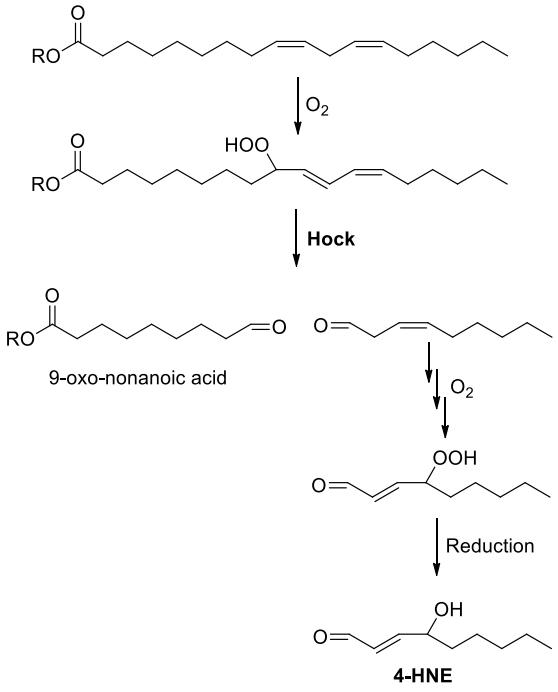

Scheme 1.18. Proposed mechanism for 4-HNE formation via lipid peroxidation followed by Hock fragmentation.

1.7 Research Objectives

Wentworth *et al.* proposed that endogenous ozone is responsible for secosterol generation *in vivo,* as they believed that ozone was the only ROS that can directly cleave the double bond in the B-ring of the sterol. We were skeptical given they used biomarkers that are not unique to ozonolysis. In fact, an alternative ozone-free pathway proposed by Brinkhorst *et al.* showed that secosterols are not unique to ozonolysis as Hock fragmentation of cholesterol 5α-OOH, the main product of $^1O_2$ oxidation can also generate secosterols. However, singlet oxygen is a high energy molecule with a microsecond timescale half-life. Moreover, cholesterol 5α-OOH is not particularly stable in solution either, as it rearranges readily to a more thermodynamically stable product, cholesterol 7α-OOH. Hock fragmentation of cholesterol 6β-OOH, the minor product of cholesterol autoxidation, can also generate secosterols. However, cholesterol 6β-OOH comprises only 2% of the total cholesterol autoxidation products.

We were interested in finding the most reasonable, physiologically relevant, pathway to secosterols, so we focused our efforts on cholesterol 7-OOH, the most abundant product of cholesterol autoxidation (Scheme 1.19). We wondered if cholesterol 7-OOH could undergo Hock fragmentation to yield products with similar properties as secosterol-A and -B, and further, if they had been misidentified as secosterol-A and -B. We compared the Hock fragmentation of cholesterol 7α-OOH with that of cholesterol 5α-OOH. We also investigated the characteristics of the products, their isolation and our attempts in their characterization, one of which provided us with an insightful detail about the mechanism of Hock fragmentation.

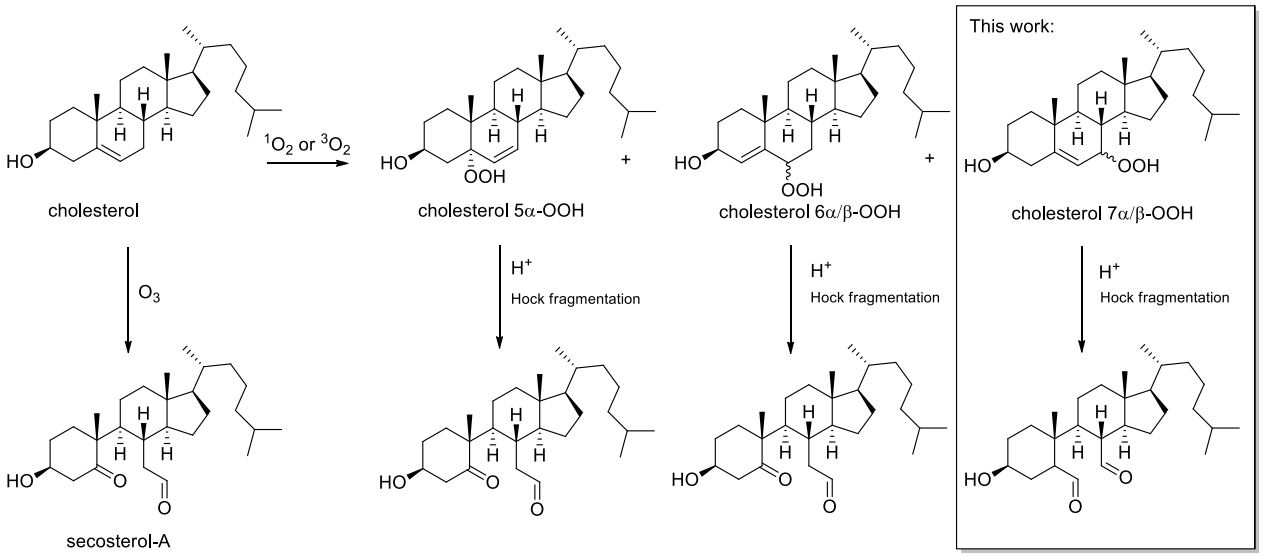

Scheme 1.19. Proposed pathways to secosterols.

1.8 References

[1] Bolland, J. L. *Quarterly Reviews*. **1949**, 3, 1.

[2] Lundberg, W. O.; Chipault, J. R.; Hendrickson, M. J. *J. Am. Oil Chem. Soc.* **1949**, 26, 109.

[3] Ingold, K. U. *Science* **1967**, 158, 248.

[4] Ingold, K. U. *Acc. Chem. Res.* **1969**, 2, 1.

[5] Maillard, B.; Ingold, K. U.; Scaiano, J. C. *J. Am. Chem. Soc*. **1983**, 105, 5095.

[6] Burton, G. W.; Doba, T.; Gabe, E. J.; Hughes, L.; Lee, F.; Prased, L.; Ingold, K. U. *J. Am. Chem. Soc*. **1985**, 107, 7053.

[7] Burton, G. W.; Ingold, K. U. *J. Am. Chem. Soc.* **1981**, 103, 6472.

[8] Bowry, V. R.; Ingold, K. U. *Acc. Chem. Res.* **1999**, 32, 27.

[9] Esterbauer, H.; Gebicki, J.; Pauhl, H.; Jurgens, G. *Free Radical Biol. Med*. **1992**, 13, 341.

[10] Berliner, J. A.; Heinecke, J. W. *Free Radical Biol. Med*. **1996**, 20, 707.

[11] Antczak, A.; Nowak, D.; Shariati, B.; Krol, M.; Piasecka, G.; Kurmanowska, Z. *Eur. Respir. J.* **1997**, 10, 1235.

[12] Montuschi, P.; Corradi, M.; Ciabattoni, G.; Nightingale, J.; Kharitonov, S. A.; Barnes, P. J. *Am. J. Respir. Crit. Care. Med*. **1999**, 160, 216.

[13] Simonian, N. A.; Coyle, J. T. *Annu. Rev. Pharmacol. Toxical*. **1996**, 36, 83.

[14] Sayre, L. M.; Zelasko, D. A.; Harris, P. L. R.; Perry, G.; Salomon, R. G.; Smith, M. A. *J. Neurochem*. **1997**, 68, 2092.

[15] Farmer, E. H.; Sutton, D. A. *J. Chem. Soc.* **1943**, 119.

[16] Farmer, E. H.; Koch, H. P.; Sutton, D. A. *J. Chem. Soc.* **1949**, 541.

[17] Frankel, E. N.; Neff, W. E.; Rohwedder, W. K. *Lipids* **1977**, 901.

[18] Porter, N. A.; Mills, K. A.; Carter, R. L. *J. Am. Chem. Soc.* **1994**, 116, 6690.

[19] Pratt, D. A.; Mills, J. H.; Porter, N. A. *J. Am. Chem. Soc.* **2003**, 125, 5801.

[20] Howard, J. A.; Ingold, K. U. *Can. J. Chem*. **1967**, 45, 785.

[21] Prein, M.; Adam, W. *Angew. Chem. Int. Ed. Engl.* **1996**, *35*, 477.

[22] Kiryu, C.; Makiuchi, M.; Miyazaki, J.; Fujinaga, T.; Kakinuma, K. *FEBS Lett.* **1999**, 443, 154.

[23] Khan, A. U. *Biochem. Biophys. Res. Commun*. **1984**, 122, 668.

[24] Ryter, S. W.; Tyrrell, R. M. *Free Radic. Biol. Med*. **1998**, 24, 1520.

[25] Wagner, D.; Przybyla, D.; Camp, R.; Kim, C.; Landgraf, F.; Lee, K. P.; Wursch, M.; Laloi, C.; Nater, M.; Hideg, E.; Apel, K. *Science* **2004**, 306, 1183.

[26] Singleton, D. A.; Hang, C. *J. Org. Chem*. **2000**, 3, 91.

[27] Singleton, D. A.; Hang, C.; Szymanski, M. J.; Meyer, M. P.; Leach. A. G.; Kuwata, K. T.; Chen, J. S.; Greer, A.; Foote, C. S.; Houk, K. N. *J. Am. Chem. Soc.* **2003**, 125, 1319.

[28] Hamberg, M.; Samuelsson, B. *Proc. Natl. Acad. Sci. USA.* **1974**, 70, 899.

[29] Adam, J.; Fitzsimmons, B. J.; Girard, Y.; Leblanc, Y.; Evans, J. F.; Rokach, J. *J. Am. Chem. Soc*. **1985**, 107, 464.

[30] Serhan, C. N.; Hamberg, M.; Samuelsson, B. *Proc. Natl. Acad. Sci. USA*. **1984**, 81, 5335.

[31] Greenberg, M. E.; Li, X-M.; Gugiu, B. G.; Gu, X.; Qin, J.; Salomon, R. G.; Hazen, S. L. *J. Biol. Chem*. **2008**, 283, 2385.

[32] Wong-Ekkabut, J.; Xu, Z.; Triampo, W.; Tang. I. M.; Tieleman, D. P.; Monticelli, L. *J. Biophys.* **2007**, 93, 4225.

[33] Stewart, C. R.; Wilson, L. M.; Zhang, Q.; Pham, C. L. L.; Waddington, L. J.; Staples, M. K.; Stapleton, D.; Kelly, J. W.; Howlett, G. *J. Biochem.* **2007**, 46, 5552.

[34] Berg. J. M.; Tymoczko, J. L.; Stryer, L. *Biochemistry, 5th ed*. NewYork, Freeman, W. H. **2002**.

[35] Holick, M. F.; MacLaughlin, J. A.; Doppelt, S. H. *Science* **1981**, 211, 590.

[36] Saito, Y.; Yoshida, Y.; Niki, E. *FEBS Lett*. **2007**, 581, 4349.

[37] Pratt, D. A.; Tallman, K. A.; Porter, N. A. *Acc. Chem. Res*. **2011**, 44, 458.

[38] Miyamoto, S.; Arai, H.; Terao, J. *Enzymatic antioxidant defenses*. Eds. Aldini, G.; Yeum, K-J.; Niki, E.; Russell, R. M. Wiley-Blackwell Publishing, Hoboken NJ, USA, **2010**. 21-23.

[39] Kulig, W.; Cwiklik, L.; Jurkiewicz, P.; Rog, T.; Vattulainen, I. *Chem. Phys. Lipids.* **2016**, 199, 144.

[40] Zielinski, Z. A. M.; Pratt, D. A. *J. Am. Chem. Soc.* **2016**, 138, 6932.

[41] VanLier, J. E.; Mast, N.; Pikuleva, I. A. *Angew. Chem. Int. Ed*. **2015**, 54, 11138.

[42] Gumulka, J.; St.Pyrek, J.; Smith, L. L. *Lipids* **1982**, 17, 197.

[43] Wentworth Jr, P.; Nieva, J.; Takeuchi, C.; Galve, R.; Wentworth, A. D.; Dilley, R. B.; DeLaria, G. A.; Savan, A.; Babior, B. M.; Janda, K. D.; Eschenmoser, A.; Lerner, R. A. *Science* **2003**, 302, 1053.

[44] Gumulka, J.; Smith, L. L. *J. Am. Chem. Soc.* **1983**, 105, 1972.

[45] Jaworski, K.; Smith, L. L. *J. Org. Chem.* **1988**, 53, 545.

[46] Paryzek, Z.; Martynow, J.; Swoboda, W. *J. Chem. Soc. Perkin Trans*. **1990**, 1, 1222.

[47] Pryor, W. A.; Wang, K.; Bermúdez, E. *Biochem. Biophys. Res. Commun*. **1992**, 188, 618.

[48] Allen, R. C.; Stjernholm, R. L.; Steele, R. H. *Biochem. Biophys. Res. Comm*. **1972**, 47, 676.

[49] Harrison, J. E.; Schultz, J. *J. Biol. Chem*. **1976**, 251, 1371.

[50] Gaut, J. P.; Yeh, G. C.; Duy Tran, H.; Byun, J.; Henderson, J. P.; Richter, G. M.; Brennan, M.; Lusis, A. J.; Belaaouaj, A.; Hotchkiss, R. S.; Heinecke, J. W. *Proc. Natl. Acad. Sci*. **2001**, 98, 11961.

[51] Khan, A. U.; Kasha, M. *Proc. Natl. Acad. Sci.* **1994**, 91, 12365.

[52] Babior, B. M.; Takeuchi, C.; Ruedi, J.; Gutierrez, A.; Wentworth Jr. P. *Proc. Natl. Acad. Sci. USA.* **2003**, 100, 3031.

[53] Nieva, J.; Wentworth Jr, P. *Trends Biochem Sci.* **2004**, 29, 274.

[54] Wentworth, Jr. P.; Wentworth, A. D.; Zhu, X.; Wilson, I. A; Janda, K. D.; Eschenmoser, A.; Lerner, R. A. *Proc. Natl. Acad. Sci. USA.* **2003**, 100, 1490.

[55] Wentworth, Jr. P.; McDunn, J. E.; Wentworth, A. D.; Takeuchi, C.; Nieva, J.; Jones, T.; Bautista, C.; Ruedi, J. M.; Gutierrez, A.; Janda, K. D.; Babior, B. M.; Eschenmoser, A.; Lerner, R. A. *Science* **2002**, 298, 2195.

[56] Datta, D.; Vaidehi, N.; Xu, Xin.; Goddard III, W. A. *Proc. Natl. Acad. Sci. USA.* **2002**, 99, 2636.

[57] Brinkhorst, J.; Nara, S. J.; Pratt, D. A. *J. Am. Chem. Soc*. **2008**, 130, 12224.

[58] Zielinski, Z. A. M.; Pratt, D. A. *J. Am. Chem. Soc*. **2016**, 138, 6932.

[59] Hock, H.; Schrader, O., *Naturwissenschaften* **1936**, 24, 159.

[60] Hock, H.; Lang, B. *Ber*. **1944**, 77B, 357 [In German].

[61] Mali, V. R.; Palaniyandi, S. S. *Free Radical Res.* **2014**, 48, 251.

-2-

Ozonolysis of Cholesterol and its Isomer, $\Delta^{6,7}$-Cholesterol

2.1 Introduction

The hydrazones derived from 2,4-dinitophenylhydrazine (DNPH) derivatization of the cholesterol ozonolysis products secosterol-A and -B have allegedly been identified in atherosclerotic plaques and brain tissue of Alzheimer's patients by Wentworth and co-workers.[1] As a result, they proposed that ozone (which they proposed to be forming endogenously via antibody-catalyzed water oxidation) is solely responsible for secosterol generation *in vivo*.[2, 3, 4]

Given the interest in the pathogenic potential of the secosterols [5, 6, 7, 8] and their use as biomarkers for oxidative stress,[9] we wondered if other, more biologically relevant oxidants ($^1O_2$, $^3O_2$) were able to generate secosterol-A and -B and/or similar products. In fact, we demonstrated that secosterol-A and -B can also arise upon acid-catalyzed Hock fragmentation of cholesterol 5α-hydroperoxide (cholesterol 5α-OOH), the major product of the reaction of cholesterol with singlet oxygen.[10] We also recently demonstrated that the acid-catalyzed Hock fragmentation of cholesterol 6β-OOH, a minor product of the reaction of cholesterol with either singlet oxygen or molecular oxygen, can also generate secosterols.[11] However, ozone and singlet oxygen are high-energy oxidants. Therefore, we wondered if cholesterol 7α and 7β-OOH, the major products of the reaction of cholesterol with molecular oxygen (via autoxidation), would undergo Hock fragmentation and provide carbonyl compounds analogous to secosterol-A and -B. The potential products of the acid-catalyzed Hock fragmentation of cholesterol 7α and 7β-OOH are shown in Scheme 2.1.

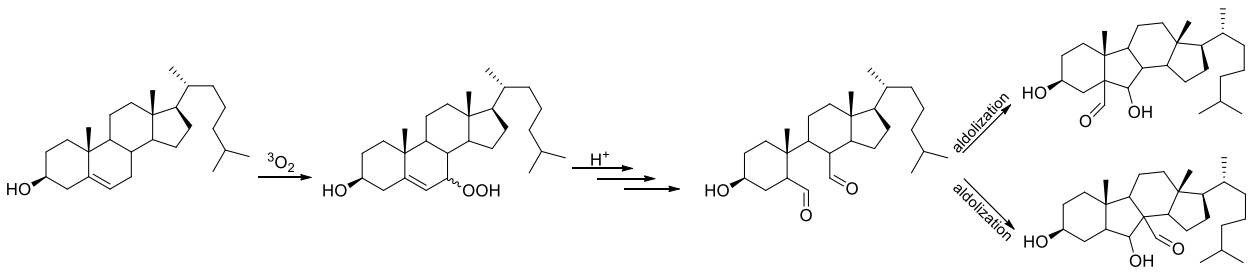

Scheme 2.1. Proposed products of the acid-catalyzed Hock fragmentation of cholesterol 7α and 7β-OOH, the main products of cholesterol autoxidation.

Since secosterol-A and -B may be formed either by cholesterol ozonolysis or by Hock fragmentation of cholesterol 5α-OOH, we surmised that the easiest way to prepare the expected products of the Hock fragmentation of cholesterol 7α and 7β-OOH was to subject the isomer of cholesterol with the double bond in the 6,7 position (i.e. $\Delta^{6,7}$-cholesterol) to ozonolysis (Scheme 2.2).

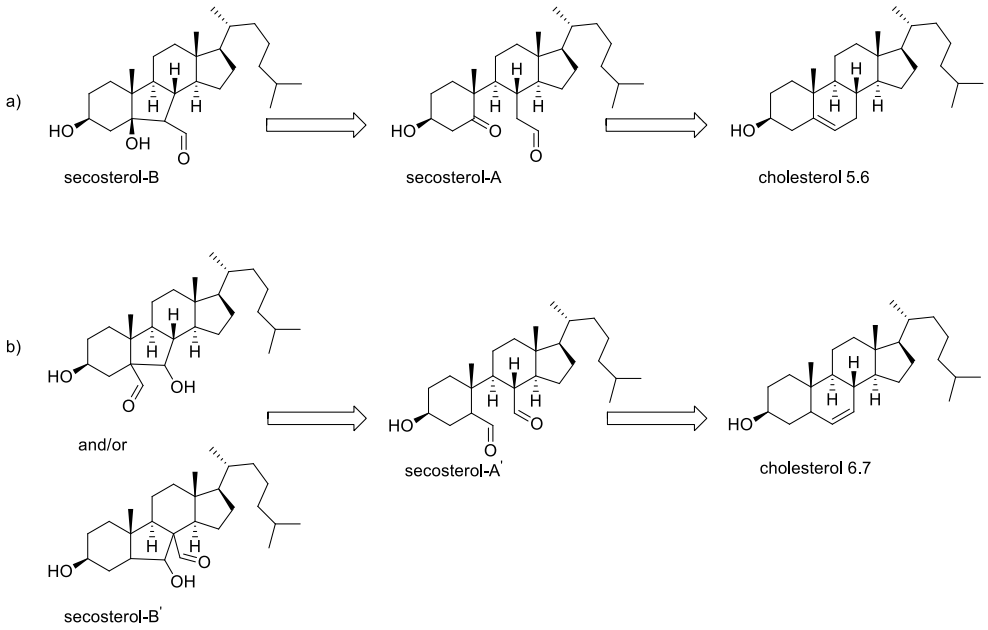

Scheme 2.2. a) Retrosynthesis of secosterol-A and -B via ozonolysis of cholesterol. b) Retrosynthesis of the proposed products (secosterol-A' and secosterol-B') of Hock fragmentation of cholesterol 7α and 7β-OOH via ozonolysis of $\Delta^{6'7}$-cholesterol.

In this chapter we first describe the synthesis of the isomer of cholesterol with the double bond in the 6,7 position ($\Delta^{6'7}$-cholesterol). We then describe the ozonolysis of $\Delta^{5'6}$-cholesterol and $\Delta^{6'7}$-cholesterol, and discuss the products formed from each.

2.2 Results

2.2.1 Synthesis of $\Delta^{6,7}$-Cholesterol

$\Delta^{6,7}$-Cholesterol was synthesized by a procedure originally reported by Corey.[12] Cholesteryl acetate, **2**, was nitrated with nitric acid and sodium nitrite to produce 3β-acetoxy-6-nitrocholest-5-ene, **3** (Scheme 2.3). A Nef reaction was next carried out to reduce the nitro group with zinc in acetic acid and water producing the corresponding 3β-acetoxycholestan-6-one, **4**. It should be pointed out that the yield increased substantially when the temperature was increased from 80 ^{o}C to 120 ^{o}C. Increasing the temperature above the boiling point of water removes the excess water from the reaction mixture and hence prevents acid dilution. While high acidity favours the Nef reaction, weak acidic conditions favour the regeneration of nitro compounds via protonation of the α-carbon. By removing water, we prevented the rise in pH and promoted the protonation of oxygen rather than the α-carbon.[13]

The resultant 3β-acetoxycholestan-6-one was brominated with bromine in dry ether to give 3β-acetoxy-7-bromocholestan-6-one, **5**. The subsequent reduction and elimination, using sodium borohydride and zinc afforded the 3β-acetoxycholest-6-ene, **6**. Hydrolysis of the acetyl protecting group by sodium hydroxide afforded the desired cholesterol isomer with the double bond at the 6,7 position, **1**.

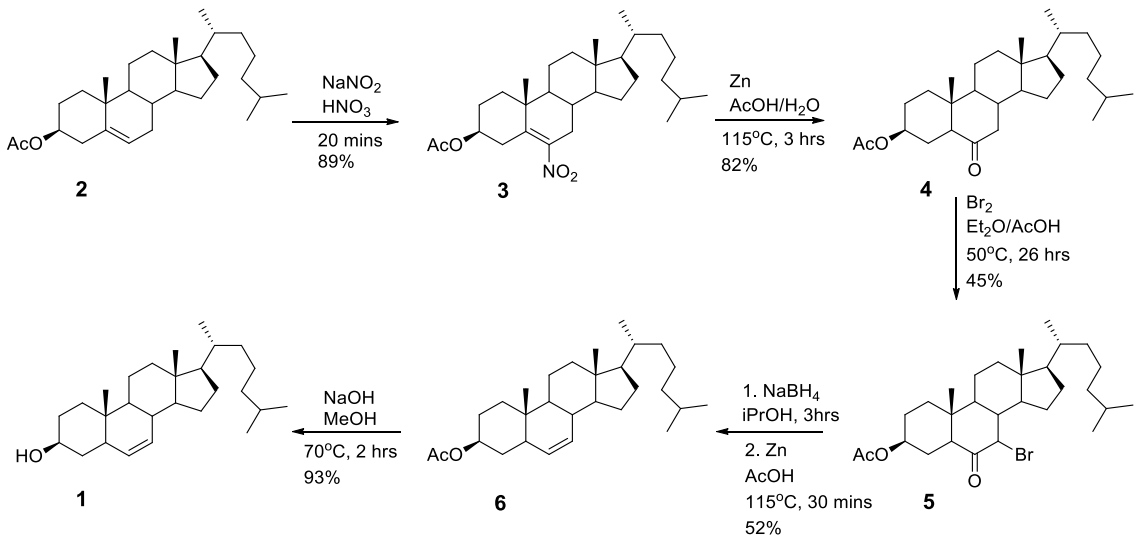

Scheme 2.3. The synthesis of $\Delta^{6,7}$-cholesterol.

2.2.2 Ozonolysis of Cholesterol Followed by DNPH Derivatization

Prior to investigating the ozonolysis of $\Delta^{6,7}$-cholesterol, **1**, we first subjected cholesterol to ozonolysis to obtain authentic secosterol-A,**7**, and secosterol-B, **8**, for comparison (Scheme 2.4). Cholesterol was dissolved in a mixture of methanol and chloroform at -78 ^{o}C while ozone was bubbled through the solution. The resultant ozonide was reduced with zinc in acetic acid to provide the keto-aldehyde product—secosterol-A (Figure 2.1) which, upon aldolization in L-proline and water/acetonitrile, yielded the aldolized product—secosterol-B (Figure 2.2).[1]

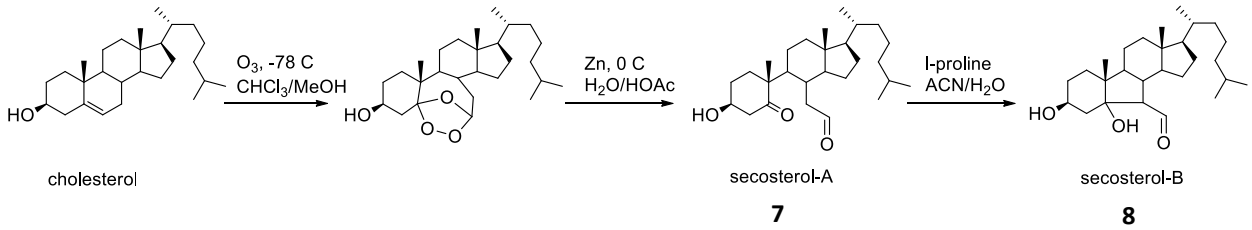

Scheme 2.4. Ozonolysis of cholesterol followed by aldolization of the keto-aldehyde product (secosterol-A, **7**) to its aldolized product (secosterol-B, **8**).

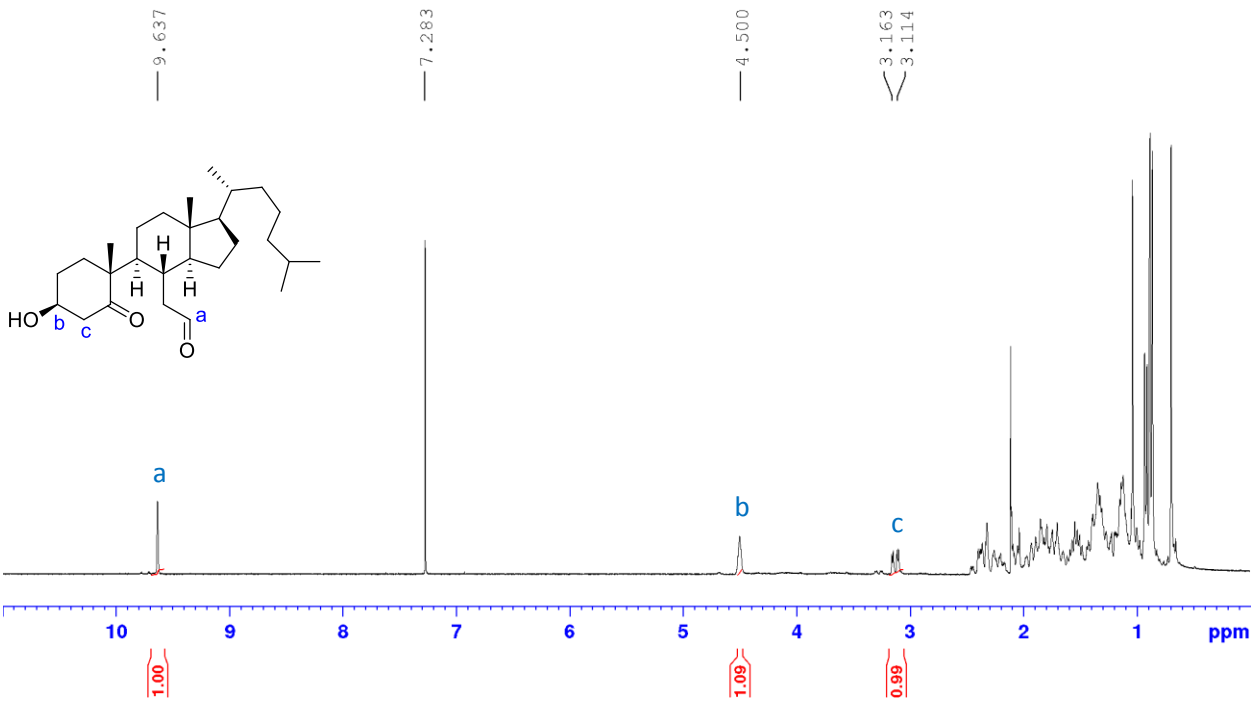

Figure 2.1. ^{1}H-NMR spectrum of secosterol-A, **7**, obtained from ozonolysis of cholesterol. The spectrum was recorded at 400 MHz with chemical shifts reported in ppm relative to $CDCl_3$.

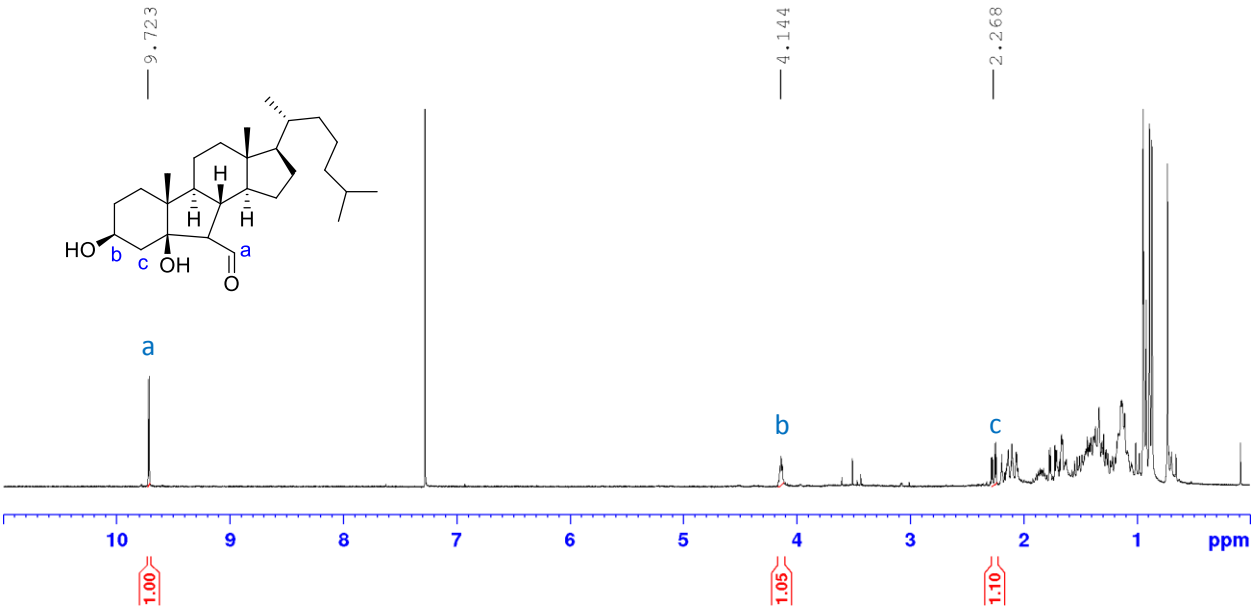

Figure 2.2. ^{1}H-NMR spectrum of secosterol-B, **8**, obtained from aldolization of secosterol-A. The spectrum was recorded at 400 MHz with chemical shifts reported in ppm relative to $CDCl_3$.

Secosterol-A and secosterol-B were then derivatized by 2,4-dinitrophenylhydrazine (DNPH) in an acidic solution affording the spectra shown in Figures 2.3 and 2.4, respectively. It appears that both *cis* and *trans*-configurations were formed albeit the *trans*-configuration was the major product. Previously, Pryor *et al.* also reported the presence of both *cis* and *trans*-configurations of DNPH derivatized secosterol-A but they did not report the appearance of the *cis*-configuration of DNPH derivatized secosterol-B.[14] Herein, it appears that both *cis* and *trans*-configuration of both DNPH derivatized secosterols were formed.

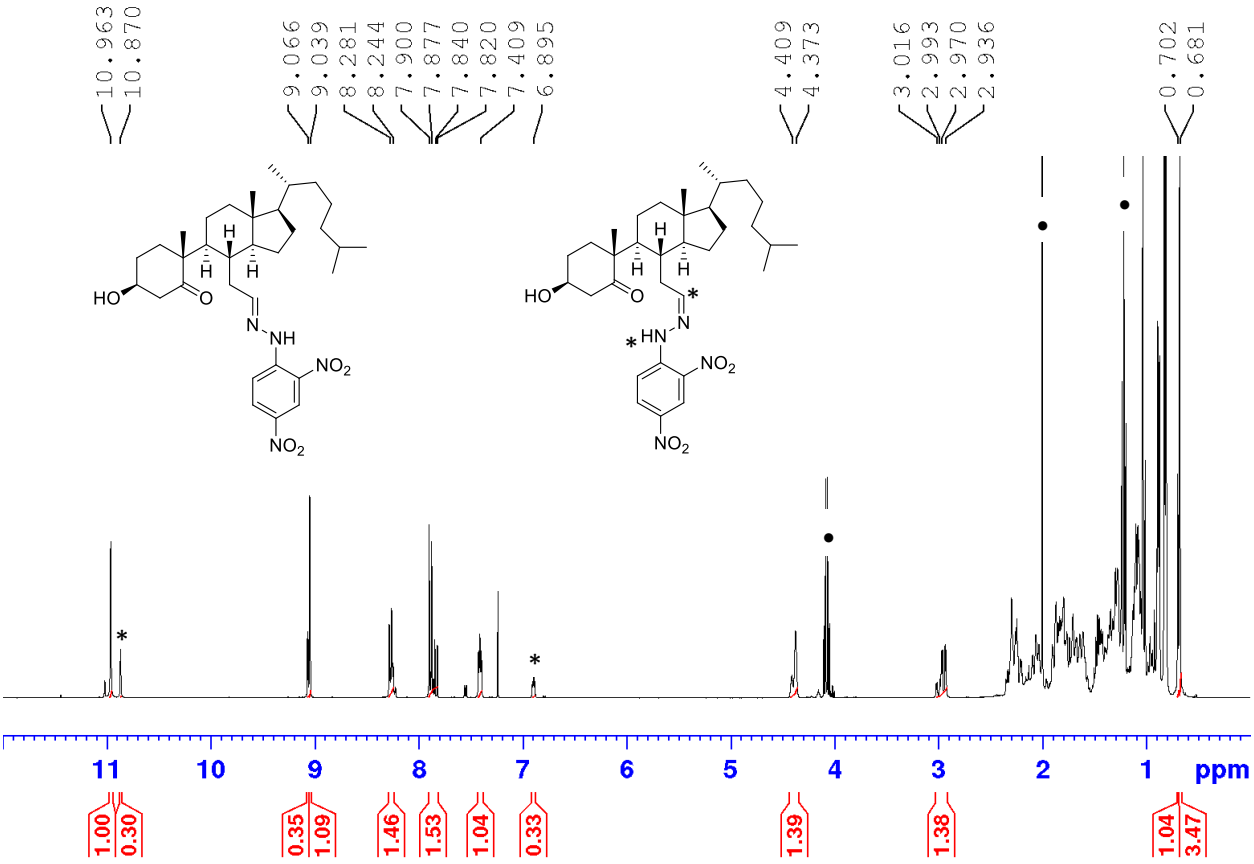

Figure 2.3. ^{1}H-NMR spectrum of 2,4-dinitrophenylhydrazone of secosterol-A, **9**. The spectrum was collected at 400 MHz with chemical shifts reported in ppm relative to $CDCl_3$. *presumed *cis*-isomer, • ethyl acetate.

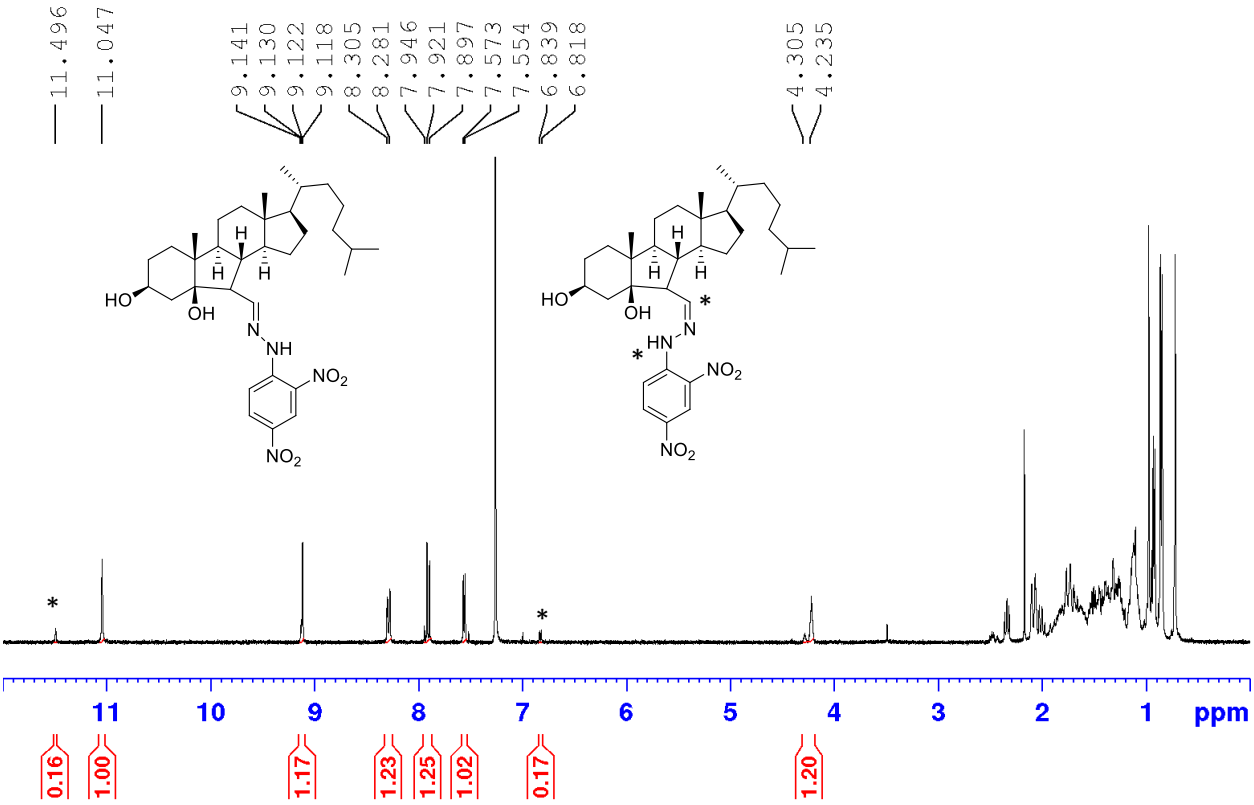

Figure 2.4. ^{1}H-NMR spectrum of 2,4-dinitrophenylhydrazone of secosterol-B, **10**. The spectrum was collected at 400 MHz with chemical shifts reported in ppm relative to $CDCl_3$. *presumed *cis*-isomer.

2.2.3 Ozonolysis of $\Delta^{6'7}$-Cholesterol

The same procedure was employed for ozonolysis of $\Delta^{6'7}$-cholesterol. However, herein we used dimethyl sulfide to reduce the resulted secondary ozonide. Powerful reducing agents such as BH_3, [15] Zn/AcOH, [16] and $LiAlH_4$ [17] as well as milder ones such as Me_2S [18] are commonly used by research groups. We preferred Me_2S work-up for the lack of requirement to concentrate the sample.

Appearance of the aldehyde peaks and disappearance of the vinylic peaks of the starting material monitored by ^{1}H-NMR of the crude product mixture confirmed that the ozonolysis of $\Delta^{6'7}$-cholesterol was successful (Figure 2.5).

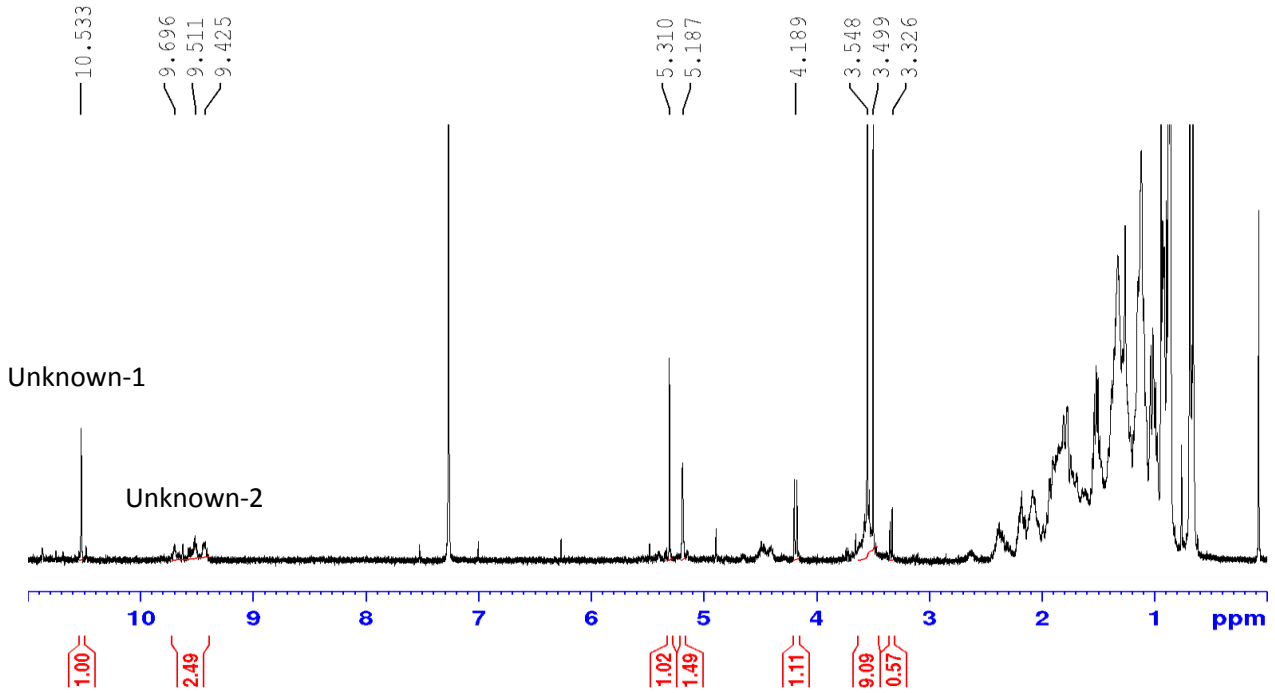

Figure 2.5. ^{1}H-NMR spectrum of crude product mixture of $\Delta^{6'7}$ cholesterol ozonolysis followed by Me_2S work up. The spectrum was collected at 400 MHz with chemical shifts reported in ppm relative to $CDCl_3$.

Flash chromatography was used in an attempt to isolate the individual products. The first product (hereafter will be referred to Unknown-1) to elute was one of the apparently major product characterized by the peak at 10.5 ppm (Figure 2.6).

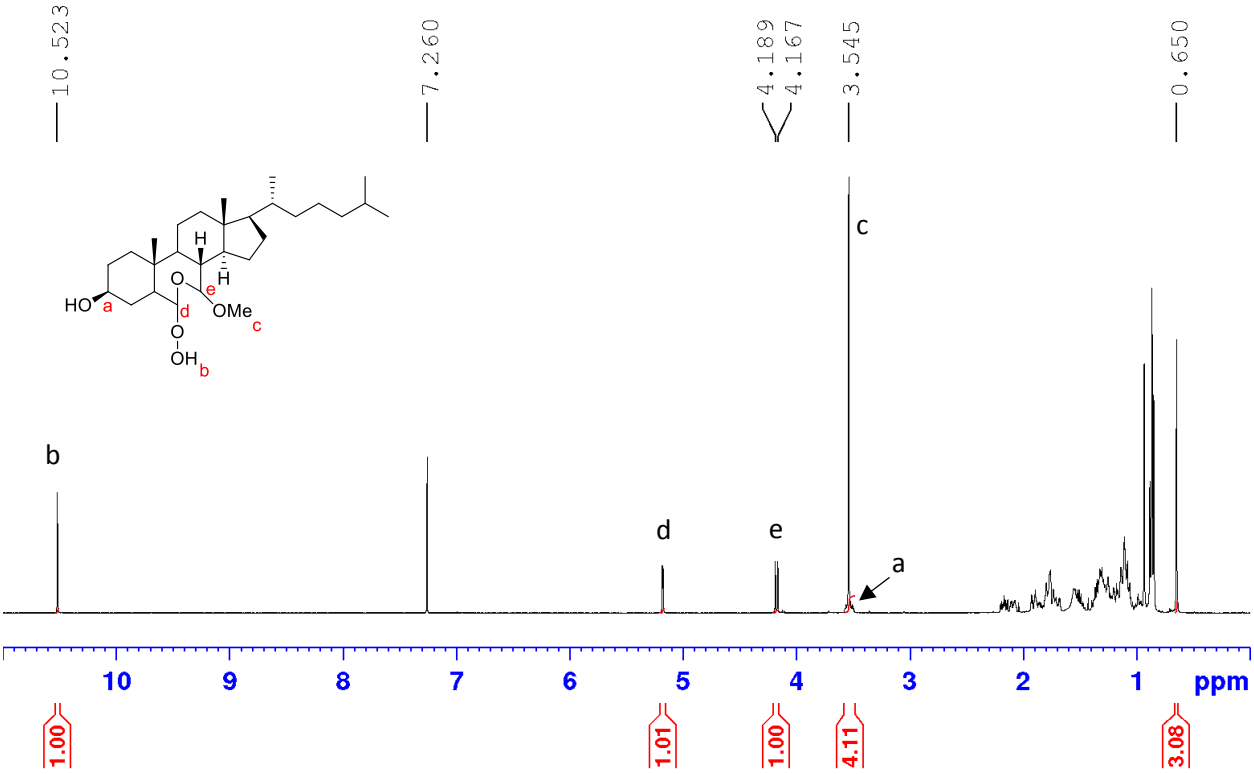

Figure 2.6. ^{1}H-NMR spectrum of Unknown-1 obtained from ozonolysis of $\Delta^{6,7}$-cholesterol followed by Me_2S work up. The tentatively assigned structure is also shown. The spectrum was collected at 400 MHz with chemical shifts reported in ppm relative to $CDCl_3$.

The signal tentatively assigned to proton-b exchanged with deuterium upon addition of D_2O to the sample, albeit slowly. This peak is within the chemical shift range of carboxylic acid protons that could arise from over ozonisation (over oxidation). However, the corresponding ^{13}C-NMR showed no peak characteristic of a carboxylic acid.

A sharp singlet peak, peak-c, corresponding to three protons had the characteristics of methoxy protons formed from incorporation of methanol. Ozonolysis of cholesterol has been reported to yield solvent-participated products,[19] but only if alcoholic solvents were used while herein we mainly used chloroform. Furthermore, our earlier attempts in cholesterol ozonolysis never yielded a product wherein solvent was incorporated. Since similar reaction conditions were used for ozonolysis of cholesterol and $\Delta^{6'7}$-cholesterol we were suspicious that the difference in their work up was causing this inconsistency where in one case we got clear secosterol-A and secosterol-B and in the other case we got a messier product mixture with apparent solvent incorporation. Therefore, a mixture of cholesterol and $\Delta^{6'7}$-cholesterol were ozonolyzed and the resulting ozonides were reduced by Me_2S (Figure 2.7).

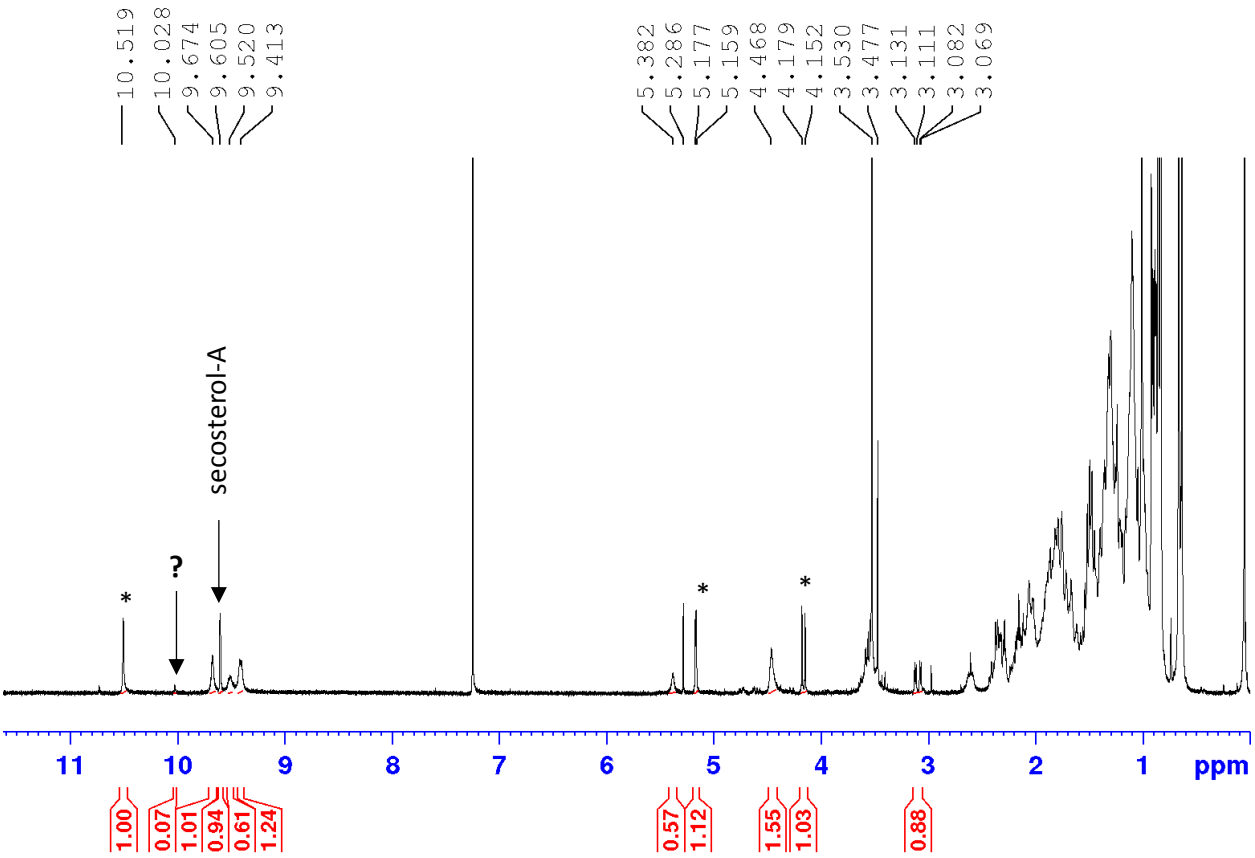

Figure 2.7. ^{1}H-NMR spectrum of crude product mixture of cholesterol and $\Delta^{6,7}$-cholesterol ozonolysis followed by Me_2S work up. The spectrum was collected at 400 MHz with chemical shifts reported in ppm relative to $CDCl_3$. * Unknown-1.

After separation and isolation of the individual products we obtained the precedented solvent-incorporated product: 7α-methoxy-3β-hydroxy-5α-B-homo-6-oxacholestane-5-hydroperoxide (Figure 2.8).[20, 21, 22]

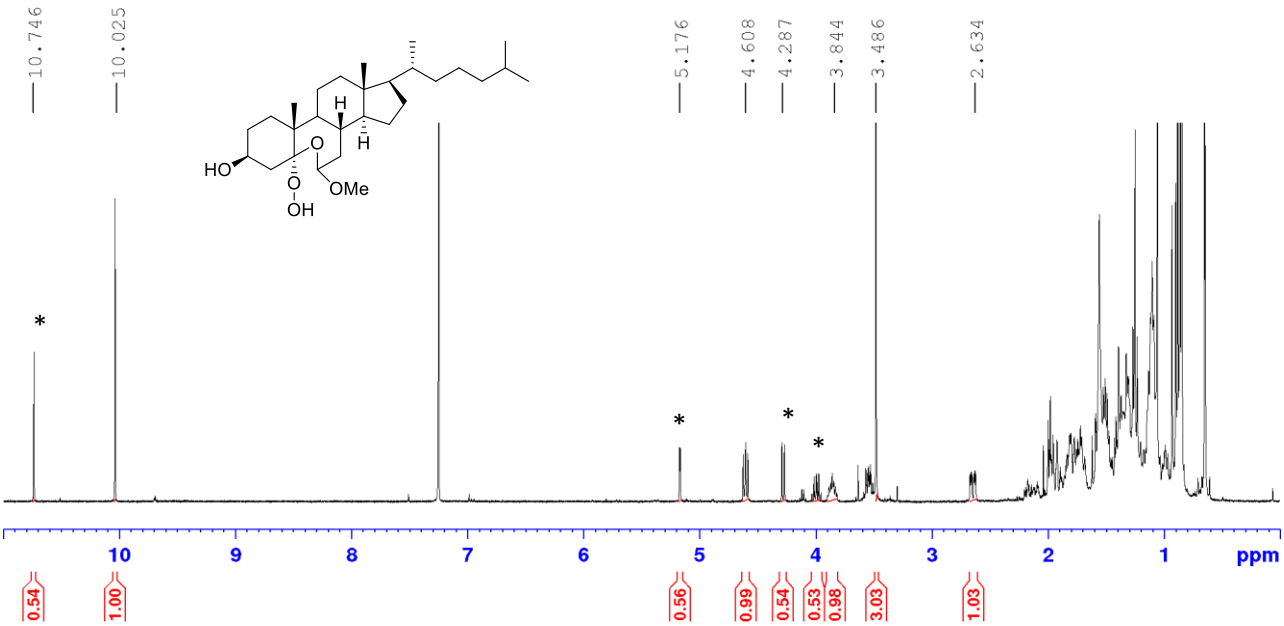

Figure 2.8. ^{1}H-NMR spectrum of 7α-methoxy-3β-hydroxy-5α-B-homo-6-oxacholestane-5-hydroperoxide obtained from ozonolysis of cholesterol followed by Me_2S work up. The spectrum is in accordance with literary reported spectra.[7, 8, 9] * impurity peaks. The spectrum was collected at 400 MHz with chemical shifts reported in ppm relative to $CDCl_3$.

Our multiple attempts to separate and isolate the rest of the mass balance of the $\Delta^{6,7}$-cholesterol ozonolysis products were not successful as the second fraction consistently consisted of a mixture of two products (hereafter will be referred to Unknown-2) (Figure 2.9). The two products consistently co-eluted with the ratio of 1:0.6. In order to see if any of these products was the anticipated dialdehyde or aldolized product (cf. Scheme 2.1), we added acid to the mixture. Aldolization is acid catalyzed therefore we expected to see a change in the ratio of the products. We dissolved the mixture in 0.1 M *p*-toluenesulfonic acid (PTSA) and stirred it at room

temperature for 20 minutes. The ratio of the two products did not change. We obtained the same results when we increased the acid concentration to 1 M PTSA (Figure 2.9).

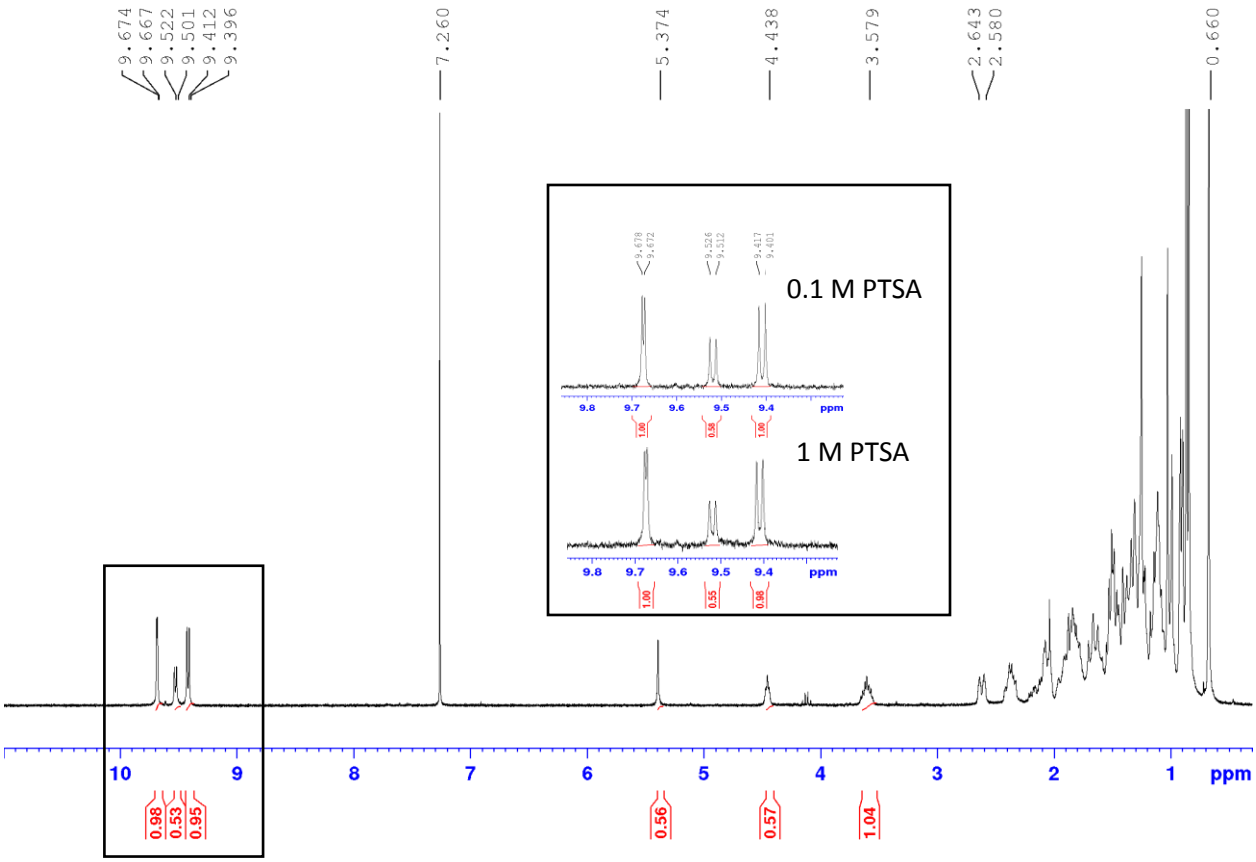

Figure 2.9. ^{1}H-NMR spectrum of the Unknown-2 mixture isolated from crude product mixture of $\Delta^{6,7}$-cholesterol ozonolysis. The spectrum was collected at 400 MHz with chemical shifts reported in ppm relative to $CDCl_3$. Inset: aldehyde region at different PTSA concentration.

In order to see if there is an equilibrium between these two products or if one would be able to convert to the other, we looked at the ratio between the peaks at different temperatures. As a matter of fact, the ratio between these two products changed as we increased the

temperature up to 50°C but adapted the initial ratio when we cooled down the sample to room temperature (Figure 2.10).

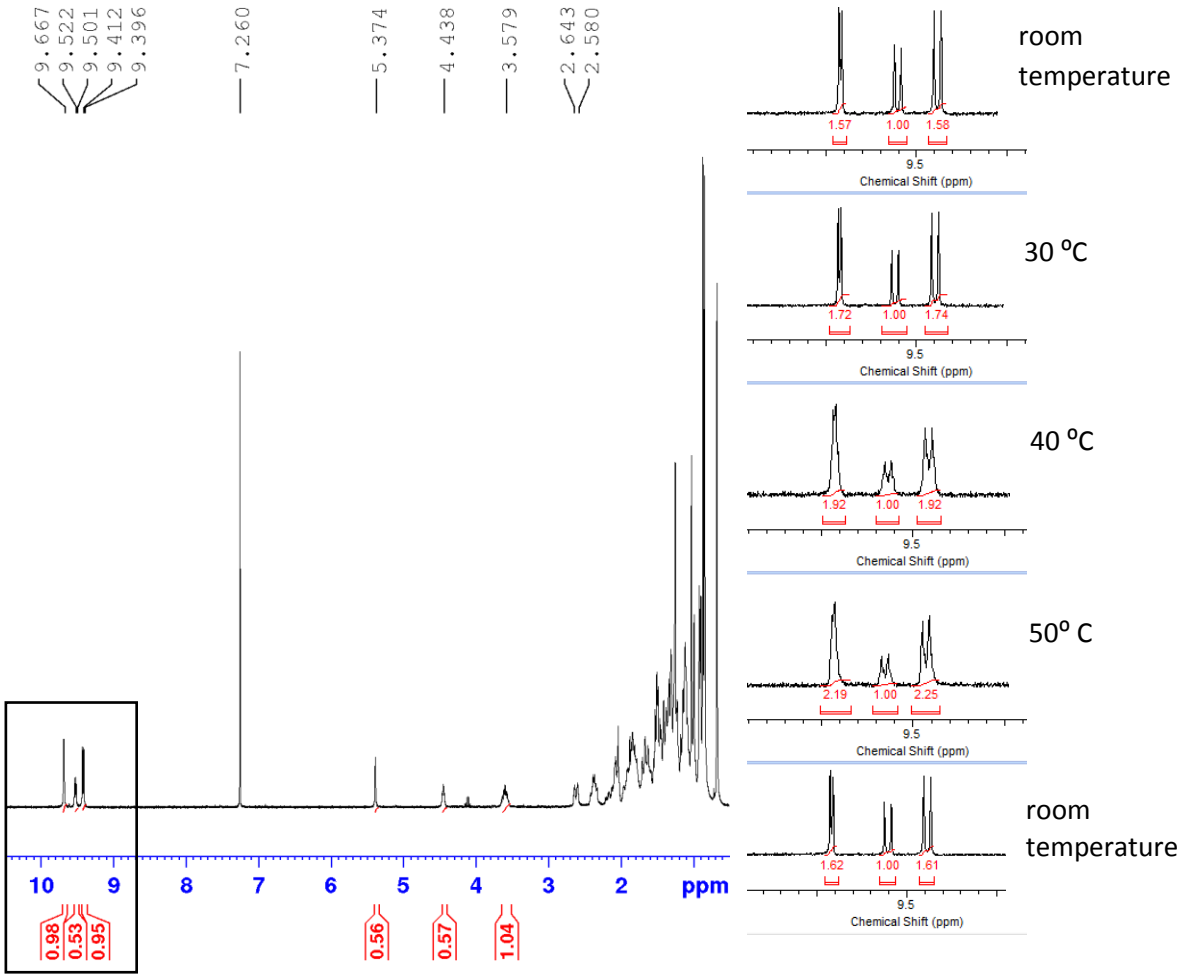

Figure 2.10. ^{1}H-NMR spectrum of the Unknown-2 mixture isolated from crude product mixture of $\Delta^{6,7}$-cholesterol ozonolysis. The spectrum was collected at 400 MHz with chemical shifts reported in ppm relative to $CDCl_3$. Inset: aldehyde region at different temperature- in order of change from top to bottom.

We proposed that Unknown-2 is a mixture of a dialdehyde structure and a hemi-acetal structure. Therefore, we oxidized the mixture by PCC in chloroform where we obtained

cholesterol-derived lactone confirming the generation of hemi-acetal from ozonolysis of $\Delta^{6'7}$-cholesterol (Figure 2.11).

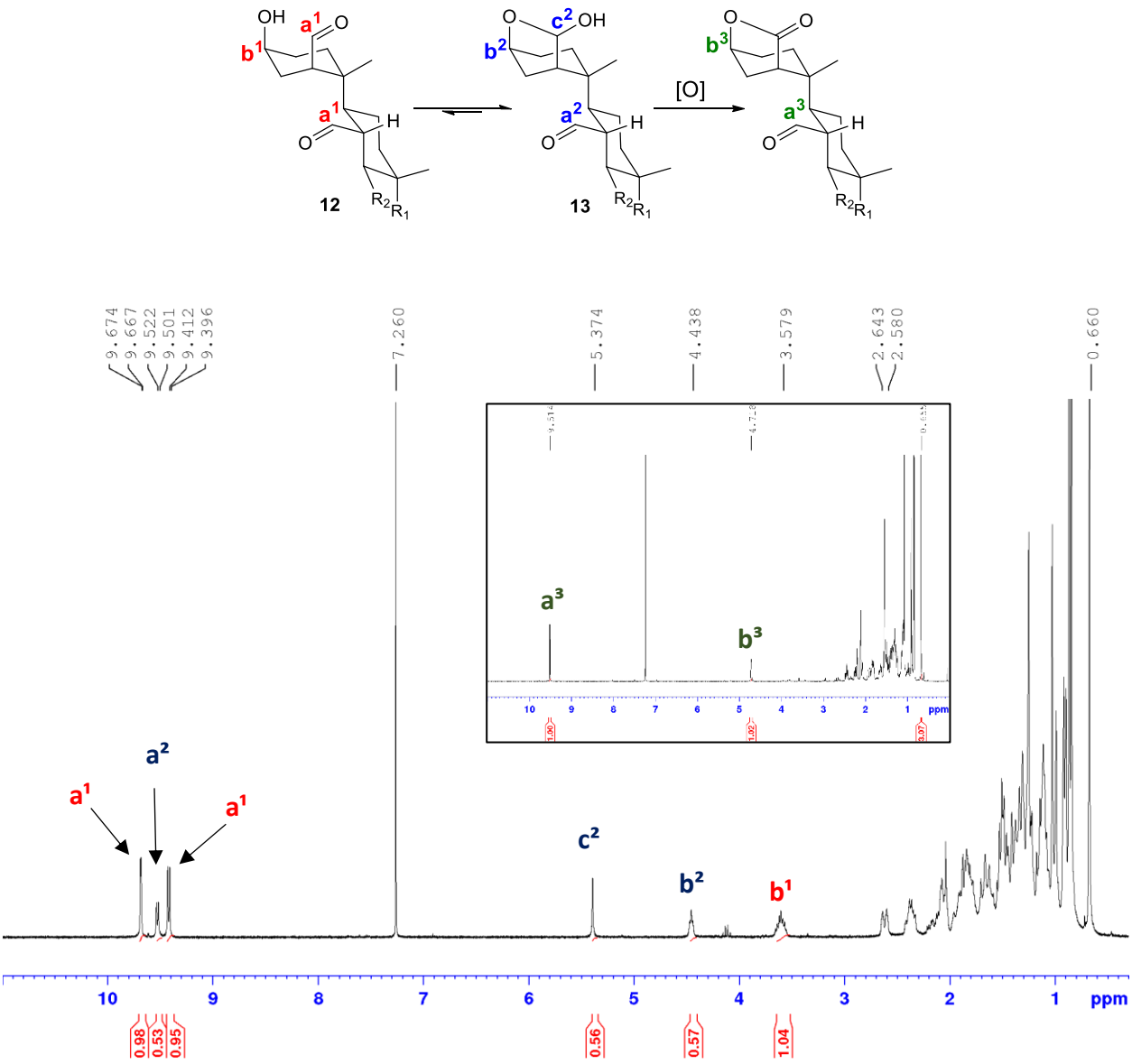

Figure 2.11. ^{1}H-NMR spectrum of the Unknown-2 mixture (Structures **12** and **13**) isolated from crude product mixture of ozonolysis of $\Delta^{6'7}$-cholesterol. The spectrum was collected at 400 MHz with chemical shifts reported in ppm relative to $CDCl_3$. Inset: Oxidized product of the hemi-acetal structure.

The crude product mixture of $\Delta^{6,7}$-cholesterol ozonolysis was also subjected to DNPH derivatization conditions. The hydrazones were injected to UPLC-MS along with DNPH derivatized secosterol-A and secosterol-B for comparison (Figure 2.12).

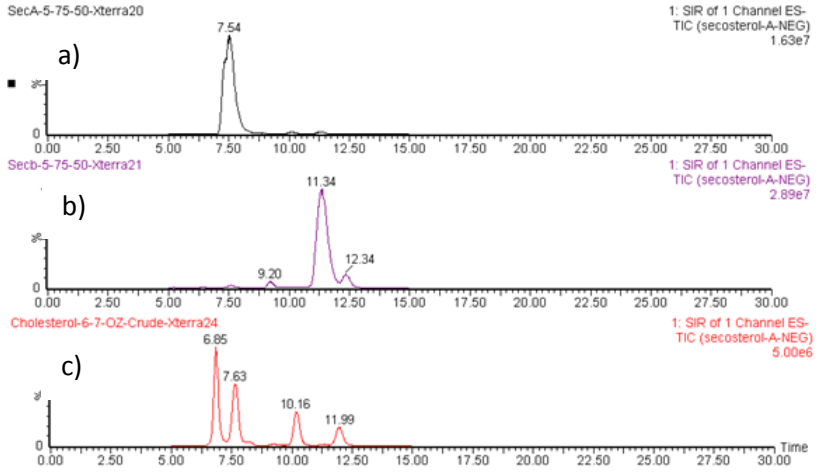

Figure 2.12. Hydrazones derived from secosterol-A (a), secosterol-B (b) and ozonolysis of $\Delta^{6,7}$-cholesterol (c). UPLC-MS analyses were performed on a C18 column (2.5 µm- 4.6 x 75 mm) with ESI^- detection (597 *m/z*). Mobile phase: 75% ACN, 20% MeOH, 5% H_2O (0.5 mL/min).

2.2.4. Computational Studies[†]

The relative energy difference between the dialdehyde structure and the anticipated aldolized products were calculated. For simplicity, the D-ring and the alkyl chain of the cholesterol were omitted from our calculations. The energy of the anticipated aldolized products were 5.5 and 6.1 kcal/mol lower than the dialdehyde structure, **11** (Figure 2.13). The method employed to calculate the energies was B3P86/6-311G (d, p).[23, 24]

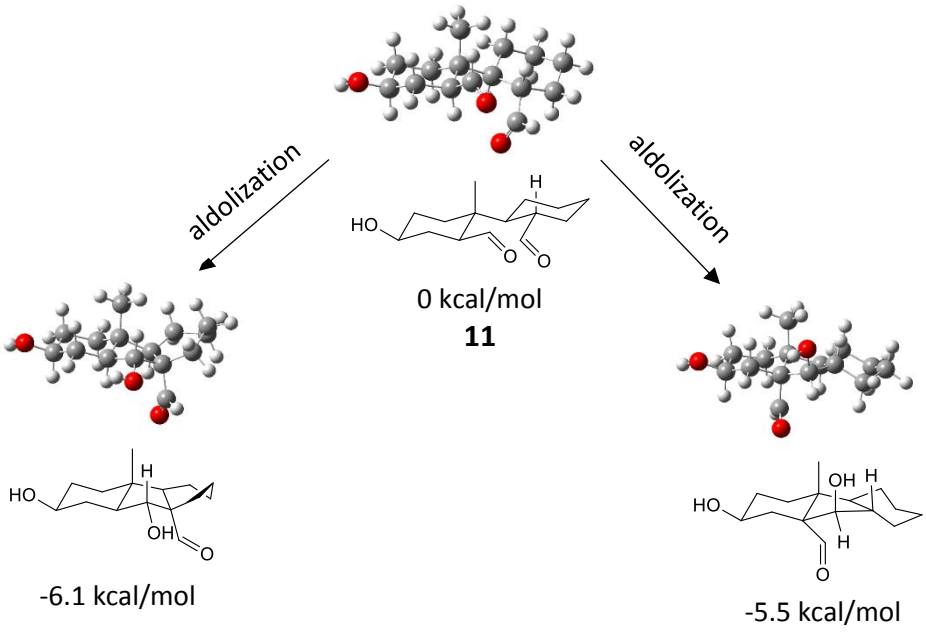

Figure 2.13. DFT calculations of the energy difference between the anticipated dialdehyde structure, **11**, and the corresponding aldolized products.

[†] All the DFT calculations were carried out by Zosia Zielinski, a doctoral candidate in the Pratt group.

Since the formation of the hemi-acetal proposed above (cf. Figure 2.11) requires ring-A of cholesterol backbone to flip, we investigated the conformational equilibria between different possible configurations. By opening the B-ring of the sterol framework, the rigidity of the cholesterol backbone decreases- it allows ring flips, bond rotations and even sometimes both. We calculated the relative energies of different dialdehyde conformations compared to the dialdehyde in its original conformation,**11** (Figure 2.14).

We can see that the structure obtained from a ring flip, **12**, and the one obtained from bond rotation, **14**, are lower in energy compared to the original dialdehyde conformation, **11**, by 3.6 kcal/mol and 3.9 kcal/mol respectively. Bond rotation in addition to a ring flip results in a conformation, **15**, that is 1.9 kcal/mol higher in energy than **11.** Structure **12** has the hydroxyl group and one of the aldehyde groups in close proximity to one another, where they can react to form a hemi-acetal structure, **13**. The hemi-acetal structure, **13**, is 6.1 kcal/mol lower in energy than the dialdehyde structure, **11** (Figure 2.14).

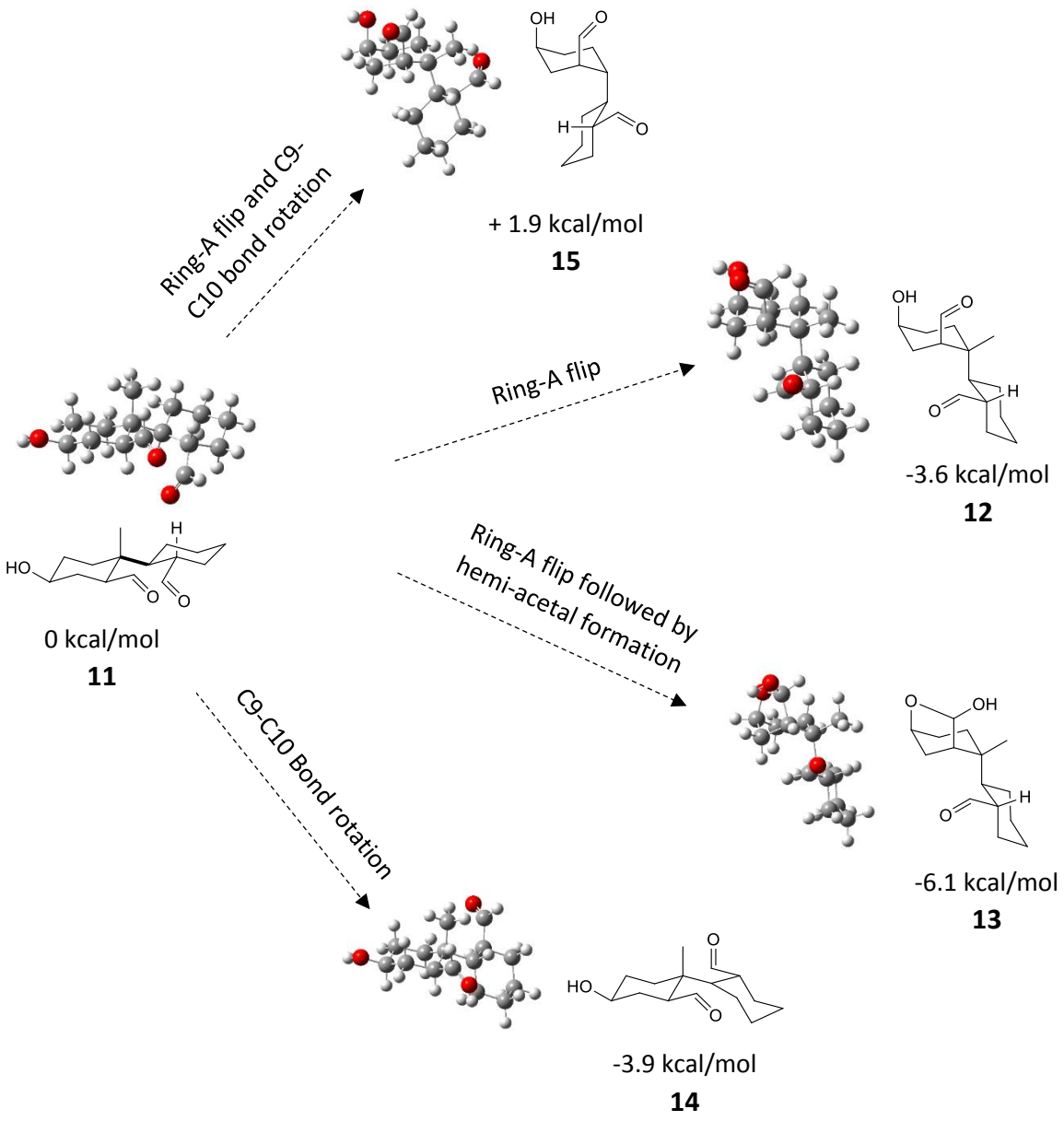

Figure 2.14. DFT calculations of the energy difference between the anticipated dialdehyde structure, **11** and its different conformations, **12**, **14**, **15**. The hemi-acetal , **13** derived from **12** is also shown.

2.3 Discussion

Ozone, a very powerful oxidant, readily attacks ethylenic linkages, resulting in separation of carbon atoms originally connected by a double bond. In 1975, Criegee suggested that ozone undergoes a [3+2] cycloaddition with the alkene to yield a cycloadduct that is generally referred to as the primary ozonide (Scheme 2.5).[25] This compound rapidly decomposes to carbonyl and carbonyl oxide products which, in a non-polar solvent, can rapidly recombine to give a so-called secondary ozonide. The secondary ozonide can be reduced to carbonyls by reducing agents such as Zn/AcOH, Me_2S, Ph_3P, Me_3P and $(NC)_2C=C(CN)_2$. The primary ozonide can also rearrange to form the intermediate Criegee zwitterion (peroxyepoxide) which upon removal of oxygen forms the corresponding epoxide.[26]

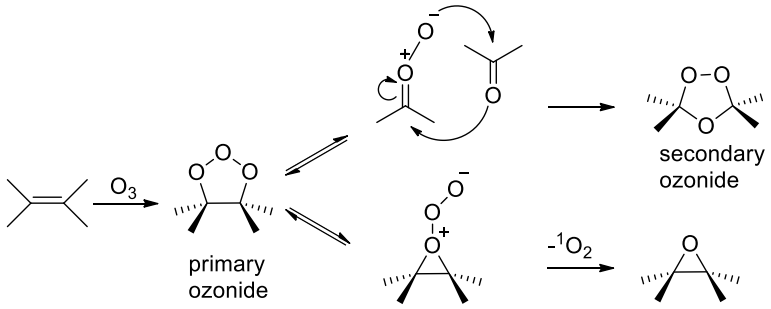

Scheme 2.5. Accepted mechanism of ozonolysis of an alkene.

Cholesterol, just like any other unsaturated lipid, reacts rapidly with ozone. In 1983, Gumulka and Smith identified that 3β-hydroxy-5-oxo-5,6-secocholestan-6-al (secosterol-A) is the major product of cholesterol ozonolysis in non-alcoholic solvents .[27] They investigated the effect of solvent participation in cholesterol ozonolysis product formation. Ozonolysis of cholesterol in

non-participating organic solvents such as chloroform generated the secondary ozonide (Scheme 2.6), **17**, which was reduced with zinc in acetic acid to yield secosterol-A, **18**, as the major product. However, when they performed the same reaction in chloroform with 50% methanol or ethanol, they reported that the corresponding alkoxy-peroxides were formed which, in 1990 was corrected to be alkoxy-hydroperoxide, **20**, by Paryzek, *et. al*. based on their extensive NMR studies.[28] Moreover, in 1997, the X-ray analysis confirmed that the product of cholesterol ozonolysis in a participating (alcoholic) solvent is in fact the proposed alkoxy-hydroperoxide, **20**.[29]

The ozonolysis that takes place in aqueous (or biphasic) media rather than organic solvent is more relevant to biological systems; however, little is known about cholesterol ozonolysis in aqueous system. We can anticipate that this could be due to the insolubility of cholesterol in aqueous media and also the explosive nature of ozone at temperatures above 0°C. However, Gumulka and Smith ozonized a 1 mg/mL aqueous dispersion of cholesterol at room temperature for two hours and obtained hydroxy-hydroperoxide, **19**, as their major product, and secosterol-A and isomeric 5,6 epoxides as their minor products. Interestingly, hydroxy-hydroperoxides, **19**, were converted to secosterol-A within 48 hours in the presence of water making secosterol-A the final major product of cholesterol ozonolysis in aqueous media.[30] Both research groups found corresponding alkoxy-hydroperoxide, **20**, as the major product when the reaction was done in a mixture of water and methanol (or ethanol). Both research groups recommended that Criegee mechanism can explain the observed product distribution of cholesterol ozonolysis in different media (Scheme 2.6).

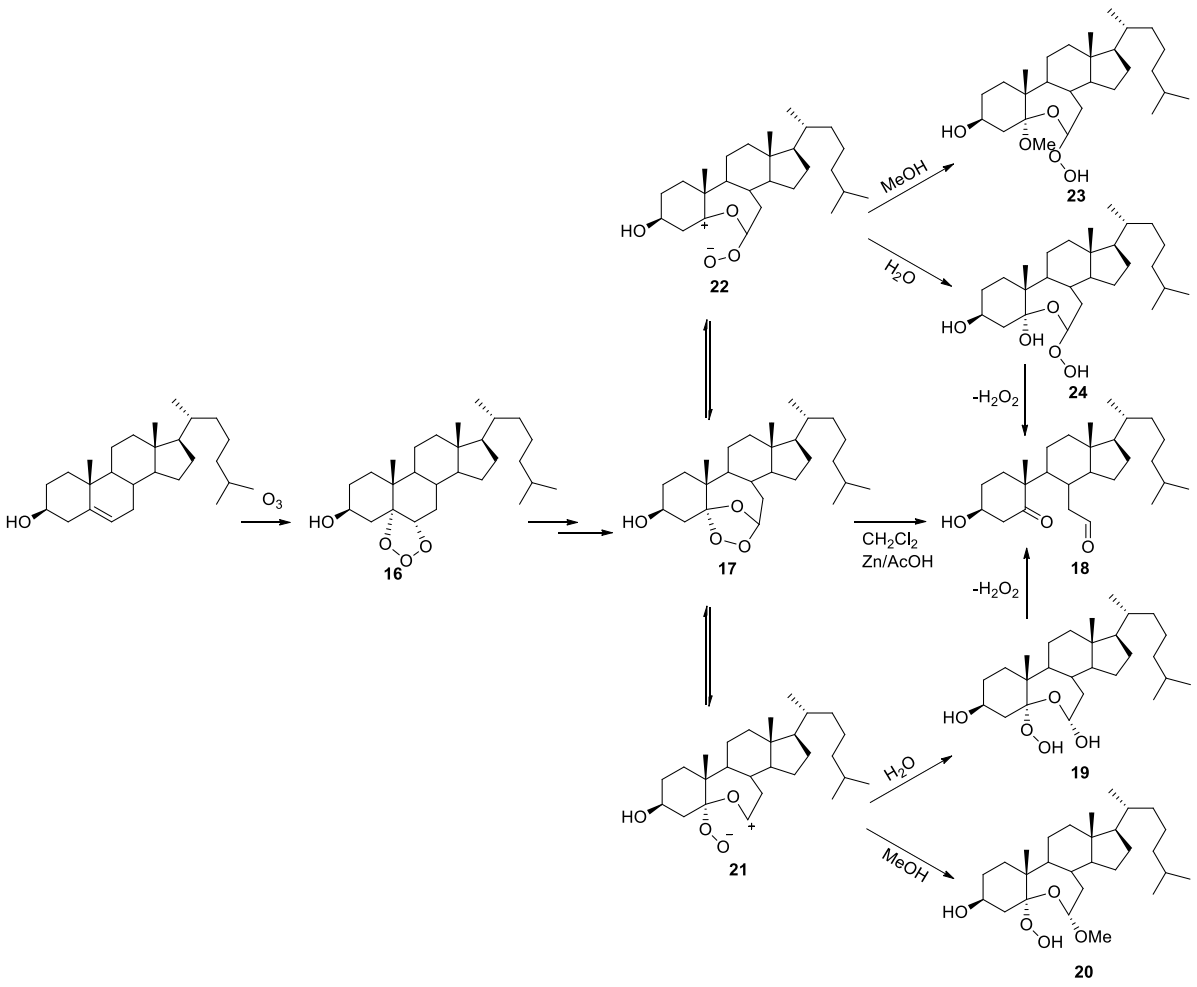

Scheme 2.6. Proposed mechanism of ozonolysis of cholesterol in participating (i.e. nucleophilic) and non-participating solvents.

To avoid the incorporation of methoxy group into the product, only 10% methanol was used to maintain the solution of chloroform at -78°C. We observed incorporation of methanol when the dimethylsulfide was used to reduce the secondary ozonide but no methanol incorporation was observed when zinc/acetic acid work-up was employed. This could be due to the difference in reduction rate of each reducing agent and/or the solvent that was used for each

reagent to reduce the secondary ozonide. The secondary ozonide is in equilibrium with the proposed zwitterions (**21** and **22**, cf. Scheme 2.6). If the reducing agent is slow and reduction is taking place in methanol, then there would be a higher probability for methanol to capture the ion and form the alkoxy-hydroperoxide (**20** and **23**). Reduction with zinc took place in acetic acid and water, hence no alkoxylated product was observed.

The ozonolysis of $\Delta^{6'7}$-cholesterol was carried out under the same reaction conditions. However, we obtained more of the methoxylated product from ozonolysis of $\Delta^{6'7}$-cholesterol compared to cholesterol (Figure 2.6). The cholesterol-derived methoxylated hydroperoxide was less than 1% of the total products formed via cholesterol ozonolysis, while the $\Delta^{6'7}$-cholesterol-derived methoxylated hydroperoxide was more than 30% of the total products formed via ozonolysis of $\Delta^{6'7}$-cholesterol. This can be due to the difference in the reactivity of the intermediates (the secondary ozonide and the zwitterions) derived from $\Delta^{6'7}$-cholesterol from those that are formed from cholesterol (Scheme 2.7). In this case, both zwitterions derived from $\Delta^{6'7}$-cholesterol (**25** and **26**) consist of secondary carbocation centres as opposed to zwitterions derived from cholesterol (**21** and **22**), where one had a secondary and the other a tertiary carbocation centre. This is consistent with the fact that the secondary ozonide derived from ozonolysis of $\Delta^{6'7}$-cholesterol may be more reactive to nucleophilic solvent.

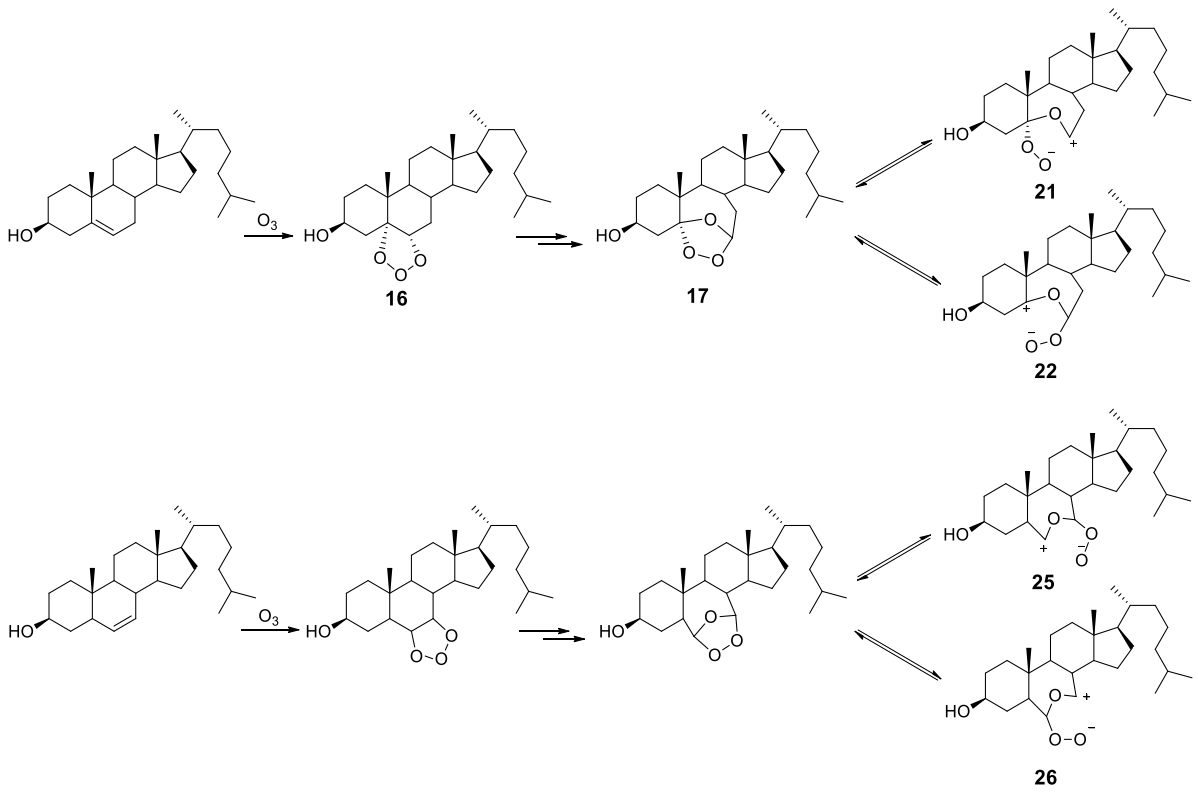

Scheme 2.7. Secondary ozonide and corresponding zwitterions derived from $\Delta^{6'7}$-cholesterol and cholesterol.

The structure of Unknown-1 was assigned using some characteristic peaks in its ^{1}H-NMR spectrum, one of which is a sharp singlet at 3.55 ppm (Peak-c, cf. Figure 2.4) assigned as methoxy protons due to its chemical shift, integration of 3H's and multiplicity of a sharp singlet peak. Peak-b could not be assigned as an aldehyde proton since it was in an exceptionally low-field region and was away from other aldehyde peaks in the region between 9.4-9.7 ppm. More importantly, this peak disappeared when D_2O was added. Accordingly, a peak at 10.53 ppm is right within the range of a carboxylic acid proton that could arise from over ozonisation (over oxidation) of the

cholesterol. However, the corresponding ^{13}C NMR reveled no quaternary carboxylic acid carbon peak.

On the other hand, hydroperoxides in general are characterized by low-field signals in their spectra.[31] The alkoxy-hydroperoxide derived from ozonolysis of cholesterol in participating solvent has a signal at around 10 ppm, which was assigned to the hydroperoxy proton by multiple research groups.[32,33] Therefore, using the Criegee mechanism, we proposed the following structure and assigned the peaks as shown in Figure 2.6. The assigned structure correlates with the corresponding C^{13} NMR and DEPT-135 spectra as well as HMQC data.

The next fraction was a mixture of two products (Unknown-2) which eluted out of the column with a consistent ratio of 1:0.6 every time. This suggests that the mixture of these two products might be in equilibrium. At first, it seemed that Unknown-2 is possibly a mixture of the dialdehyde, **11**, and one of the anticipated aldolized products (Scheme 2.1).

Since aldolization is acid catalyzed, we added acid to the mixture to push the equilibrium toward the aldolized product but the ratio of the products did not change by increasing the acid concentration. The lack of disappearance of the dialdehyde peaks suggested that the dialdehyde structure was not capable of aldolizing (even after addition of acid). By contrast, our DFT calculations[‡] showed that the aldolized products are much lower in energy (5.5 and 6.1 kcal/mol) than the anticipated dialdehyde structure, **11**. Intramolecular aldolization depends on the distance of the aldehyde groups in the structure. If the most stable conformation pushes the

[‡]All the DFT calculations were carried out by Zosia Zielinski, a doctoral candidate in the Pratt group.

aldehyde groups far away from each other in space, then the rate slows down. This led us to propose the following mechanism to justify the observed results (Scheme 2.8).

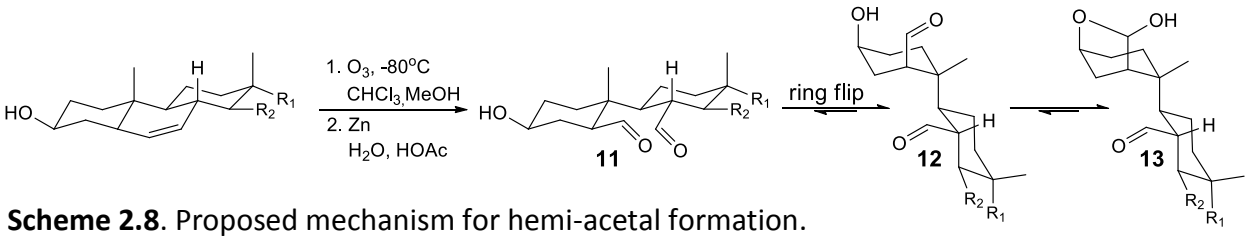

Scheme 2.8. Proposed mechanism for hemi-acetal formation.

Breakage in ring-B of the cholesterol backbone allows ring-A to flip to form the dialdehyde structure, **12**. This places the two aldehyde groups far away from each other, decreasing their ability to react with one another and aldolize. This new configuration, however, put the aldehyde and hydroxyl group in a close proximity to one another, and their reaction can form the corresponding hemiacetal, **13**. Since **12** and **13** are in equilibrium and they have similar chromatographic characteristics, we decided to oxidize the hemi-acetal to a lactone to be able to separate them. Upon multiple purifications the lactone product was isolated, which supported the presence of the hemi-acetal structure in our mixture.

The relative energy of the hemi-acetal structure, **13**, to the ring-flipped dialdehyde structure, **12**, was calculated. Unexpectedly, the hemi-acetal structure was 2.5 kcal/mol more stable than **12**. This was somewhat contradictory to our experimental results. The theoretical ratio of dialdehyde to hemi-acetal which was calculated using the energy difference between **12** and **13** is 1:59. However, the experimental ratio of dialdehyde to hemiacetal is 1:0.6. This indicates that the dialdehyde structure, **12**, is more stable than hemiacetal, **13**, which, contradicts

our computational results. Even though we are comparing gas phase calculations to condensed phase measurements, we still expected to predict relative energies well.

Structure **12** is lower in energy compared to **11** by 3.6 kcal/mol, however, the structure obtained from bond rotation, **14**, is even more stable by 3.9 kcal/mol. Nonetheless, this structure seems to be inert to any further intramolecular reactions since all of its functional groups are further apart in space. Bond rotation in addition to ring flip, **15**, locates the aldehyde and hydroxyl groups in close proximity to one another to form the hemi-acetal but this structure is 1.9 kcal/mol higher in energy than **11**. Hence, formation of hemi-acetal through **15** is generally omitted due to its high energy. Amongst the two thermodynamically stable products, **12** is the only possible primary precursor for hemiacetal structure. While almost all of **12** gets converted to **13**, structure **14** is inert to further intramolecular reactions; therefore, the observed experimental ratio should be due to the distribution between **12** and **14**. As a matter of fact, the theoretical ratio calculated using computational energy differences (0.3 kcal/mol) between **12** and **14** is analogous to experimental ratio of 1:0.6. However, the increase in temperature changed the product ratio to 1:0.4. We anticipated that by changing the temperature, we affected the equilibrium between **12** and **13** and that changed the ratio of our products.

Nonetheless, the anticipated aldolized products are more stable than **11**, **12** and **14** but we did not observe them in the mixture. We anticipated that the aldolization might not be kinetically favored, even if the final product is lower in energy. Furthermore, the dialdehyde ,**11**, transforms into the two most thermodynamically stable conformations (**12** and **14**) which, are incapable of undergoing aldolization due to distanced aldehydes, hence, the aldolized product was never observed.

The crude product mixture of the ozonolysis of $\Delta^{6'7}$-cholesterol was derivatized by DNPH. The corresponding chromatogram showed multiple hydrazones within the relative retention times of secosterol-A and secosterol-B (Figure 2.13). We can speculate that these are probably hydrazones of dialdehyde conformations **12** and **14** and the proposed hemi-acetal structure **13**. In general, addition of DNPH to these structures traps them in their specific conformations due to steric interactions. Furthermore, the derivatization of structure **12** can prevent the formation of **13**, increasing its concentration to a detectable level. In addition, DNPH derivatization of each aldehyde within a structure might have a different effect on the overall polarity of the structure, increasing the diversity of the products.

In summary, due to the breakage in one of the cholesterol cyclic systems and the resulting flexibility of the cholesterol backbone during ozonolysis, we did not obtain the products that we expected. In addition, methoxylation of the intermediate in ozonolysis of $\Delta^{6'7}$-cholesterol resulted in a by-product lowering our yield which was not ideal either. In general, we realized that ozonolysis of $\Delta^{6'7}$-cholesterol is much more complex and sensitive than ozonolysis of cholesterol due to the reactivity of the intermediates.

2.4. Experimental

All chemicals and solvents were purchased from Sigma Aldrich Co. LLC and used as received, unless otherwise stated. 2,4-dinitrophenylhydrazine (DNPH) was purified by recrystallization from n-butane prior to use. All the carbon assignments correspond to cholesterol back-bone numbering system.

3β-Acetoxy-6-nitrocholest-5-ene (3): A suspension of cholesteryl acetate (5 g) in concentrated HNO_3 (150 mL) was stirred vigorously. $NaNO_2$ salt (3 × 2.5 g) was added at 0, 5 and 10 minutes to the mixture which was stirred vigorously at room temperature under atmospheric pressure for 20 minutes. The reaction mixture was then poured over ice and was incubated in the fridge for an hour. Formed crystals were filtered and dissolved in 600 mL ether and light petroleum mixture (1:1, v/v) and were washed extensively with water and concentrated $NaHCO_3$ solution. The collected ethereal layer was then concentrated to a thick oil under vacuum. The concentrated oil was recrystallized from methanol to give pure 3β-acetoxy-6-nitrocholest-5-ene as white crystals (89 % yield). ^{1}H-NMR (400 MHz, $CDCl_3$) δ 4.63 (m, 1H), 2.75 (dd, *J*=4.4, 13.6 Hz, 1H), 2.14 (s, 1H), 2.12-1.10 (Comp, 27H), 1.11 (s, 3H), 0.90 (d, *J*=6.4 Hz, 3H), 0.85 (dd, *J*= 1.7, 6.4 Hz, 6H), 0.67 (s, 3H). Analytical data were in accordance with those reported in the literature.[34]

***3β-Acetoxycholestan-6-one (4)*:** A sample of 3β-acetoxy-6-nitrocholest-5-ene (2.5 g) in acetic acid (57 mL) and water (7 mL) was stirred and refluxed (115 ^{o}C) until a homogenous solution was formed. Activated zinc powder (0.4 g) was added gradually to the vigorously stirred refluxing solution. More zinc (2 × 0.4 g) was added after 1 and 2 hours, and the reaction was refluxed for another hour. The suspension was dissolved in 400 mL ether and was washed

extensively with water and concentrated $NaHCO_3$ solution. Ether was removed by suction to form a thick oil which was recrystallized from methanol to give pure 3β-acetoxycholestan-6-one as white needle-like crystals (82% yield). ^{1}H-NMR (400 MHz, $CDCl_3$) δ 4.64 (m, 1H), 2.29 (dd, *J*=4.4, 13.6 Hz, 1H), 2.23 (dd, *J*= 3.4, 13.4 Hz, 1H), 2.03 (t, *J*= 3.4 Hz, 1H), 2.00-0.92 (Comp, 29H), 0.88 (d, *J*=6.4 Hz, 3H), 0.84 (dd, *J*= 1.7, 6.4 Hz, 6H), 0.74 (s, 3H), 0.63 (s, 3H). Analytical data were in accordance with those reported in the literature.[31]

3β-Acetoxy-7-bromocholestan-6-one (5): To a solution of 3β-acetoxycholestan-6-one (2 g) in glacial acetic acid (10 mL) and distilled ether (23 mL) incubated in an ice bath, bromine (215 µl) was added dropwise. The resulting solution was then refluxed at 50 ^oC for 26 hours. The resulting mixture was concentrated to a small volume under vacuum. The concentrated solution was incubated in an ice bath while ice-cold water was added to form a brown solid precipitation. The precipitate was filtered and dissolved in a methanol/acetone mixture for recrystallization to give pure 3β-acetoxy-7-bromocholestan-6-one as fine white crystals. (45% yield). ^{1}H-NMR (400 MHz, $CDCl_3$) δ 4.71 (m, 1H), 4.16 (d, *J*=3.4 Hz, 1H), 3.26 (dd, *J*= 2.7, 12.4 Hz, 1H), 2.00-0.92 (Comp, 29H), 0.90 (d, *J*=6.4 Hz, 3H), 0.85 (dd, *J*= 1.7, 6.4 Hz, 6H), 0.75 (s, 3H), 0.67 (s, 3H). Analytical data were in accordance with those reported in the literature.[12]

3β-Acetoxycholestan-6-ene (6)**:** To a solution of 3β-acetoxy-7-bromocholestan-6-one (1.4 g) in *iso*-propanol (50 mL) was added a solution of sodium borohydride (14 mg) in *iso*-propanol (34 mL). The reaction mixture was stirred at room temperature for 3 hours and the excess hydride was decomposed by dilute sulphuric acid. The resultant reaction mixture was concentrated under vacuum to form a thick oil which was diluted by ether (200 mL) and methylene chloride (20 mL) and was washed with water extensively. The collected ethereal layer

was dried by magnesium sulphate and concentrated to a thick oil under vacuum. The oily residue was dissolved in acetic acid (100 mL) where zinc dust (20 mg) was slowly added to the mixture. The reaction mixture was refluxed for 30 minutes. The hot solution was filtered and the filtrate was concentrated to half the volume under the reduced pressure. The concentrated solution was diluted by ether and was washed with water multiple times. The ethereal layer was concentrated by vacuum to a light-yellow solid which was recrystallized from an ethanol/water mixture to give pure 3β-acetoxycholestan-6-ene as white flat crystals (52% yield). ^{1}H-NMR (400 MHz, $CDCl_3$) δ 5.46 (d, *J*= 13.6 Hz, 1H), 5.22 (d, *J*= 13.6 Hz, 1H), 4.71 (m, 1H), 2.10-0.90 (Comp, 30H), 0.88 (d, *J*=6.4 Hz, 3H), 0.84 (dd, *J*= 1.7, 6.4 Hz, 6H), 0.77 (s, 3H), 0.67 (s, 3H). Analytical data were in accordance with those reported in the literature.[12]

$\Delta^{6'7}$-Cholesterol (1): A solution of 3β-acetoxycholestan-6-ene (1.0 g) and NaOH (0.2 g) in methanol (50 mL) was boiled at 70 ^{o}C for 2 hours. The resulting solution was then poured into a mixture of EtOAc and 5% citric acid (1:1, v:v) and the organic phase was washed with water multiple times. Magnesium sulphate was used to dry the organic layer, which was then concentrated under vacuum. The solid residue was recrystallized from methanol to give pure $\Delta^{6'7}$-cholesterol as white flat crystals (93% Yield). ^{1}H-NMR (400 MHz, $CDCl_3$) δ 5.46 (d, *J*= 13.6 Hz, 1H), 5.22 (d, *J*= 13.6 Hz, 1H), 3.75 (m, 1H), 2.00-0.90 (Comp, 28H), 0.88 (d, *J*=6.4 Hz, 3H), 0.84 (dd, *J*= 1.7, 6.4 Hz, 6H), 0.77 (s, 3H), 0.67 (s, 3H). Analytical data were in accordance with those reported in the literature.[12]

3β-Hydroxy-5-oxo-5,6-secocholestan-6-al (secosterol-A) (7): A solution of cholesterol (1.0 g) in a mixture of chloroform (90 mL) and methanol (10 mL) (9:1, v:v) was ozonized at -78 ^{o}C for 30 minutes. Me_2S work up: Me_2S (1.5 mL) was added to the product mixture, which was stirred in an ice bath for 2 hours. The mixture was concentrated under vacuum and was used for analysis as a crude product mixture. Zinc work up: the reaction mixture was stirred in an ice bath under vacuum to remove chloroform. The concentrated product mixture was re-dissolved in acetic acid (45 mL) and water (5 mL), and zinc powder (0.65 g) was added and the mixture was stirred at room temperature for three hours. The product mixture was then diluted with dichloromethane (100 mL) and washed with water three times (3 × 50 mL). The organic layer was collected and dried over magnesium sulphate, then concentrated under vacuum. The product was purified by a preparative silica column (ethyl acetate: hexane, 1:5) to give pure secosterol-A as a white solid (62% yield). ^{1}H-NMR (300 MHz, $CDCl_3$) δ 9.59 (bs, 1H), 4.46 (m, 1H), 3.09 (dd, *J*= 4.0,13.9 Hz, 1H), 2.10-1.00 (Comp, 28H), 0.99 (s, 3H), 0.87 (d, *J*=6.4 Hz, 3H), 0.83 (dd, *J*= 1.7, 6.4 Hz, 6H), 0.65 (s, 3H). Analytical data were in accordance with those reported in the literature.[1]

3β-Hydroxy-5β-hydroxy-B-norcholestane-6β-carboxaldehyde (secosterol-B) (8): L-proline (42 mg) was added to a solution of secosterol-A (150 mg) in acetonitrile (9.5 mL) and water (0.5 mL) (19:1, v:v) and the reaction mixture was stirred for 2 hours at room temperature. The product mixture was concentrated under vacuum and was re-dissolved in ethyl acetate (20 mL) and washed with water (3 × 10 mL). The organic layer was dried over magnesium sulphate and was concentrated under vacuum. A preparative silica column (ethyl acetate: hexane, 1:5) was used to purify the product to give secosterol-B as a white solid (83% yield). ^{1}H-NMR (300 MHz, $CDCl_3$) δ 9.68 (d, *J*= 3.1 Hz, 1H), 4.10 (m, 1H), 2.22 (dd, *J*= 2.9, 9.0 Hz, 1H), 2.10-1.00 (Comp,

28H), 0.91 (s, 3H), 0.89 (d, *J*=6.4 Hz, 3H), 0.83 (dd, *J*= 1.7, 6.4 Hz, 6H), 0.68 (s, 3H). Analytical data were in accordance with those reported in the literature.[1]

2,4-Dinitrophenylhydrazone of secosterol-A (9): 2,4-dinitrophenylhydrazine (DNPH) (52 mg) was dissolved in *p*-toluenesulphonic acid (1 mg) and acetonitrile (150 mL) and was stirred at room temperature for 10-20 minutes. Secosterol-A (100 mg) was added to the homogenous DNPH solution and was stirred at room temperature for four hours. The mixture was concentrated under vacuum and the residue was re-dissolved in ethyl acetate (10 mL) which was washed with water (3 × 20 mL). The organic layer was dried over magnesium sulphate and concentrated under vacuum. A preparative silica column (ethyl acetate: hexane, 1:5) was used to give pure hydrazone derivatized secosterol-A as yellow crystals (55% yield). ^{1}H-NMR (500 MHz, $CDCl_3$) δ 10.97 (s, 1H), 9.09 (d, *J*= 2.5 Hz, 1H), 8.29 (dd, *J*= 2.6, 9.4 Hz, 1H), 7.90 (d, *J*= 9.7 Hz, 1H), 7.40 (q, *J*= 6.7 Hz, 1H), 4.40 (m, 1H), 2.96 (dd, *J*= 4.2, 13.6 Hz, 1H), 2.10-1.00 (Comp, 28H), 1.01 (s, 3H), 0.90 (d, *J*=6.4 Hz, 3H), 0.83 (dd, *J*= 1.7, 6.4 Hz, 6H), 0.69 (s, 3H). Analytical data were in accordance with those reported in the literature.[1]

2,4-Dinitrophenylhydrazone of secosterol-B (10)**:** 2,4-dinitrophenylhydrazine (DNPH) (52 mg) was dissolved in 0.1 M HCl in ethanol (150 mL) and was stirred at room temperature for 10-20 minutes. Secosterol-B (100 mg) was added to the homogenous DNPH solution and was stirred at room temperature for four hours. The mixture was concentrated under vacuum and the residue was re-dissolved in ethyl acetate (10 mL), then washed with water (3 × 20 mL). The organic layer was dried over magnesium sulphate and concentrated under vacuum. A preparative silica column (ethyl acetate: hexane, 1:5) was used to give pure hydrazone derivatized secosterol-B as yellow crystals (60% yield). ^{1}H-NMR (400 MHz, $CDCl_3$) δ 11.01 (s, 1H), 9.08 (d, *J*= 2.4 Hz, 1H),

8.25 (dd, *J*= 2.6, 9.8 Hz, 1H), 7.87 (d, *J*= 9.8 Hz, 1H), 7.53 (d, *J*= 7.2 Hz, 1H), 4.19 (m, 1H), 2.31 (dd, *J*= 7.3, 9.0 Hz, 1H), 2.10-1.00 (Comp, 28H), 0.94 (s, 3H), 0.89 (d, *J*=6.4 Hz, 3H), 0.82 (dd, *J*= 1.7, 6.4 Hz, 6H), 0.69 (s, 3H). Analytical data were in accordance with those reported in the literature.[1]

Ozonolysis of $\Delta^{6'7}$-cholesterol: A mixture of $\Delta^{6'7}$ cholesterol (0.75 g) in chloroform (67.5 mL) and methanol (7.5 mL) was ozonized at -78^{o}C for 1 hour. The product mixture was concentrated to a thick oil under vacuum. The concentrated residue was dissolved in acetic acid (34 mL) and water (4 mL), then zinc powder (0.46 g) was added and the reaction was stirred at room temperature for 3 hours. The reaction mixture was diluted in dichloromethane (75 mL) and was washed with water (3 × 50 mL). Sample was dried over magnesium sulphate and was concentrated under vacuum. A preparative silica column (ethyl acetate: hexane, 1:6) was used to separate the products, whose spectral characteristics are provide in Figures 2.5, 2.7, 2.8 and 2.9.

Cholesterol-derived lactone **:** cholesterol-derived hemiacetal (13) (100 mg) was dissolved in dichloromethane (30 mL), and pyridinium chlorochromate (77.2 mg) and celite (800 mg) were added. The reaction mixture was stirred at room temperature under argon for 2 hours. The product mixture was filtered through packed celite and the filtrate was diluted with dichloromethane and was washed with water multiple times. The organic layer was dried by magnesium sulfate and was concentrated under vacuum. Preparative TLC (60G F_{254} on 20 × 20 cm glass plate with Merk Millipore)(ethyl acetate: hexane, 1:4) was used to isolate the lactone product. ^{1}H-NMR (400 MHz, $CDCl_3$) δ 9.51 (d, *J*= 5.5 Hz, 1H), 4.72 (m, 1H), 2.44 (ddd, *J*= 5.5, 10.7 Hz, 1H), 2.27 (m, 2H), 2.20 (t, *J*= 1.9 Hz, 1H), 2.12 (t, J= 1.7 Hz, 2H), 2.07 (m, 2H), 1.90 (m, 1H), 1.84 (m, 1H), 1.80 (m, 2H), 1.63 (m, 2H), 1.55-1.11 (Comp, 13H) , 1.07 (s, 3H), 0.90 (d, *J*=6.4 Hz,

3H), 0.84 (dd, *J*= 1.7, 6.4 Hz, 6H), 0.67 (s, 3H). ^{13}C-NMR (400 MHz, $CDCl_3$) δ 203.5, 176.9, 76.4, 54.5, 52.2, 49.0, 47.5, 41.1, 41.0, 38.6, 38.4, 37.4, 37.2, 35.2, 34.9, 32.1, 28.9, 27.2, 24.9, 23.7, 22.9, 21.9, 21.7, 21.5, 20.3, 17.8, 10.8.

2.5. References

[1] Wentworth Jr, P.; Nieva, J.; Takeuchi, C.; Galve, R.; Wentworth, A. D.; Dilley, R. B.; DeLaria, G. A.; Savan, A.; Babior, B. M.; Janda, K. D.; Eschenmoser, A.; Lerner, R. A. *Science* **2003**, 302, 1053.

[2] Wentworth Jr, P.; Jones, L. H.; Wentworth, A. D.; Zhu, X.; Larsen, N. A.; Wilson, I. A.; Xu, X.; Goddard III, W. A.; Janda, K. D.; Eschenmoser, A.; Lerner, R. A. *Science* **2001**, 293, 1806.

[3] Nieva, J.; Wentworth Jr, P. *Trends. Biochem. Sci.* **2004**, 29, 274.

[4] Wentworth Jr, P.; Wentworth, A. D.; Zhu, X.; Wilson, I. A.; Janda, K. D.; Eschenmoser, A.; Lerner, R. A. *Proc. Natl. Acad. Sci.* **2003**, 100, 1490.

[5] Bieschke, J.; Zhang, Q.; Powers, E. T.; Lerner R. A.; Kelly J. W. *Biochemistry* **2011**, 44, 4977.

[6] Stewart, C. R.; Wilson, L. M.; Zhang, Q.; Pham, C. L.; Waddington, L. J.; Staples, M. K.; Stapleton, D.; Kelly, J. W.; Howlett, G. J. *Biochemistry* **2007**, 46, 5552.

[7] Tomono, S.; Yasue. Y.; Miyoshi, N.; Ohshima, H. *Biochemistry* **2013**, 77, 651.

[8] Bosco, D. A.; Folwer, D. M.; Zhang, Q.; Nieva, J.; Powers, E. T.; Wentworth Jr, P.; Kelly J. W. *Nat. Chem. Biol.* **2006**, 2, 249.

[9] Wentworth Jr, P.; Nieva, J. *Science* **2002,** 298, 2195.

[10] Brinkhorst, J.; Nara, S. J.; Pratt, D. A. *J. Am. Chem. Soc*. **2008**, 130, 12224.

[11] Zielinski, Z. A. M.; Pratt, D. A. *J. Am. Chem. Soc*. **2016**, 138, 6932.

[12] Corey, E. J.; Gregoriou, A. *J. Am. Chem. Soc.* **1959**, 81, 3127.

[13] Halberstadt, E. S.; Hughes, E. D.; Ingold, C. K. *J. Chem. Soc*. **1950**, 2441.

[14] Pryor, W. A.; Wang, K.; Bermúdez, E. *Biochem. Biophys. Res. Commun*. **1992**, 188, 618.

[15] Flippin, L. A.; Gallagher, D. W.; Jalali-Araghi, K. *J. Org. Chem*. **1989**, 54, 1430.

[16] Dai, P.; Trullinger, T. K.; Liu, X.; Dussault, P. H. *J. Org. Chem.* **2006**, 71, 2283.

[17] Greenwood, F. L. *J. Org. Chem.* **1955**, 20, 803.

[18] Chen, L.; Wiemer, D. F. *J. Org. Chem.* **2002**, 67, 7561.

[19] Gumulka, J.; Smith, L. L. *J. Am. Chem. Soc.* **1983**, 105, 1972.

[20] Paryzek, Z.; Martynow, J.; Swoboda, W. *J. Chem. Soc., Perkin Trans.* 1. **1990**, 1222.

[21] Smith, L. L.; Ezell, E. L.; Jaworski, K. *Steroids* **1996**, 61, 104.

[22] Paryzek, Z.; Rychlewska, U. *J. Chem. Soc., Perkin Trans. 2*. **1997**, 2313.

[23] Becke, A. D. *J. Chem. Phys.* **1993**, 98, 5648.

[24] Perdew, J. P. *phys. Rev*. **1986**, 33, 8822.

[25] Criegee, R. *Angew. Chem. Int. Ed. Engl.* **1975**, 14, 745.

[26] Martinez, R. I.; Herron, J. T.; Huie, R. E. *J. Am. Chem. Soc.* **1981**, 103, 3807.

[27] Gumulka, J.; Smith, L. L. *J. Am. Chem. Soc.* **1983**, 105, 1972.

[28] Paryzek, Z.; Martynow, J.; Swoboda, W. *J. Chem. Soc., Perkin Trans. 1.* **1990**, 1220.

[29] Paryzek, Z.; Urszula, R. *J. Chem. Soc., Perkin Trans. 2.* **1997**, 2313.

[30]Gumulka, J.; Smith, L. L. *J. Am. Chem. Soc.* **1983**, 105, 1972.

[31] Lillie, T. S.; Ronald, R. C. *J. Org. Chem*. **1985**, 50, 5084.

[32] Paryzek, Z.; Martynow, J.; Swoboda, W. *J. Chem. Soc., Perkin Trans.* 1. **1990**, 1222.

[33] Paryzek, Z.; Rychlewska, U. *J. Chem. Soc., Perkin Trans. 2*. **1997**, 2313.

[34] Choucair, B.; Dherbomez, M.; Roussakis, C.; El-Kihel, L. *Tetrahedron* **2004**, 60, 11477.

-3-

Hock Fragmentation of Cholesterol 7α- and 7β-Hydroperoxide

3.1 Introduction

Cholesterol 7α and 7β-hydroperoxides (cholesterol 7α- and 7β-OOH) are the primary products of cholesterol autoxidation.[1] Cholesterol autoxidation begins with H-atom abstraction from C7 and less so from C4 to form an allylic radical.[2] Oxygen addition to either side of the allylic radical generates the corresponding peroxyl radical. The most thermodynamically stable products are cholesterol 7α- and 7β-peroxyl radicals, which ultimately get trapped by an H-atom donor to form cholesterol 7α- and 7β-OOH respectively (Scheme 3.1).

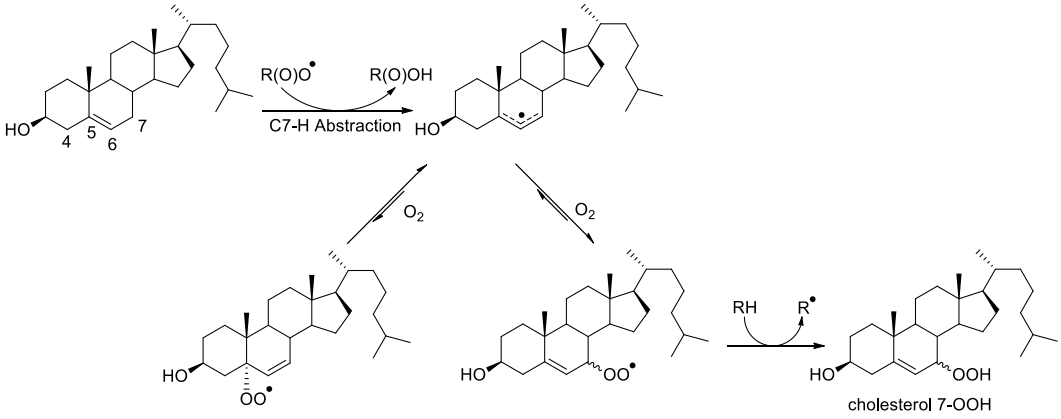

Scheme 3.1. The primary pathway of cholesterol autoxidation.

Herein, we propose that acid-catalyzed Hock fragmentation of cholesterol 7-OOH may lead to the formation of secosterols similar in structure, and therefore chromatographic properties and mass spectra, to the secosterols that derived from ozonolysis of cholesterol or Hock fragmentation of cholesterol 5α-OOH. This could be significant *in vivo* not only due to the stability and greater abundance of cholesterol 7-OOH in solution compared to other

regioisomeric hydroperoxides, but also due to the lack of requirement for highly energetic oxidants such as singlet oxygen or ozone.[2, 3, 4]

Acid-catalyzed Hock fragmentation of cholesterol 7-OOH takes place by the protonation of the hydroperoxide under acidic conditions, such as the derivatization conditions used to identify secosterol-A and secosterol-B (2,4-dinitrophenylhydrazine (DNPH) and HCl in EtOH).[5] Migration of the sp^2 carbon to the electron deficient oxygen is the next step, which is presumed to be concerted with the departure of water.[6] The water then attacks the oxocarbenium ion to form a hemi-acetal intermediate which can lead to the anticipated dialdehyde structure. The dialdehyde structure can undergo intramolecular aldolization to generate the two possible aldol products. Under acidic conditions cholesterol 7α- and 7β-OOH can also undergo dehydration to generate 7-ketocholesterol (Scheme 3.2).

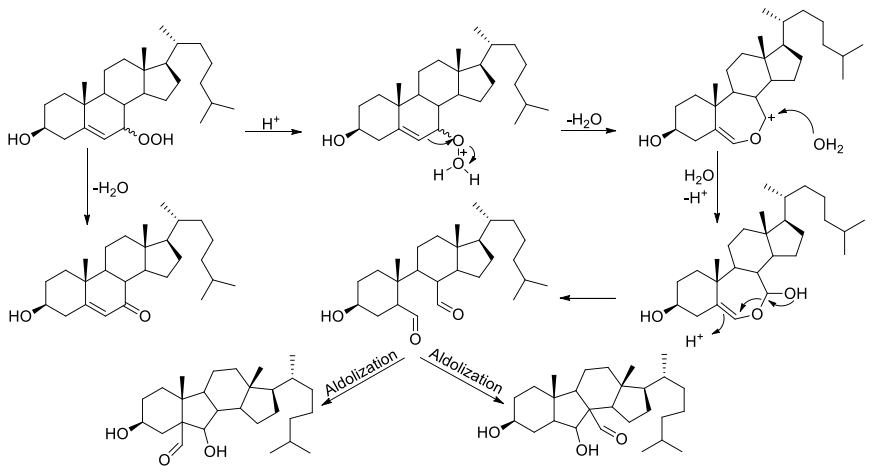

Scheme 3.2. Proposed scheme of acid-catalyzed Hock fragmentation of cholesterol 7-OOH with the three expected products. The dehydration pathway which competes with Hock fragmentation in acidic conditions is also shown.

3.2 Results

3.2.1 Synthesis of Cholesterol 7α-Hydroperoxide

Cholesterol 5α-OOH was obtained by Rose Bengal photosensitized oxidation of cholesterol in pyridine and was isomerized to cholesterol 7α-OOH in chloroform as suggested by Beckwith and co-workers.[1] In our initial attempts of oxidizing cholesterol with $^1O_2$ we obtained several cholesterol oxidation products: cholesterol 5α-OOH, the main product of cholesterol photo-oxidation; cholesterol 6α and 6β-OOH, the minor products of cholesterol photo-oxidation;[7, 8,9] and cholesterol 7α and 7β-OOH, products derived from the rearrangement of cholesterol 5α-OOH, were all present (Figure 3.1).[10]

Cholesterol 5α-OOH can undergo a radical rearrangement to form cholesterol 7α-OOH which can undergo a subsequent radical rearrangement to generate cholesterol 7β-OOH. Dehydration of cholesterol 7α and 7β-OOH generates 7-ketocholesterol, which would start to appear in the corresponding spectra if the reaction was run for longer time (Scheme 3.3).

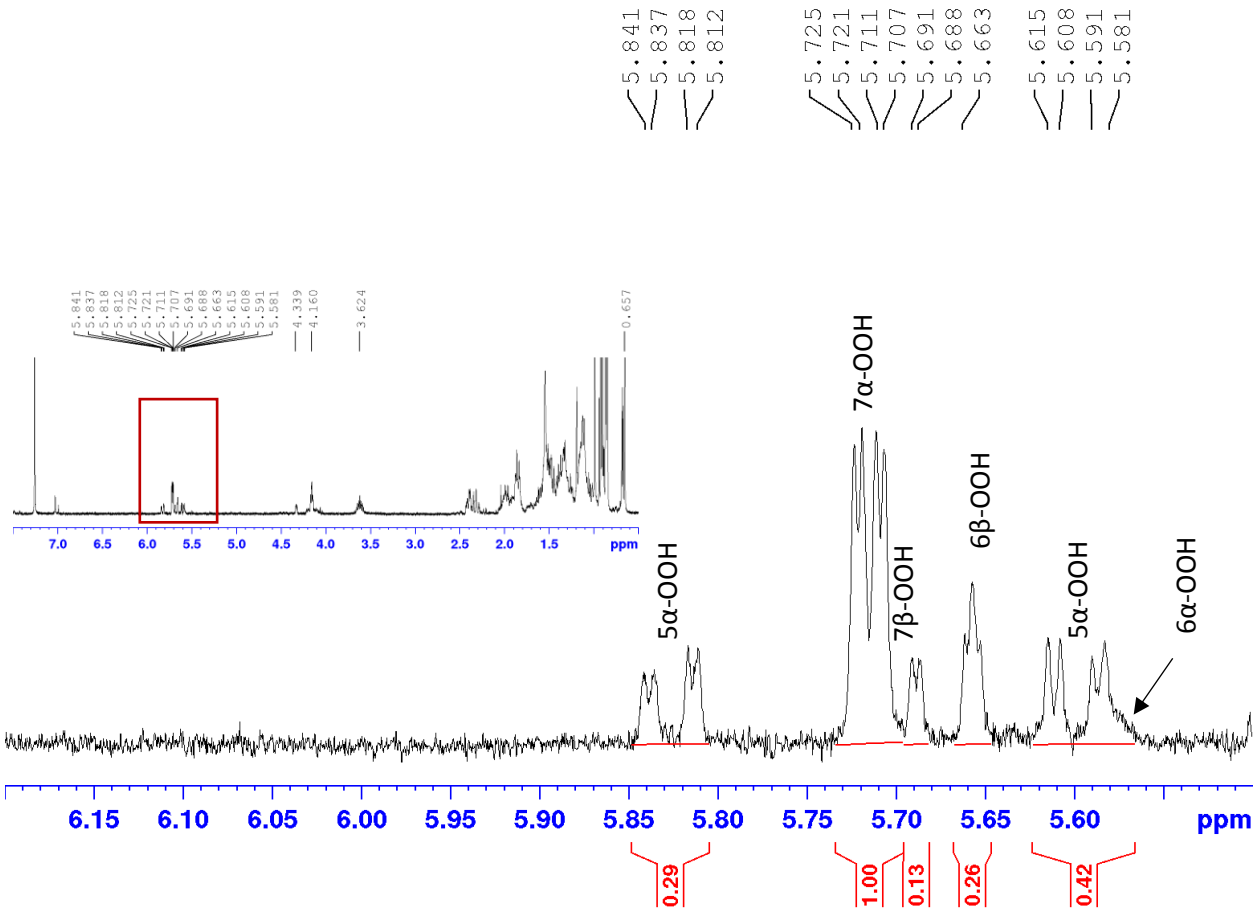

Figure 3.1. Alkene region of the ^{1}H-NMR spectrum of a crude cholesterol photo-oxidation product mixture. Cholesterol 5α-OOH, cholesterol 7α/β-OOH and cholesterol 6α/β-OOH are shown. The spectrum was recorded at 400 MHz with chemical shifts reported in ppm relative to $CDCl_3$. Peaks are assigned based on literature values.[11] Inset: full spectrum.

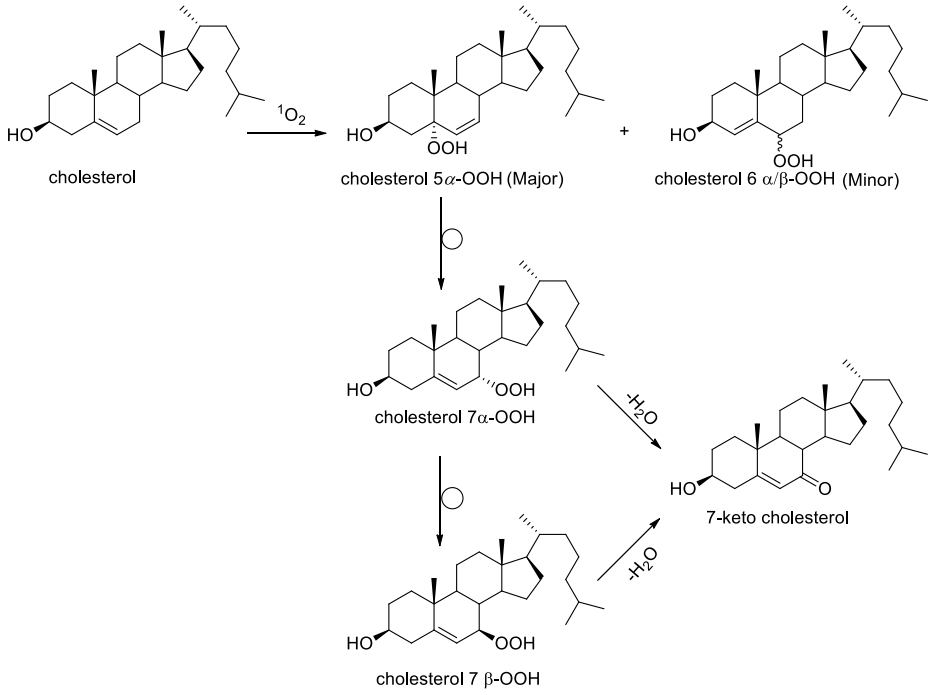

Scheme 3.3. Products of cholesterol photo-oxidation.

To prevent the formation of cholesterol 7α and 7β-OOH, 1 equivalent of butylated hydroxytoluene (BHT), a peroxyl radical-trapping antioxidant, was added. BHT prevents radical rearrangement of cholesterol 5α-OOH to cholesterol 7α-OOH and subsequent rearrangement to cholesterol 7β-OOH. This helped to obtain a cleaner product mixture where pure cholesterol 5α-OOH was obtained after purification and removal of BHT. Cholesterol 5α-OOH was rearranged to cholesterol 7α-OOH in chloroform for 12 hours. Cholesterol 7α-OOH obtained from radical rearrangement of cholesterol 5α-OOH is shown in Figure 3.2.

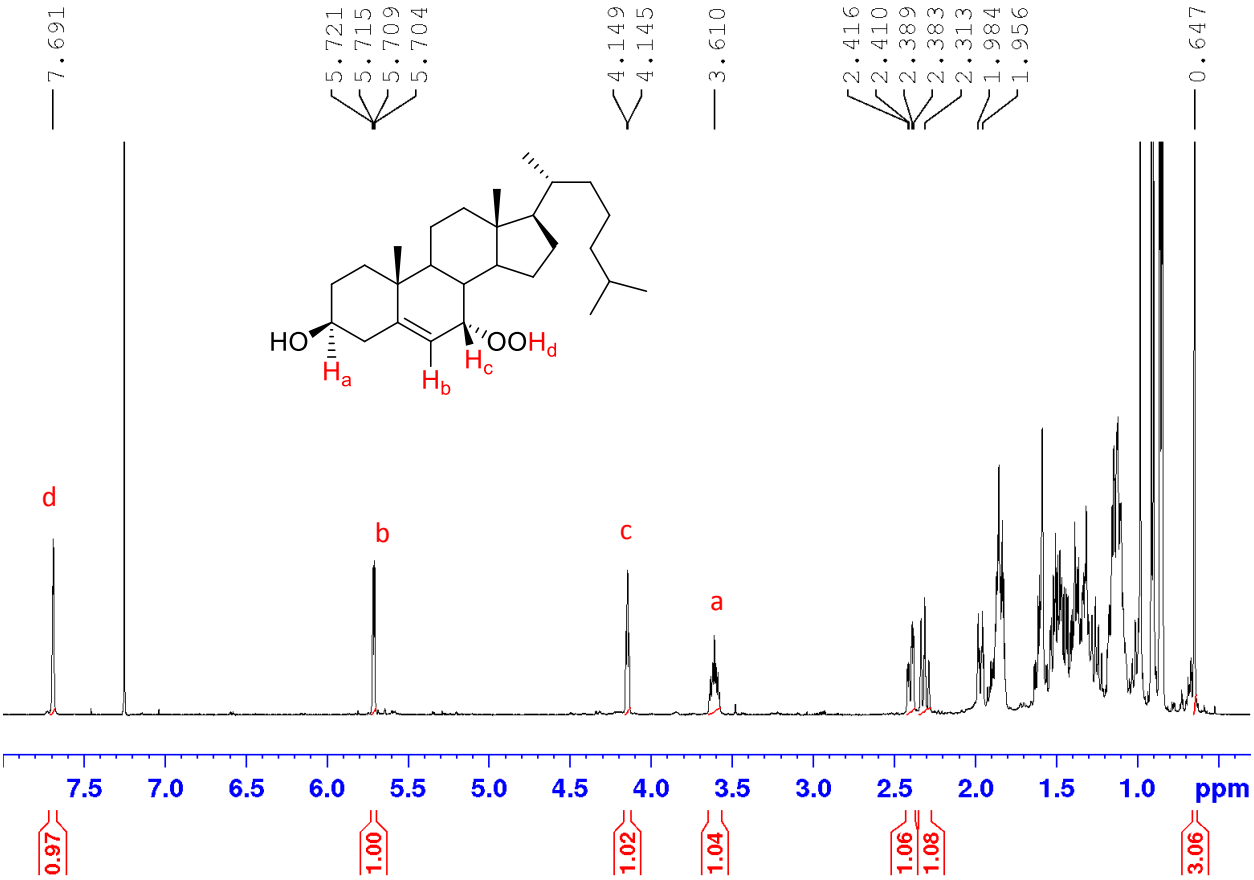

Figure 3.2. ^{1}H-NMR spectrum of cholesterol 7α-OOH in $CDCl_3$. The spectrum was recorded at 400 MHz with chemical shifts reported in ppm relative to $CDCl_3$.

Radical rearrangement of cholesterol 5α-OOH to cholesterol 7α-OOH is relatively fast compared to the rearrangement of cholesterol 7α-OOH to cholesterol 7β-OOH. Therefore, immediately after complete rearrangement of cholesterol 5α-OOH to cholesterol 7α-OOH, the solvent was removed to slow any further rearrangement.

3.2.2 Preliminary Studies of the Hock Fragmentation of Cholesterol 7α-OOH

Cholesterol 7α-OOH was subjected to various combinations of acids and solvents to explore the conditions under which it may undergo Hock fragmentation. We initially performed the reaction in acetonitrile with 10 equivalents of trifluoroacetic acid (TFA). We monitored the reaction by ^{1}H-NMR, paying particular attention to the disappearance of vinyl peaks of the starting material and appearance of aldehyde peaks of the products. The resulting ^{1}H-NMR spectrum after two hours showed, very much to our surprise, that the reaction did not proceed as expected; no aldehydic protons were observed and largely starting material remained (Figure 3.3.a).

In anticipation that the Hock fragmentation of cholesterol 7α-OOH might be much slower than cholesterol 5α-OOH, we let the reaction run for a longer time. After 32 hours, 7-ketocholesterol and 7α-hydroxycholesterol were formed as dominant products. Due to the acidic conditions of the reaction, cholesterol 7α-OOH had undergone dehydration to yield 7-ketocholesterol, but again, no Hock products (aldehyde peaks) were observed (Figure 3.3.b).

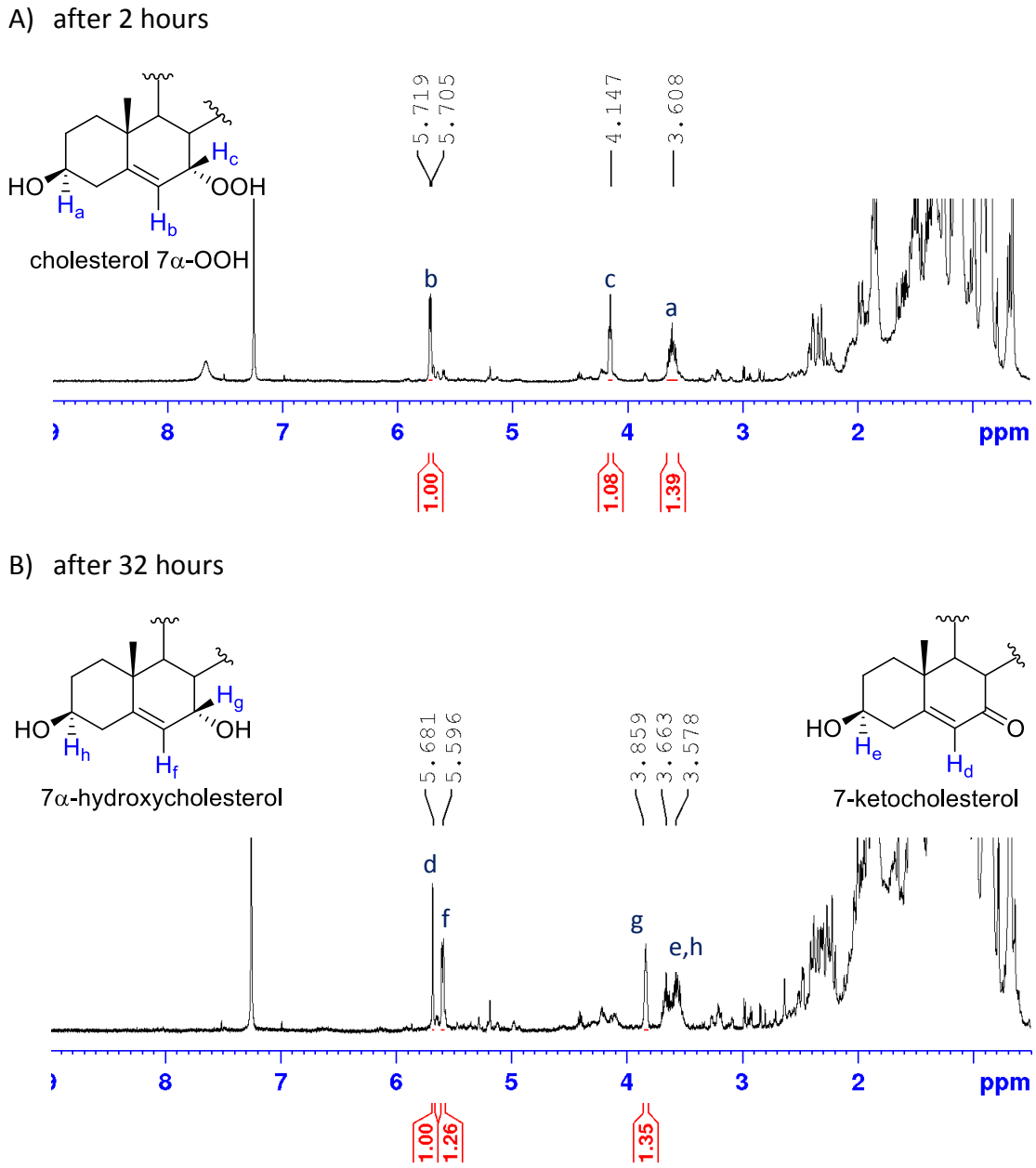

Figure 3.3. ^{1}H-NMR spectrum of the crude product mixture of Hock fragmentation of cholesterol 7α-OOH in acetonitrile with 10 equivalents of TFA, after two hours (A), and after 32 hours (B). The spectrum was recorded at 400 MHz with chemical shifts reported in ppm relative to $CDCl_3$. Peaks are assigned based on literature values.[12,13]

In the course of these studies, we observed that cholesterol 7α-OOH was not particularly soluble in acetonitrile, and therefore, we changed the reaction conditions to chloroform with 10 equivalents of p-toluenesulfonic acid (PTSA) where again no aldehydic protons were observed. We then changed the reaction conditions to isopropanol with 10 equivalents of hydrochloric acid. This time, after two hours, we observed distinct aldehyde peaks in the 9.5-10 ppm region (Figure 3.4).

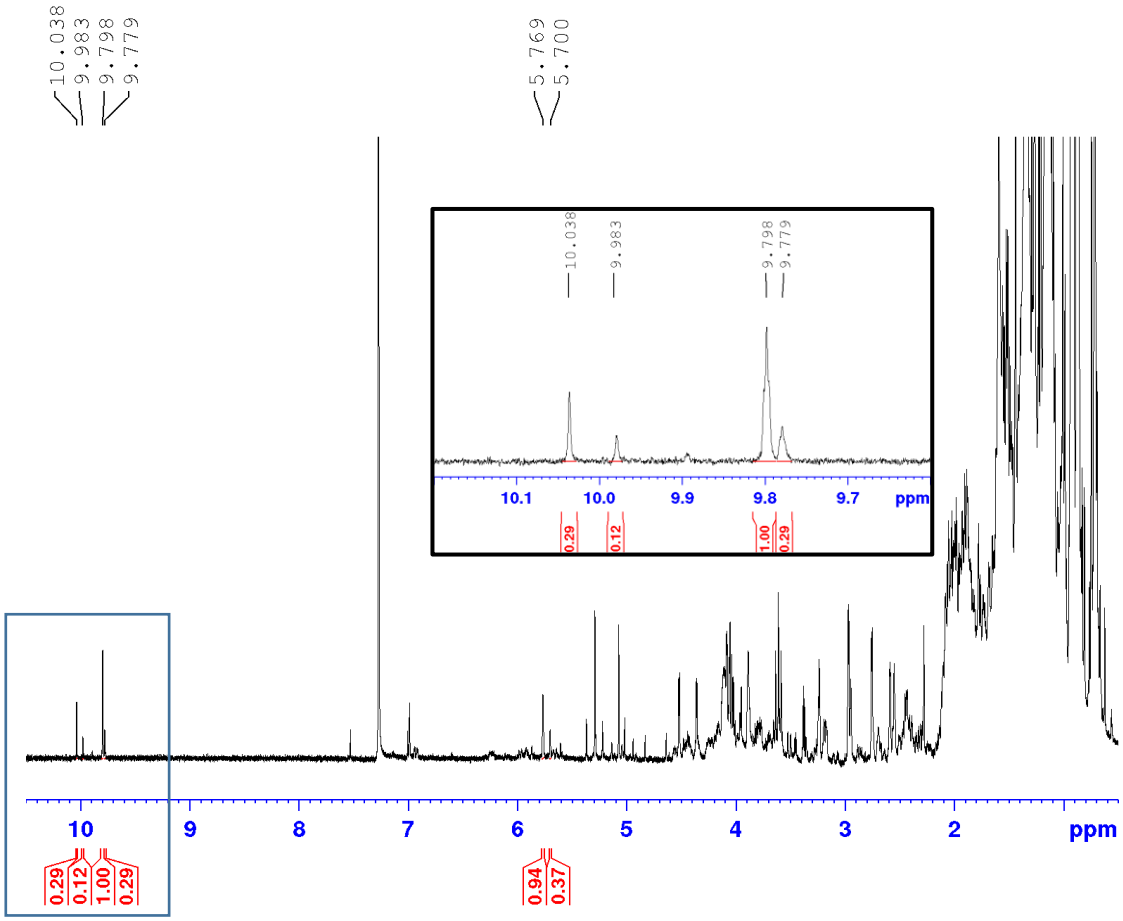

Figure 3.4. ^{1}H-NMR spectrum of the crude product mixture of Hock fragmentation of cholesterol 7α-OOH with 10 equivalents of HCl in isopropanol. The spectrum was recorded at 400 MHz with chemical shifts reported in ppm relative to $CDCl_3$. Inset: down-field region of spectrum.

The upfield (alkyl) region of the spectrum is far too complex for interpretation; however, it is evident that there are a lot of acetal peaks present in the spectrum. This is likely due to the aldehyde products forming acetals with isopropanol, which had been previously observed to occur with cholesterol 5α-OOH Hock fragmentation.[4] Therefore, we thought that changing from isopropanol to ethanol (or better, methanol) would reduce the number of protons corresponding to acetal or hemi-acetal groups which would reduce the complexity of the corresponding ^{1}H-NMR spectra. We also performed the reaction in isopropanol with twice the acid concentration. Under these reaction conditions, aldehydic protons started to appear as soon as 10 minutes into the reaction confirming the expectation that the reaction is acid-catalyzed.

3.2.3 Products of the Hock Fragmentation of Cholesterol 7α-OOH

Our numerous attempts to isolate the products of Hock fragmentation of cholesterol 7α-OOH for further characterization proved to be extremely challenging. We speculated that this difficulty could be due to many competing equilibria involving mono and/or di hemi-acetal and acetal formation from the putatively formed dialdehyde or aldolized products. Therefore, we opted to do the separation, isolation and eventually characterization of the products when performing the Hock fragmentation under 2,4-dinitrophenylhydrazine (DNPH) derivatization conditions. DNPH-derivatized products are generally more stable, and easier to detect by UV/Vis and/or negative ion ESI mass spectrometry, which can aid in their isolation and characterization.[14]

Wentworth and co-workers employed two different reaction conditions to derivatize their so called secosterols:[15] they derivatized the aldehydes obtained from atheromatous artery specimens with a solution of DNPH in 1 M HCl in ethanol, while their authentic secosterols (obtained via cholesterol ozonolysis) were derivatized with DNPH in p-toluenesulfonic acid in acetonitrile. We did not use the later conditions, since the Hock fragmentation of cholesterol 7α-OOH was deemed not to be successful in acetonitrile or when p-toluenesulfonic acid was used. We also wanted to perform the reaction similar to what was used to analyze the specimens from atherosclerotic plaques for easier comparison and consistency which clearly was not a concern for Wentworth and co-workers. Therefore, cholesterol 7α-OOH was subjected to acid-catalyzed Hock fragmentation under DNPH derivatization conditions, where DNPH (3 equivalents) was first added to 1 M HCl in methanol and, upon its complete dissolution, cholesterol 7α-OOH was added to the mixture. The mixture was stirred at room temperature for three hours. Product mixtures were examined by TLC, HPLC-UV, HPLC-MS and a wide range of NMR techniques.

Separation and isolation of products again proved to be extremely challenging. Multiple flash chromatography columns were performed on each product mixture in order to separate and isolate the major products. Collected fractions were then examined by ^{1}H-NMR spectroscopy. In all the fractions obtained, the NMR spectra were consistent with the presence of multiple species. Therefore, a combination of preparative TLC, normal-phase and reverse-phase semi-preparative HPLC were employed to purify and isolate the products. Three of the predominant products were purified and analyzed extensively. Other fractions were also collected but due to the multiple attempted purifications, their yield was too low for further analysis.

The DNPH derivatized crude product mixture of the Hock fragmentation of cholesterol 7α-OOH was injected on a normal-phase HPLC column and the eluent was analyzed by UV/Vis spectroscopy. The following chromatogram (Figure 3.5) was obtained where the initial peaks (*i*-peaks), Peak-A, Peak-B and Peak-C were subsequently analyzed.

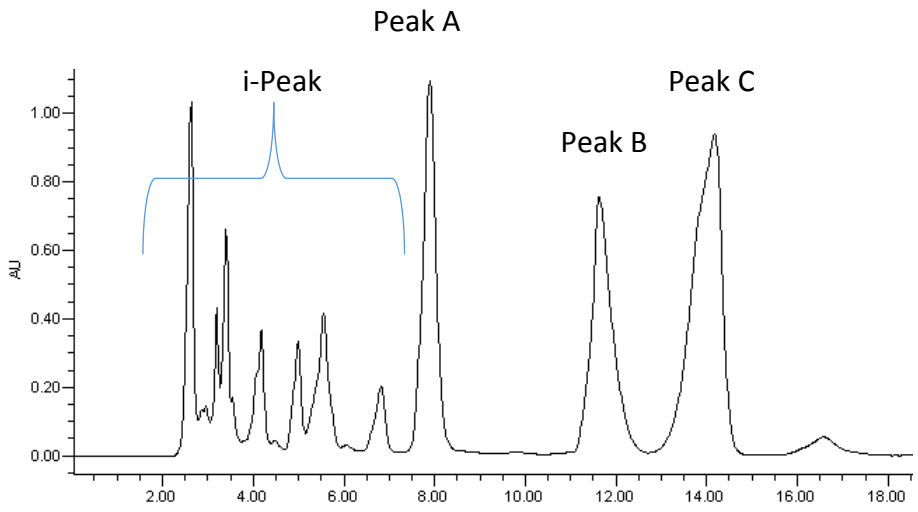

Figure 3.5. Chromatogram obtained from a crude DNPH derivatized product mixture of Hock fragmentation of cholesterol 7α-OOH (3 equiv. DNPH, 1 M HCl in MeOH). Normal-phase column (5 µm-10 x 150mm) and UV-vis detector (360 nm) with a mobile phase of 2% isopropanol in hexane at 4 mL/min was used.

No attempt was made to separate the initial peaks (i-peaks, cf. Figure 3.5) by normal phase. Instead, the entire eluent in this area was pooled, concentrated and analyzed by reverse-phase HPLC-MS (negative ion ESI). The mass scan range was between 400 to 650 *m/z* to include the expected mass of DNPH derivatized secosterols of 597 *m/z*. Surprisingly the majority of the peaks in this region did not feature mass spectra with the expected mass range, which suggests

that the majority of these peaks do not correspond to DNPH-derivatized cholesterol. They are most likely DNPH by-products with a mass around 198 *m/z*, which is outside our selected mass scan limit. There was trace amount of products with the expected mass of 597 *m/z* however, since the majority of the peaks in the i-peak region lacked any cholesterol and had very poor resolution in both normal and reverse-phase HPLC, we did not pursue further isolation and/or purification of this fraction.

One of the major peaks to elute from the column was Peak-A (cf. Figure 3.5) corresponding to Unknown-A. Unknown-A was one of the most consistent products of the Hock fragmentation of cholesterol 7α-OOH. When we performed the reaction in different solvents such as methanol, ethanol and water, Unknown-A was consistently one of the major products. We strongly believe that the small peaks marked with asterisk correspond to the diastereomer of Unknown-A; however, more studies need to be done to confirm this (Figure 3.6).

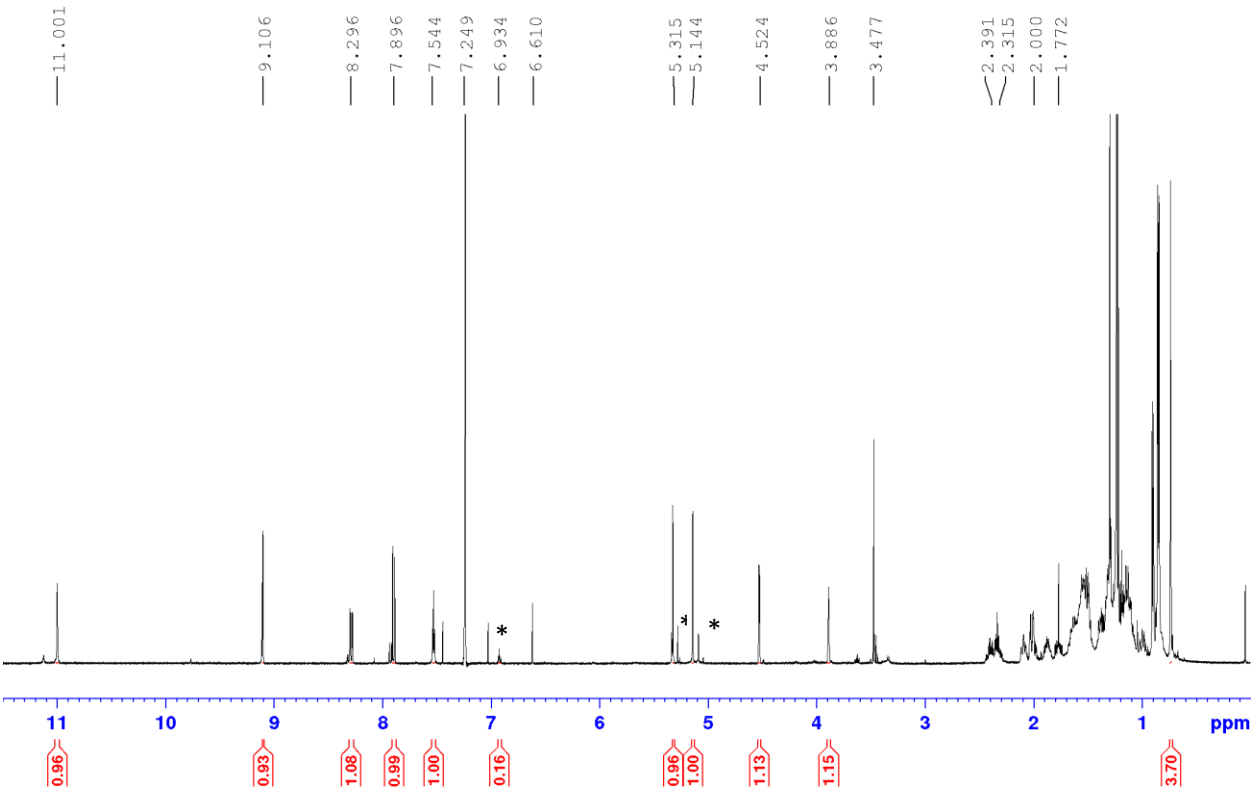

Figure 3.6. ^{1}H-NMR spectrum of Unknown-A. The spectrum was recorded at 400 MHz with chemical shifts reported in ppm relative to $CDCl_3$. * Proposed diastereomer of Unknown-A.

The second major peak to elute from the column was Peak-B corresponding to Unknown-B (cf. Figure 3.5). Once again, we strongly believe that the small peaks marked with asterisk correspond to the diastereomer of Unknown-B; however, more studies need to be done to confirm this (Figure 3.7).

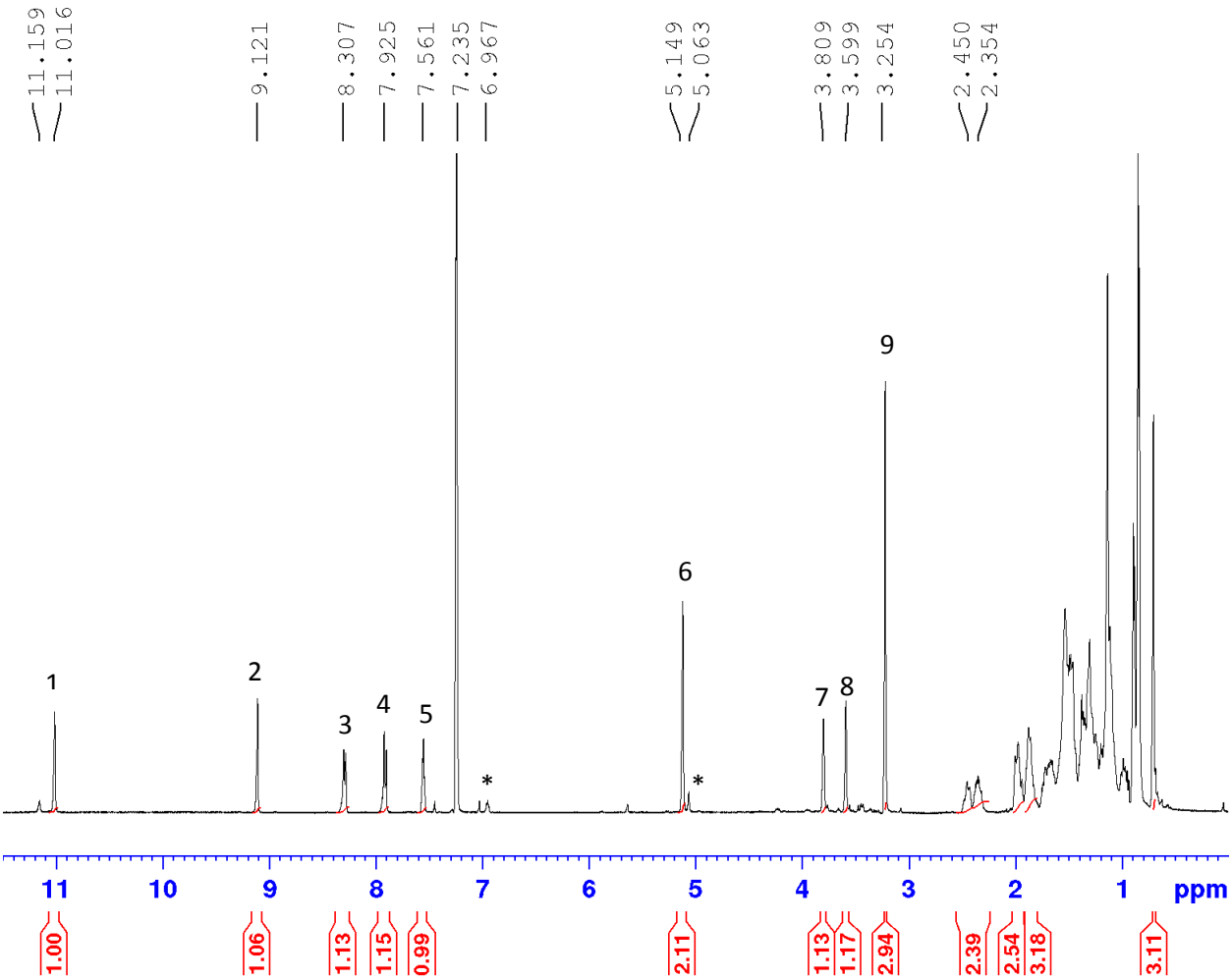

Figure 3.7. ^{1}H-NMR spectrum of Unknown-B. The spectrum was recorded at 400 MHz with chemical shifts reported in ppm relative to $CDCl_3$. * Proposed diastereomer of Unknown-B.

Peak-1 corresponds to the only proton that exchanged with a deuteron, albeit at a very slow rate. The COSY spectrum corresponding to Unknown-B is shown in Figure 3.8. Herein, we can see that the imine proton coupled to two protons in the up-field region of 2.35 and 2.45 ppm. The coupling of the aromatic protons of the DNPH moiety to one another was also observed. The

only other interpretable coupling belonged to protons corresponding to peak-7 and peak-8, which suggests that the two oxygen-baring carbons are adjacent to one another.

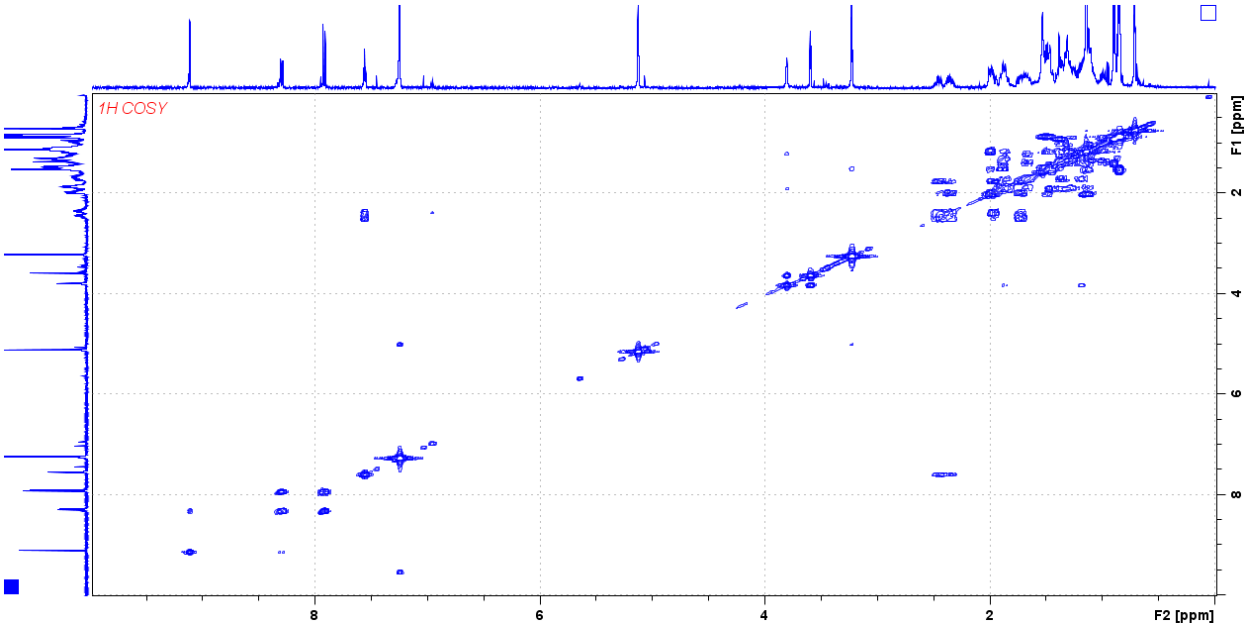

Figure 3.8. COSY NMR spectrum of Product-B. The spectrum was recorded at 400 MHz with chemical shifts reported in ppm relative to $CDCl_3$.

For further analysis, ^{13}C NMR, DEPT-90, DEPT-135, HMQC and MS were also employed. The number of carbons observed was one too many suggesting an incorporation of a methoxy group into the structure. In our HMQC studies we observed a correlation between the protons corresponding to Peak-6 to only one carbon recommending the presence of an exomethylene group and our MS analysis revealed an unexpected mass of 611 *m/z* instead of 597 *m/z*.

Peak-C (cf. Figure 3.5) was also isolated and analyzed by ^{1}H-NMR. There was no imine proton present in this structure but two characteristic peaks were present; one singlet peak at

6.19 ppm and a multiplet at 3.69 ppm. We anticipated that this last fraction most likely corresponds to DNPH-derivatized 7-ketocholesterol -product of cholesterol 7-OOH dehydration (Figure 3.9).

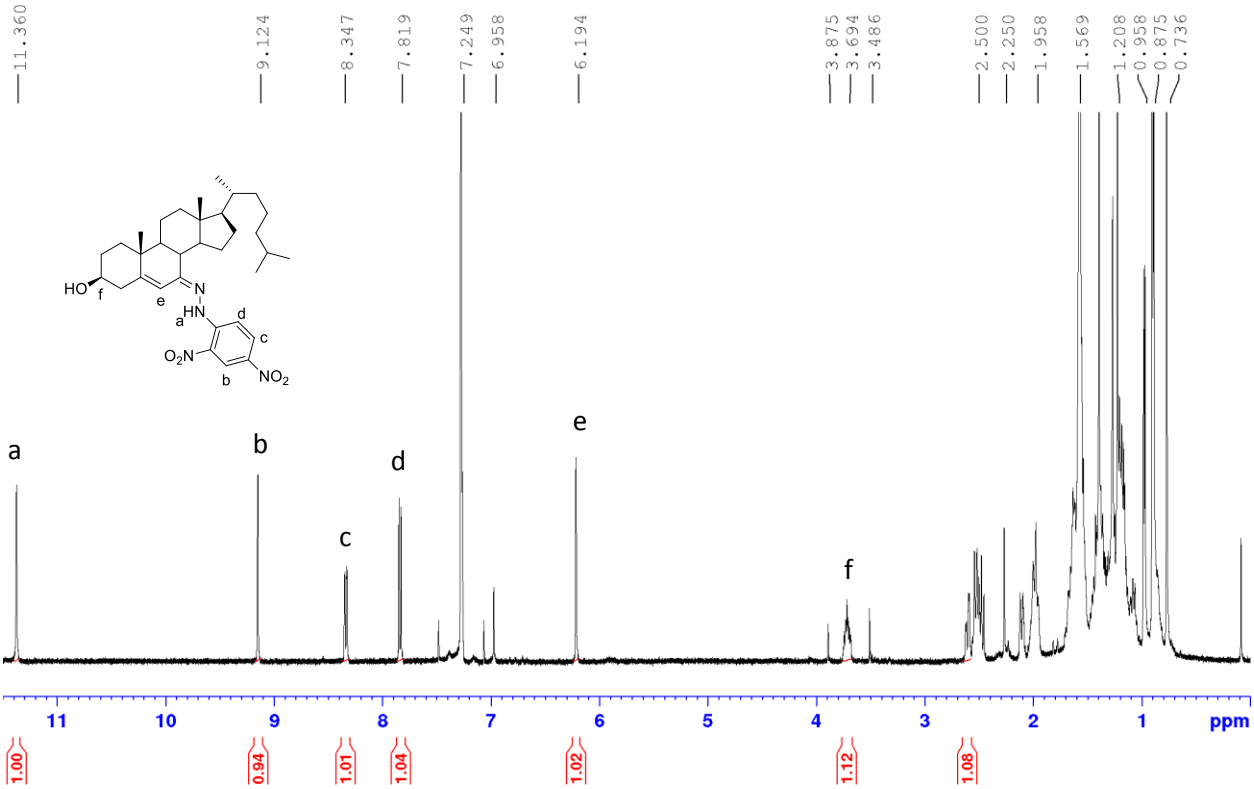

Figure 3.9. ^{1}H-NMR spectrum of hydrazone derivatized 7-ketocholesterol (Unknown-C). The spectrum was recorded at 400 MHz with chemical shifts reported in ppm relative to $CDCl_3$.

To further confirm the structure of Unknown-C we isolated pure 7-ketocholesterol from a cholesterol autoxidation mixture and subjected it to DNPH derivatization conditions. The ^{1}H-NMR spectrum of the authentically synthesized DNPH-derivatized 7-ketocholesterol

corresponded to that of Unknown-C. We further confirmed this by comparing the HPLC-UV chromatograms of authentic DNPH-derivatized 7-ketocholesterol with Unknown-C.

We also performed the Hock fragmentation of cholesterol 7α-OOH under DNPH derivatization condition in ethanol (instead of methanol) where we consistently obtained Unknown-A and Unknown-C (hydrazone derivatized 7-ketocholesterol) amongst our product mixture. Unknown-B was also obtained but with some modifications as the sharp singlet peak at 3.25 ppm (Peak-9, cf. Figure 3.7) corresponding to three protons (presumably the methoxy protons) was replaced by two sets of multiplets corresponding to two protons and three of methyl protons at 1.2 ppm (Figure 3.10). Furthermore, Unknown-B was not observed at all when the reaction was performed in water which suggests that alkoxylation plays a predominant role in Unknown-B formation.

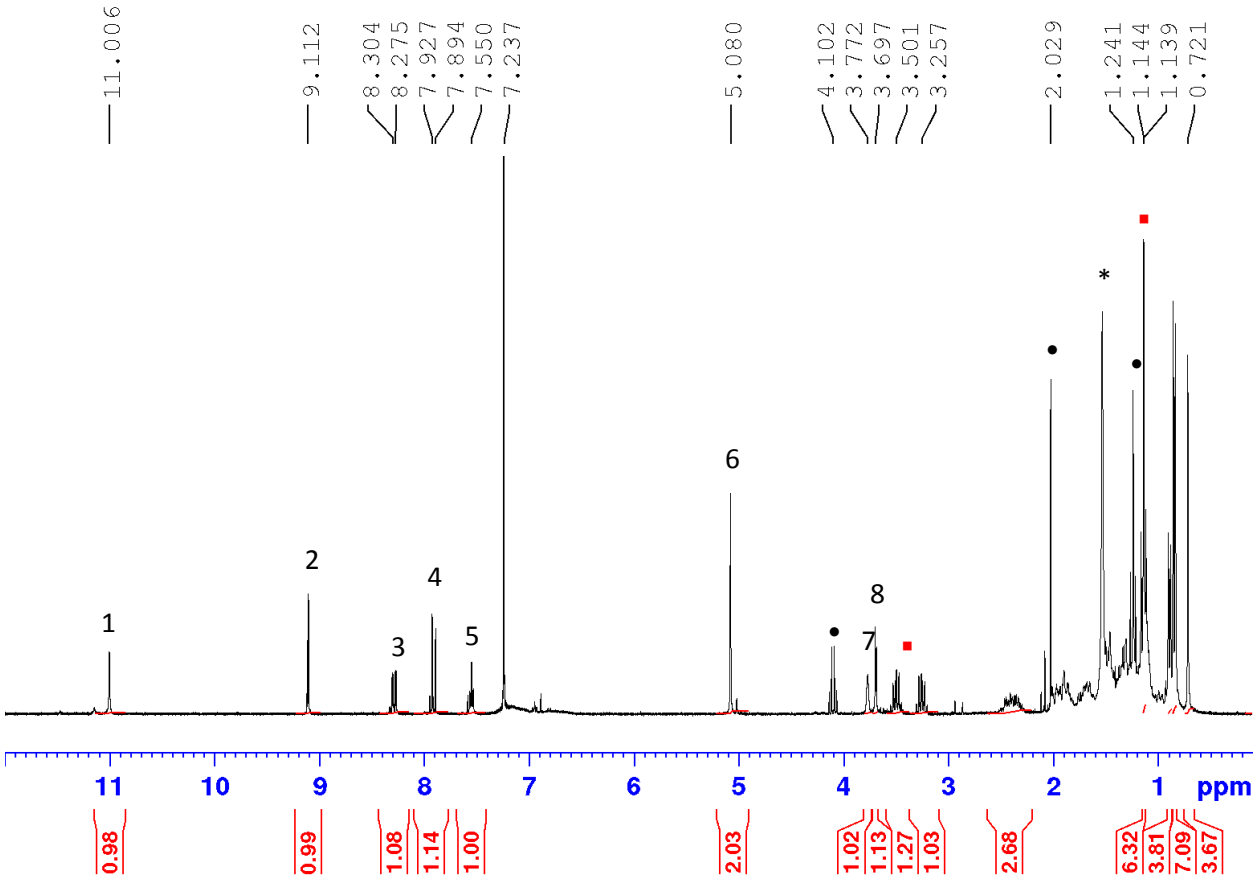

Figure 3.10. ^{1}H-NMR spectrum of Unknown-B when the reaction was performed in ethanol The spectrum was recorded at 400 MHz with chemical shift reported in ppm relative to $CDCl_3$. Numbering similar to Figure 3.7. • ethyl acetate, * water. ▪ proposed ethoxy peaks.

Since the collected MS data alongside 1D ,2D and carbon NMRs were not sufficient to elucidate the structures of Unknown-A and -B, we tried to crystalize the isolated products to obtain an x-ray crystallographic structure. Unfortunately, none of our attempts to crystalize these products were successful.

3.2.4 Hock Fragmentation and Dehydration of Cholesterol 7α-OOH (in the absence of DNPH)

In parallel with the forgoing studies, we examined the rate of the Hock fragmentation of cholesterol 7α-OOH in the absence of DNPH. At first we examined the rate of the Hock fragmentation of cholesterol 7α-OOH compared to the rate of the dehydration of cholesterol 7α-OOH, since under acidic conditions these two reactions compete with one another. Reactions were monitored by ^{1}H-NMR where we paid particular attention to the disappearance of the vinyl protons of cholesterol 7α-OOH and growth of the vinyl protons of 7-ketocholesterol (product of cholesterol 7-OOH dehydration). In general, the rate of the Hock fragmentation seemed to be more substantial than the rate of dehydration. Due to the slow rate of dehydration, only a trace amount (1.2 % of total products) of 7-ketocholesterol was generated in 0.001 M HCl in d_4-methanol after 100 minutes (Figure 3.11).

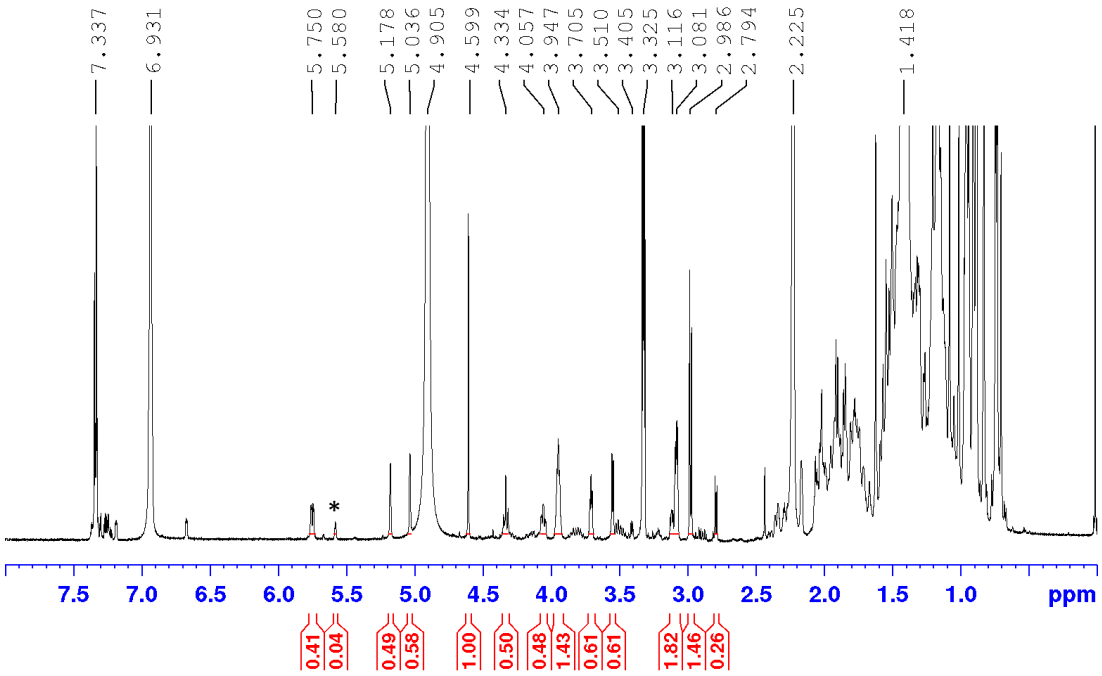

Figure 3.11. ^{1}H-NMR spectrum of the crude product mixture of the Hock fragmentation of cholesterol 7α-OOH in d_4-methanol with 0.001 M HCl after 100 minutes. The spectrum was recorded at 400 MHz with chemical shifts reported in ppm relative to $CDCl_3$. * 7-ketocholesterol.

We also examined the rate of Hock fragmentation of cholesterol 7α-OOH compared to cholesterol 5α-OOH. The reaction was monitored by ^{1}H-NMR, where we observed the disappearance of vinyl peaks of the corresponding starting material as function of time (Figure 3.12).

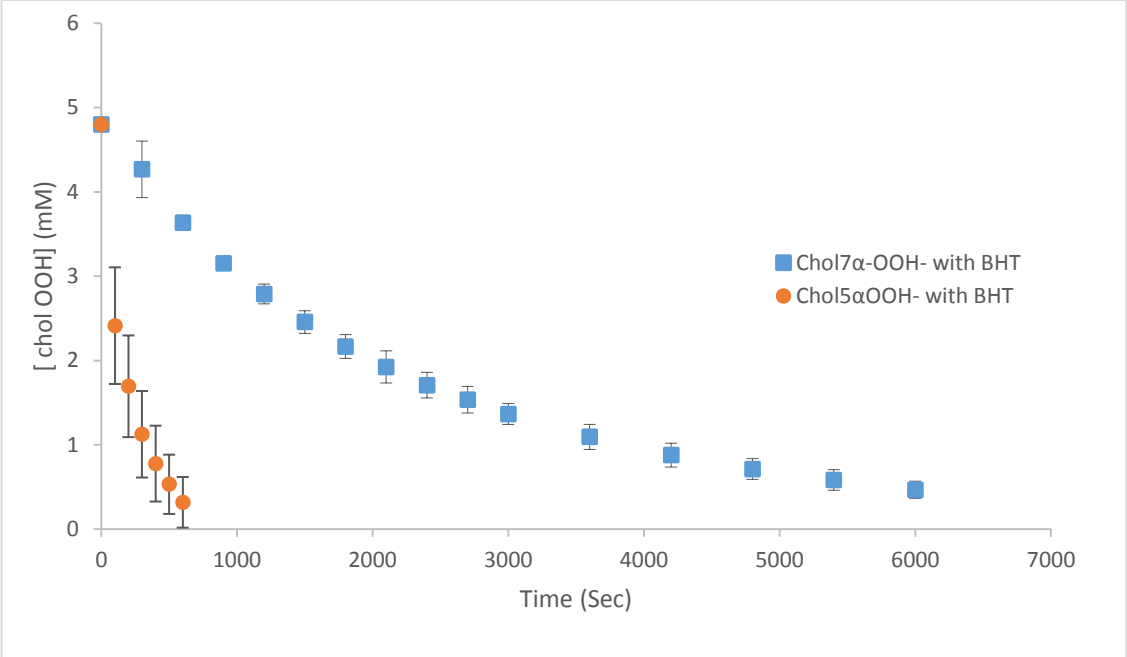

Figure 3.12. Conversion of 4.8 mM cholesterol 7α-OOH (blue, ▪) and 4.8 mM cholesterol 5α-OOH (orange, ●) to Hock products with 0.001M HCl in d_4-methanol as a function of time in the presence of BHT. The disappearance of the vinyl proton of cholesterol hydroperoxide was monitored by ^{1}H-NMR recorded at 300 MHz. Benzyl alcohol was used as an internal standard.

Herein, we could clearly see that the rate of the Hock fragmentation of cholesterol 5α-OOH was much faster than cholesterol 7α-OOH. When the natural log of the concentration of cholesterol hydroperoxide as a function of time was plotted, a linear relationship was observed indicating a first order reaction with respect to cholesterol hydroperoxides (Figure 3.13). The half-life for cholesterol 7α-OOH in 0.001M HCl in d_4-methanol in the presence of BHT was around 30 minutes (k_{obs}= 4 x10^{-4} s^{-1}) while the half-life for cholesterol 5α-OOH in the same reaction conditions was ten times shorter at only 3 minutes (k_{obs}= 4 x10^{-3} s^{-1}).

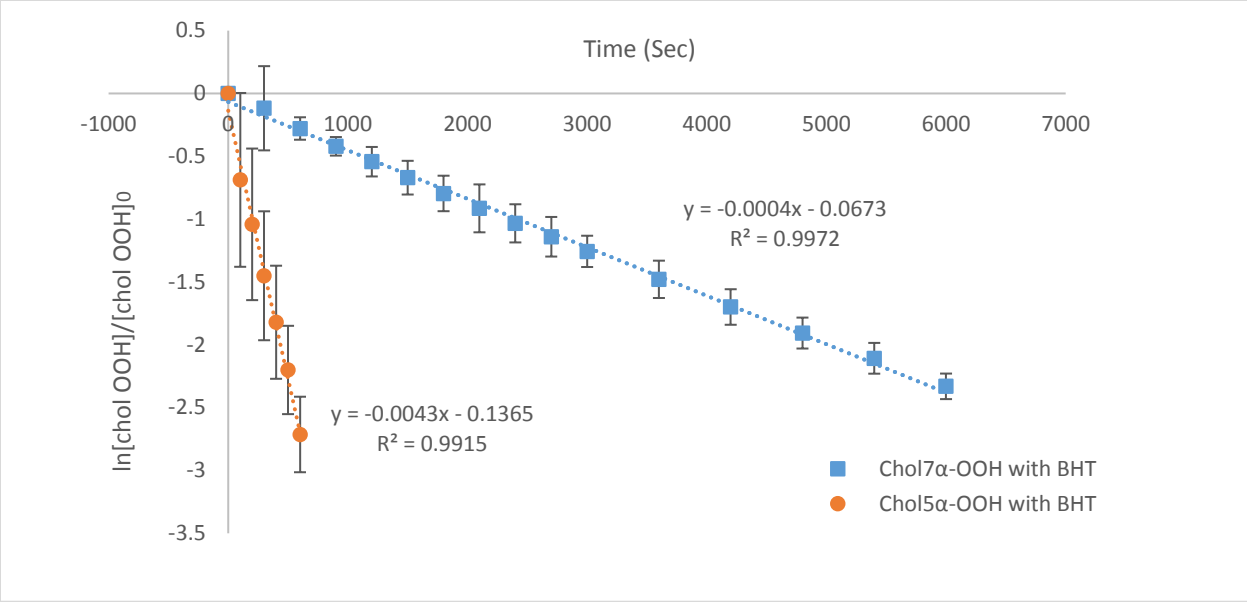

Figure 3.13. The natural logarithm of the concentration of cholesterol 7α-OOH (blue, ▪) and cholesterol 5α-OOH (orange, •) as a function of time in the presence of BHT. The disappearance of the vinyl proton of cholesterol hydroperoxide was monitored by ^{1}H-NMR recorded at 300 MHz. Benzyl alcohol was used as an internal standard.

We also studied the effect of BHT in the Hock fragmentation of cholesterol 7α-OOH. We monitored the Hock fragmentation of 4.8 mM of cholesterol 7α-OOH in d_4-methanol with 0.001 M HCl for 100 minutes with and without 1 equivalent of BHT (Figure 3.14). Herein we observed that BHT had no effect on the rate of Hock fragmentation of cholesterol 7α-OOH.

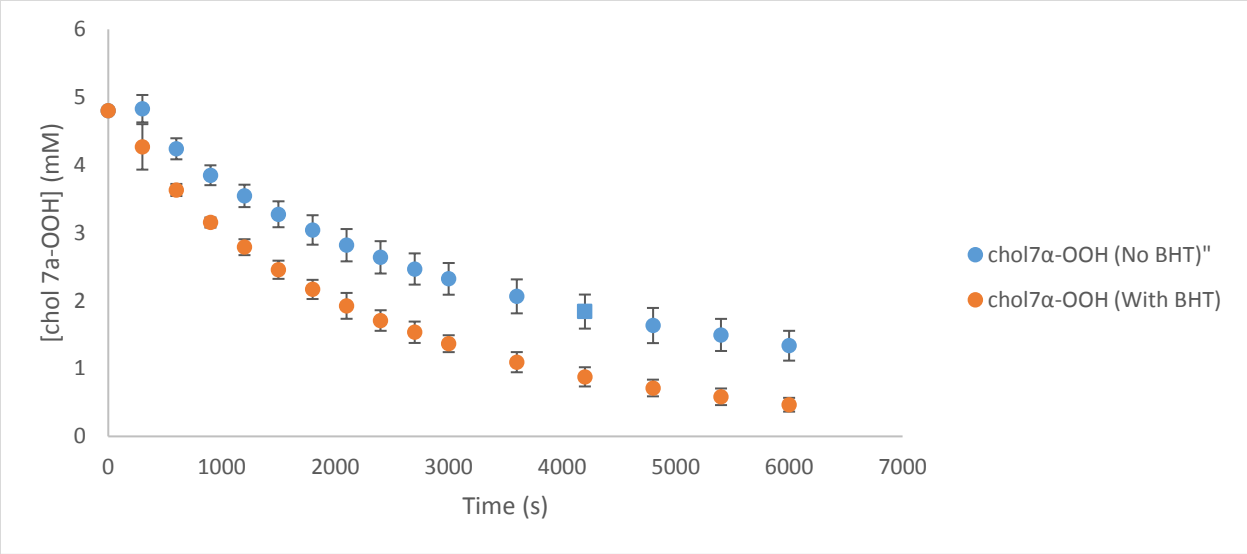

Figure 3.14. Cholesterol 7α-OOH (4.8 mM) in 0.001 M HCl in d_4-methanol conversion as a function of time in the presence (orange, •) and absence (blue, ▪) of BHT. The disappearance of the vinyl proton of cholesterol 7α-OOH was monitored by ^{1}H-NMR recorded at 300 MHz. Benzyl alcohol was used as an internal standard.

Upon cholesterol autoxidation *in vivo,* both α and β stereoisomers of cholesterol 7-OOH are generated.[16] Hence, a mixture of cholesterol 7α-OOH and cholesterol 7β-OOH was subjected to acid-catalyzed Hock fragmentation. The Hock fragmentation of 3.2 mM of cholesterol 7-OOH isomers with 0.001 M HCl in d_4-methanol and 1 equivalent of BHT was monitored to investigate the difference in the rate of Hock fragmentation between the α and β stereoisomers. Surprisingly, unlike cholesterol 7α-OOH, cholesterol 7β-OOH did not undergo Hock fragmentation to a measurable extent at 0.001 M HCl (Figure 3.15).

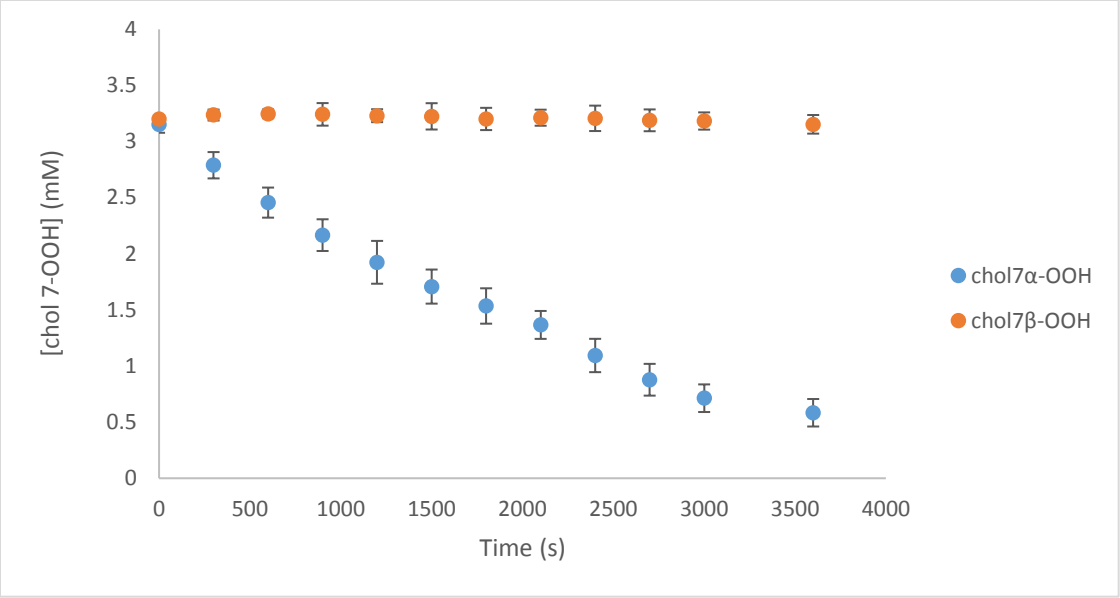

Figure 3.15. Cholesterol 7α-OOH (3.2 mM, ▪) and cholesterol 7β-OOH (3.2 mM, •) conversion as a function of time in the presence of BHT. The disappearance of the vinyl proton of cholesterol 7-OOH was monitored by ^{1}H-NMR recorded at 300 MHz. Benzyl alcohol was used as an internal standard.

At last, we also studied the effect of acid concentration on cholesterol 7α-OOH Hock fragmentation (Figure 3.16). The data sets were fit to first order decay with respect to cholesterol 7α-OOH concentration as a function of time, shown in Figure 3.17. At the lower acid concentration of 0.0001 M HCl, the rate of the Hock fragmentation of cholesterol 7α-OOH was very slow (k_{obs}= 1 x10^{-5} s^{-1}), while the higher acid concentration of 0.01 M HCl afforded a much faster rate (k_{obs}= 2.5 x10^{-3} s^{-1}). The half-life of cholesterol 7α-OOH in 0.01 M, 0.001 M and 0.0001 M HCl in d_4-methanol was determined to be 4.7 min, 30 min and 23 hours, respectively.

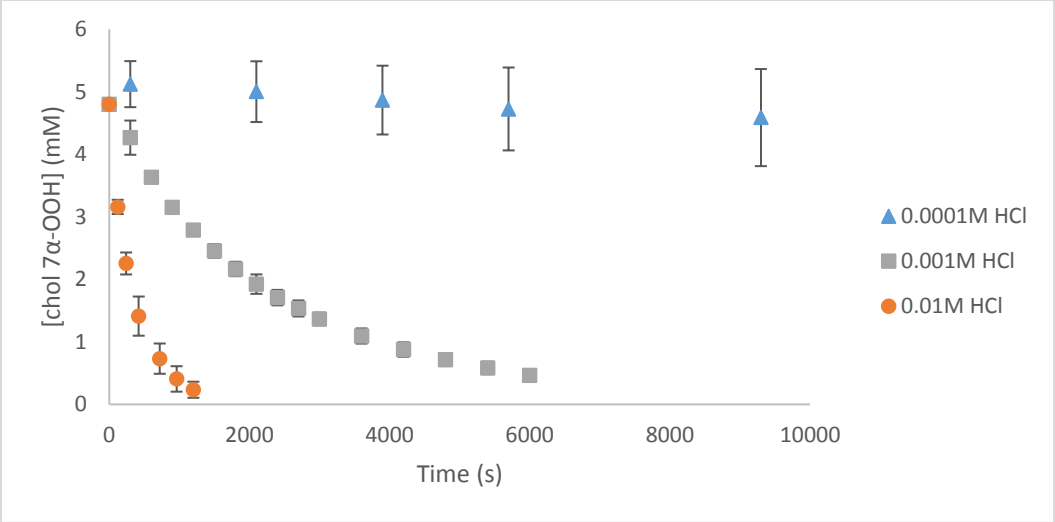

Figure 3.16. Cholesterol 7α-OOH (4.8 mM) conversion as a function of time in the presence of BHT at different acid concentration. The disappearance of the vinyl proton of cholesterol 7α-OOH was monitored by ^{1}H-NMR recorded at 300 MHz. Benzyl alcohol was used as an internal standard.

The values of the observed rate constants were plotted as a function of HCl concentration. The linear relation indicated that the reaction is first order with respect to acid concentration as well (Figure 3.18). The overall second order rate constant of the reaction was determined to be 0.2 M^{-1} s^{-1}.

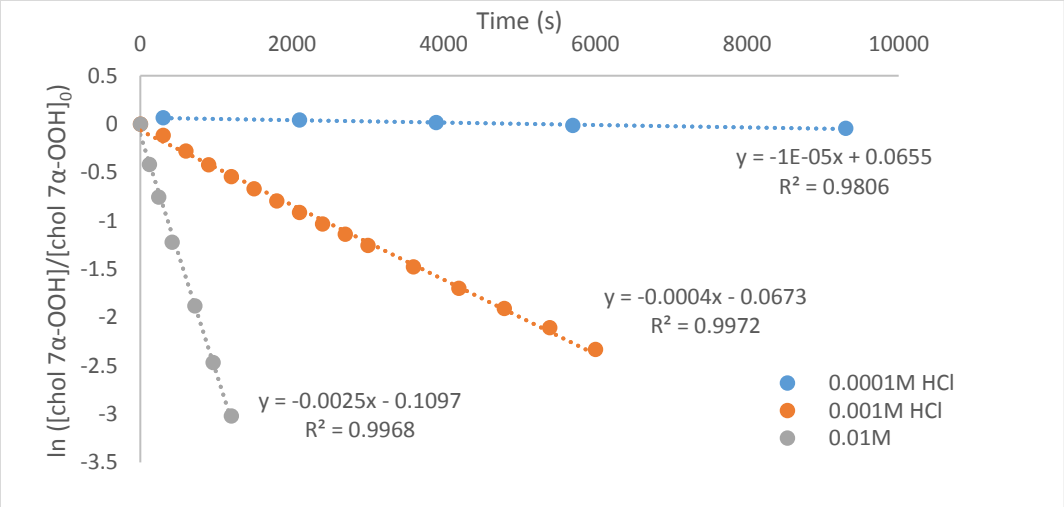

Figure 3.17. The natural logarithm of the decomposition of cholesterol 7α-OOH at different acid concentration as a function of time in the presence of BHT. The disappearance of the vinyl proton of cholesterol 7α-OOH was monitored by ^{1}H-NMR recorded at 300 MHz. Benzyl alcohol was used as an internal standard.

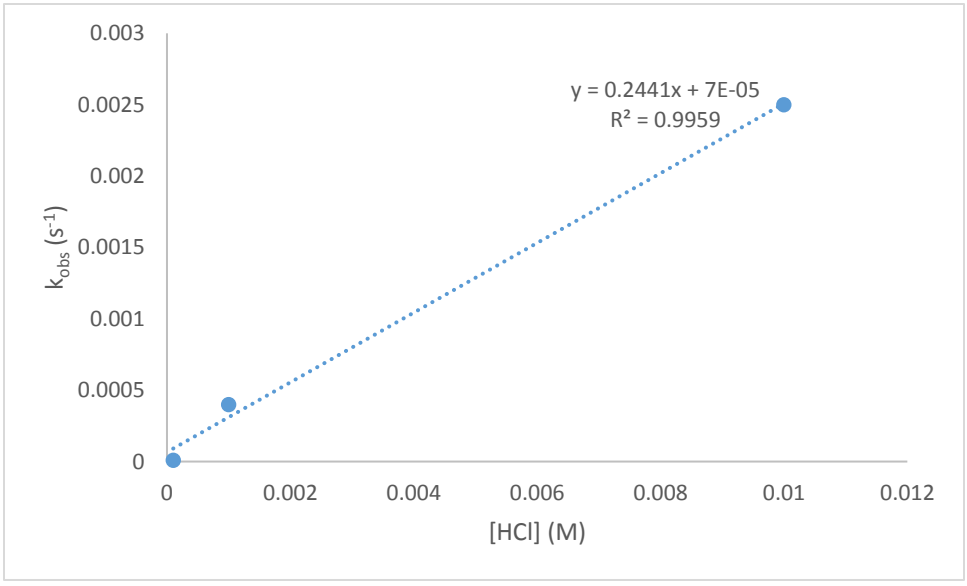

Figure 3.18. The observed rate constant of the Hock fragmentation of cholesterol 7α-OOH as a function of acid concentration.

3.2.5 Hock Fragmentation of Cholesterol 7α-OOH under DNPH Derivatization Conditions

Wentworth *et. al.* derivatized both arterial plaques and brain tissue extracts with 2,4-dinitrophenylhydrazine (DNPH) to identify secosterol-A and -B.[9] Since we showed that both cholesterol 5α-OOH[4] and cholesterol 6-OOH[2] were not stable to the derivatization conditions (yielding the same secosterols), we wondered if cholesterol 7α-OOH would undergo similar chemistry. Hence, we subjected cholesterol 7α-OOH and cholesterol 5α-OOH (for comparison) to typical DNPH derivatization conditions and monitored the reaction by ^{1}H-NMR, UPLC-MS and HPLC-UV.

The preliminary analysis of the crude product mixtures of the Hock fragmentation of cholesterol 7α-OOH and cholesterol 5α-OOH under DNPH derivatization conditions were first carried out by ^{1}H-NMR. Predictably, ^{1}H-NMR spectra of the crude product mixtures were too complex to be fully interpreted or effectively monitored. Therefore, we used HPLC-UV with detection of the DNPH chromophore at 360 nm to analyze the Hock fragmentation of cholesterol hydroperoxides under DNPH derivatization conditions.

We initially compared the products of cholesterol ozonolysis with the products of acid-catalyzed Hock fragmentation of cholesterol 7α-OOH and cholesterol 5α-OOH. Chromatograms are shown in Figure 3.19 where we used similar chromatographic conditions to those used by Wentworth and co-workers. Under these conditions, a peak at around 11.2 minutes, which corresponded to authentic DNPH-derivatized secosterol-B, was present in the chromatograms of the crude product mixture of cholesterol ozonolysis, cholesterol 5α-OOH Hock fragmentation and cholesterol 7α-OOH Hock fragmentation. Not only did this indicated that cholesterol 7α-OOH

could undergo Hock fragmentation, but also demonstrated that its products have similar chromatographic characteristics to secosterols under Wentworth's chromatographic conditions.

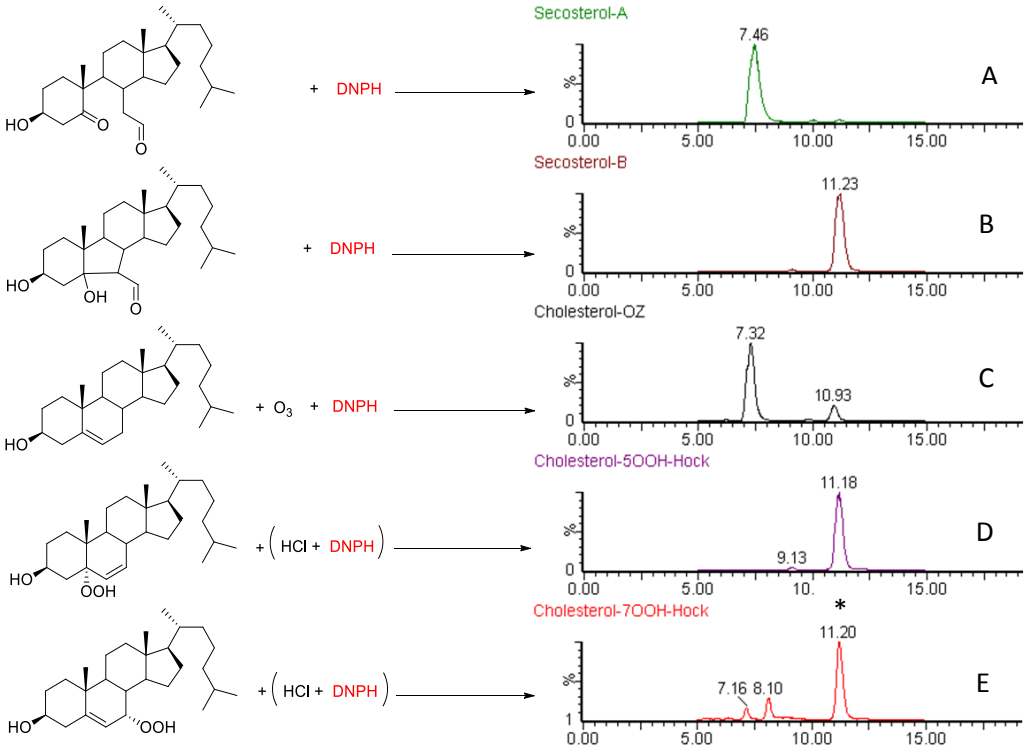

Figure 3.19. DNPH-hydrazones derived from secosterol-A (A), secosterol-B (B), ozonolysis of cholesterol (C) as well as Hock fragmentation of cholesterol 5α-OOH (D) and cholesterol 7α-OOH (E). UPLC-MS analyses were performed on a C18 column (2.5 µm- 4.6 × 75 mm) with ESI-detection. Mobile phase: 75% ACN, 20% MeOH, 5% H_2O (0.5 mL/min). * Combination of 597, 579, 615 and 611 *m/z*.

Although the peak at 11.2, which was essentially indistinguishable from that of secosterol-B, consistently appeared in each experiment we carried out with cholesterol 7α-OOH, the number and abundance of other products observed in the chromatograms differed. We therefore, systematically investigated the effect of DNPH and acid concentration on product formation and distribution under DNPH derivatization conditions.

As was shown in our kinetic studies, in the absence of DNPH, the Hock fragmentation of cholesterol 7α-OOH and cholesterol 5α-OOH were acid dependent. Herein, we performed a similar experiment in the presence of DNPH and monitored the reaction by HPLC-UV. In the Hock fragmentation of cholesterol 5α-OOH under DNPH derivatization conditions, the peaks corresponding to DNPH-derivatized secosterol-A and -B grew as the acid concentration was increased (Figure 3.20). In the case of cholesterol 7α-OOH, the concentration of the majority of the products increased confirming that Hock fragmentation of cholesterol 7α-OOH in the presence of DNPH is acid catalyzed as well (Figure 3.21).

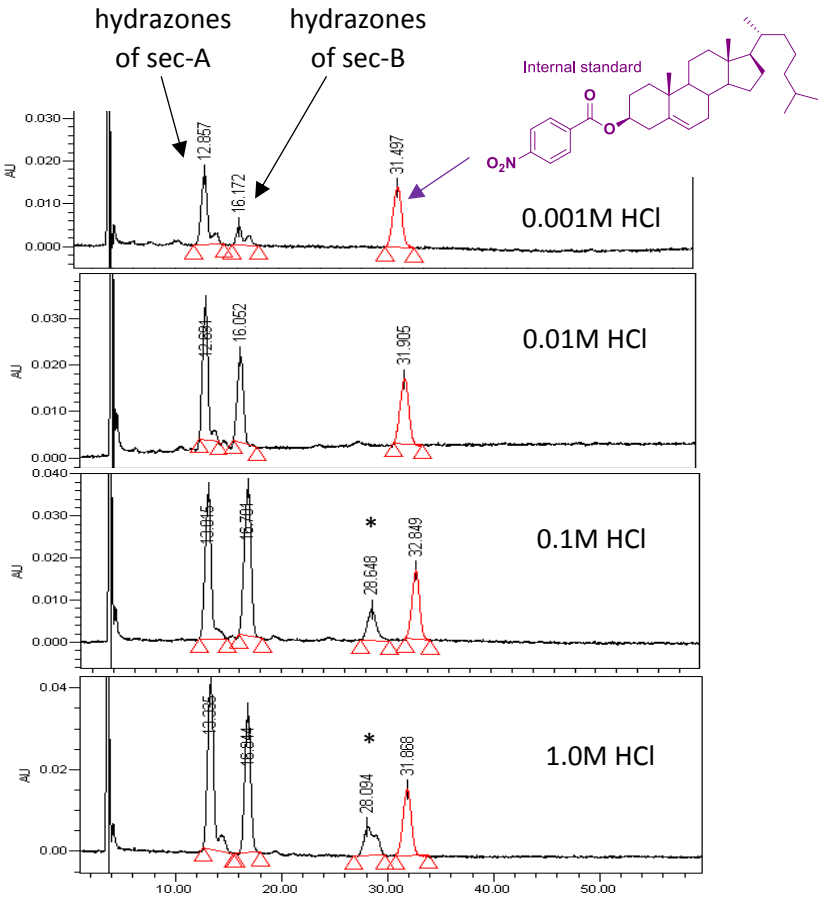

Figure 3.20. Chromatograms of the crude product mixtures of Hock fragmentation of cholesterol 5α-OOH under DNPH derivatization conditions for 2 hours at different acid concentrations. HPLC-UV analyses were performed on a C18 column (5 µm- 4.6 × 150 mm). Mobile phase: 75% ACN, 19% MeOH, 6% H_2O (0.5 mL/min). * Dehydrated hydrazones.

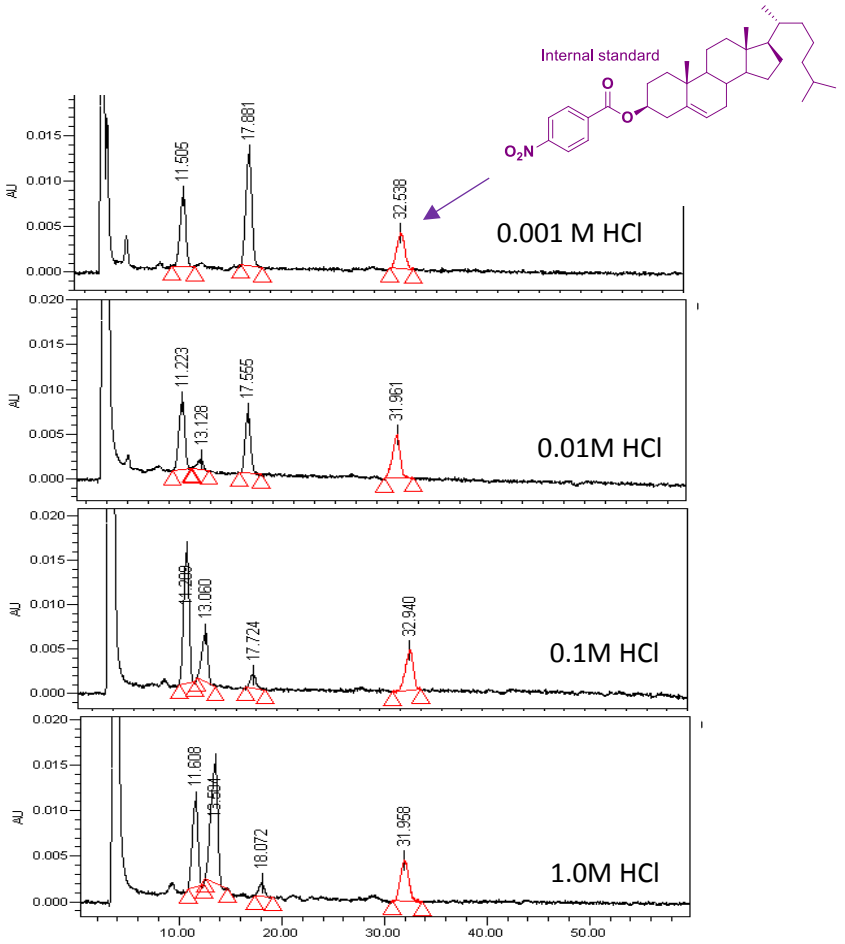

Figure 3.21. Chromatograms of the crude product mixtures of Hock fragmentation of cholesterol 7α-OOH under DNPH derivatization conditions for 2 hours at different acid concentrations. HPLC-UV analyses were performed on a C18 column (5 µm- 4.6 × 150 mm). Mobile phase: 75% ACN, 18% MeOH, 7% H_2O at 0.5 mL/min.

We also studied the effect of DNPH concentration on product stability and distribution, where the reaction was monitored at different DNPH concentrations. Interestingly, DNPH concentration affected the product distribution of Hock fragmentation of cholesterol 5α-OOH. At low DNPH concentrations secosterol-B was the dominant product, while at high DNPH

concentrations secosterol-A was more dominant (Figure 3.22). We performed similar experiment with cholesterol 7α-OOH where at lower DNPH concentrations multiple products were obtained, while at higher DNPH concentrations only three dominant products were observed (Figure 3.23).

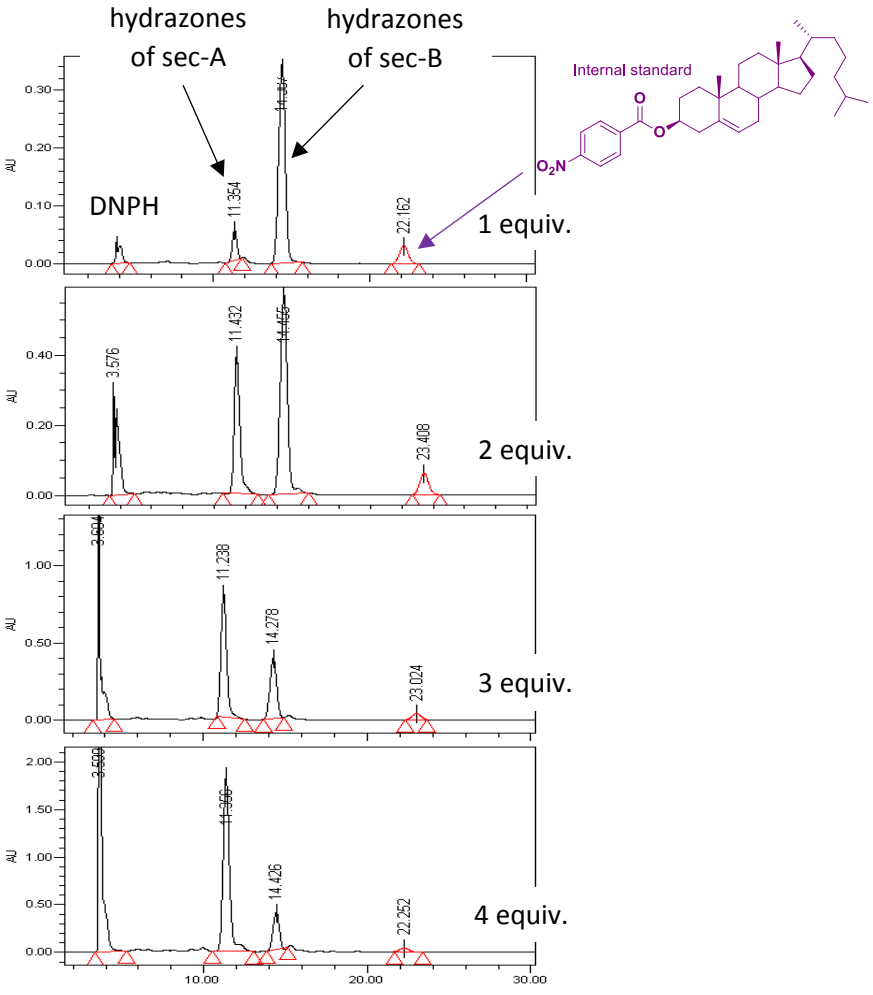

Figure 3.22. Cholesterol 5α-OOH Hock fragmentation under DNPH derivatization conditions for 2 hours at different DNPH concentrations (equivalent amounts relative to cholesterol 5α-OOH). HPLC-UV analyses were performed on a semi-preparative C18 column (5 µm- 10 × 150 mm). Mobile phase: 75% ACN, 18% MeOH, 7% H_2O (4.0 mL/min).

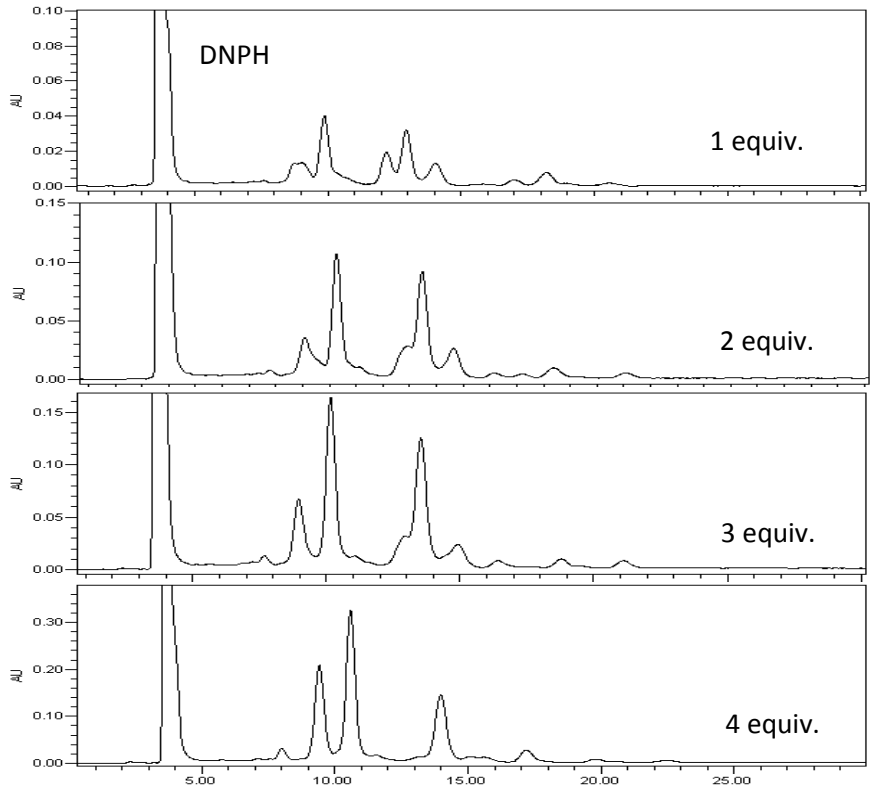

Figure 3.23. Cholesterol 7α-OOH Hock fragmentation under DNPH derivatization conditions for 2 hours at different DNPH concentrations (equivalent amounts relative to cholesterol 7α-OOH). HPLC-UV analyses were performed on a semi-preparative C18 column (5 µm- 10 × 150 mm). Mobile phase: 75% ACN, 18% MeOH, 7% H_2O at 4.0 mL/min. N.B. Internal standard was not included.

3.3 Discussion

Wentworth and co-workers proposed that the cholesterol-derived carbonyls detected in atherosclerotic plaques and brain tissues are generated via ozonolysis of cholesterol. Herein we propose that the Hock fragmentation of cholesterol 7-OOH, the main product of cholesterol autoxidation, can also generate cholesterol-derived carbonyls, albeit without the requirements of the high energy molecules such as O_3 and $^1O_2$.

In our preliminary studies of the Hock fragmentation of cholesterol 7α-OOH, we observed the incapability of cholesterol 7α-OOH to undergo Hock fragmentation in acetonitrile and chloroform using TFA and PTSA, respectively. Hock fragmentation of cholesterol 7α-OOH appeared to be most successful with HCl in alcoholic solvents. We speculate that since the equilibrium for the protonated hydroperoxide would be very poor in a non-polar and/or non-protic solvents and since this equilibrium precedes rate-determining fragmentation, we observed better results in alcoholic solvents (Scheme 3.4). We also speculate that cholesterol 5α-OOH can undergo Hock fragmentation in non-alcoholic solvents because the barrier of its rate-determining step is lower due to its more stable oxocarbenium ion character in the transition state (Scheme 3.5).

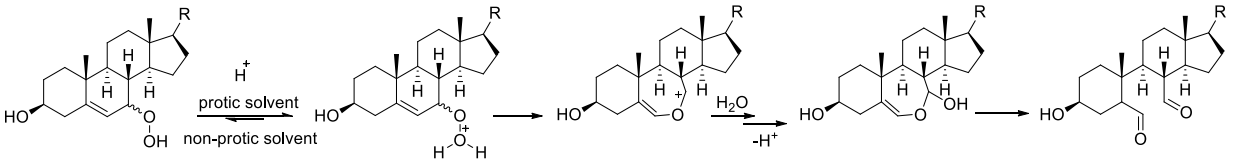

Scheme 3.4. Proposed mechanism of the Hock fragmentation of cholesterol 7-OOH where the intermediate oxocarbenium ion is shown.

As a matter of fact, previous DFT calculations done in our group showed that the intermediate oxocarbenium ion derived from cholesterol 5α-OOH Hock fragmentation has a minimum energy that is around 5 kcal/mol lower than the oxocarbenium ion derived from cholesterol 7α-OOH.[17] This also supports the overall slower rate of the Hock fragmentation of cholesterol 7α-OOH compared to the Hock fragmentation of cholesterol 5α-OOH observed in our kinetic study (Figure 3.11).

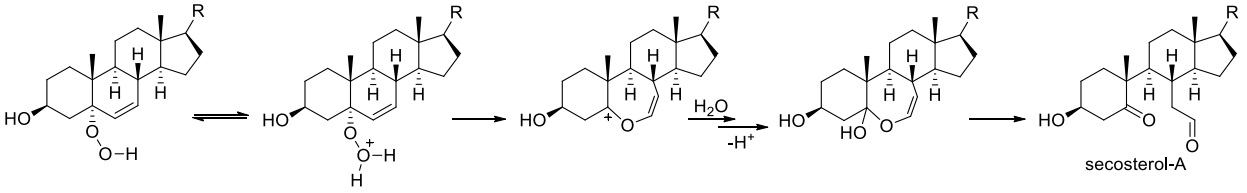

Scheme 3.5. Proposed mechanism of the Hock fragmentation of cholesterol 5α-OOH where the intermediate oxocarbenium ion is shown.

Cholesterol 7α-OOH was converted to 7-ketocholesterol and 7α-hydroxycholesterol after 32 hours in TFA and acetonitrile (Figure 3.3). The 1.26:1 ratio of 7α-hydroxycholesterol to 7-ketocholesterol prompted us to propose the Russell mechanism where self-reaction of two cholesterol 7α-peroxyl radicals (cholesterol 7α-OO•) forms a linear tetraoxide intermediate which upon decomposition, generates singlet oxygen, 7-ketocholesterol and 7α-hydroxycholesterol (Scheme 3.6). This has been observed before by Uemi *et. al.* in 2011 where they observed a Russell-like reaction of cholesterol 7α-OO•.[18] Their chemiluminescence studies showed an emission band with a maximum intensity at 1270 nm, characteristic of $^1O_2$ decay, suggesting that $^1O_2$ was formed alongside 7-ketocholesterol and 7α-hydroxycholesterol which were monitored by HPLC/MS/MS with UV detection at 210 nm.

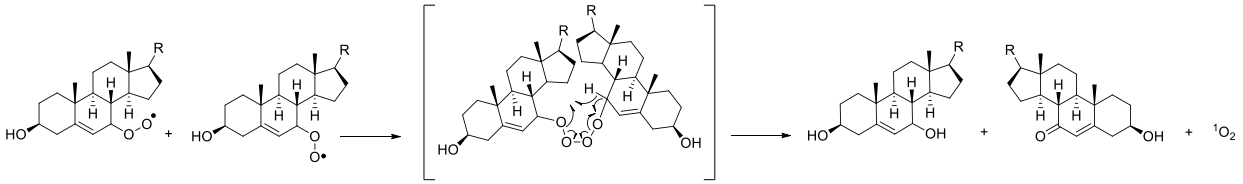

Scheme 3.6. Russell mechanism of the self-reaction of cholesterol 7-peroxyl radical generating singlet oxygen, 7-ketocholesterol and 7-hydroxycholesterol.

However, Uemi and co-workers observed these products by introducing cerium ions (Ce^{4+}) to a solution of cholesterol 7-OOH to generate cholesterol 7-OO•, while our reaction mixture consisted of only acetonitrile, cholesterol 7α-OOH and TFA. Hence, in our case it may be that the concentration of cholesterol 7-OO• was too low to undergo Russell termination at a significant rate. However, both 7-ketocholesterol and 7α-hydroxycholesterol could also be

generated via other pathways. 7-ketocholesterol could also be generated via dehydration of cholesterol 7-OOH and 7α-hydroxycholesterol could form via homolytic bond cleavage of cholesterol 7-OOH by heat or light. Therefore, it seems fortuitous that peroxyls derived from autoxidation terminate via the Russel mechanism and yield the same products in a 1:1 ratio.

The Hock fragmentation of cholesterol 7α-OOH in the presence of DNPH provided three dominant hydrazones. One of the products was the DNPH-derivatized 7-ketocholesterol (Unknown-C, cf. Figures 3.5 & 3.9). 7-Ketocholesterol is a well known product of cholesterol 7α and 7β-OOH dehydration that has been detected in human atherosclerotic plaques.[19, 20, 21] As a matter of fact, quantitative analysis of total oxysterols in human femoral plaques,[22] atherosclerotic plaques,[23] and oxidized LDL[24] showed that 7-ketocholesterol is one of the major oxysterols *in vivo*. However, surprisingly, Wentworth and co-workers never reported the presence of 7-ketocholesterol in their atherosclerotic plaque assay. This again prompts some skepticism regarding the rigour of the detection/identification techniques that were used by Wentworth and co-workers.

We had a very hard time to assign the structures of the two other isolated products (Unknown-A and Unknown-B, cf. Figure 3.5), even by employing a number of spectroscopic techniques such as ^{13}C NMR, DEPT-90, DEPT-135, COSY, HMQC and ESI-MS (Appendix I). This not only shows the complexity of the structure but also shows that in some cases spectroscopic techniques are inadequate in assigning a structure unambiguously. Additionally, the yield of the hydrazones was consistently low, which made the attempts to obtain crystals for x-ray structural determination difficult.

In our kinetic studies, we showed that the rate of the Hock fragmentation of cholesterol 5α-OOH is faster than cholesterol 7α-OOH. This is presumably due to the more stable oxocarbenium ion character in the transition state of the Hock fragmentation of cholesterol 5α-OOH as opposed to the less stable oxocarbenium ion character in the transition state of the Hock fragmentation of cholesterol 7α-OOH (Schemes 3.4 and 3.5).

The effect of BHT on the Hock fragmentation of cholesterol 7α-OOH (Figure 3.14) was also studied. BHT is known to slow radical rearrangement of cholesterol 5α-OOH to cholesterol 7α-OOH. The radical rearrangement is believed to be a step-wise mechanism, where initial H-atom abstraction from the hydroperoxide yields a peroxyl radical. β-fragmentation of oxygen occurs and the dioxygen moiety migrates across the same face from C5 to C7.[25, 26] This is slowed in the presence of BHT, since the peroxyl radical formed in the first step will abstract a labile H-atom from BHT to regain the hydroperoxide (Scheme 3.7).

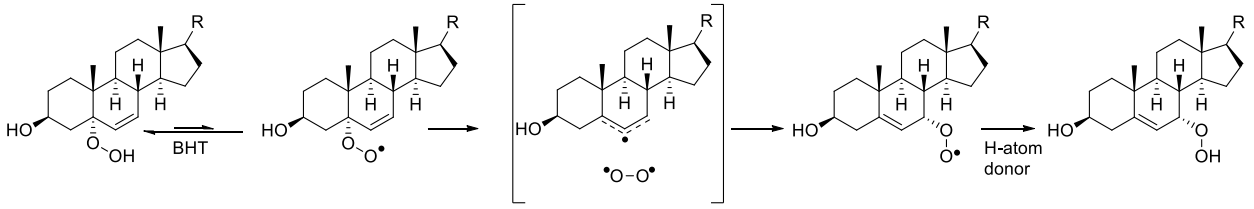

Scheme 3.7. Radical rearrangement of cholesterol 5α-OOH to cholesterol 7α-OOH.

Cholesterol 7α-OOH can also undergo rearrangement to generate cholesterol 7β-OOH. The mechanism of radical rearrangement of cholesterol 7α-OOH to cholesterol 7β-OOH is very similar to the one shown in Scheme 3.7, except O_2 migration is not concerted- the O_2 in this case must diffuse away and reattach from the other face, making it a slow process. [27] In fact, even in

the absence of BHT, there is not enough cholesterol 7β-OOH formed to affect the rate of Hock fragmentation of cholesterol 7α-OOH. Therefore, it was not surprising that cholesterol 7α-OOH Hock fragmentation was not affected in the presence of BHT. Nevertheless, autoxidation of cholesterol in biological systems generates more of the β-isomer than the α-isomer,[28, 29] therefore, we also studied the rate of the Hock fragmentation of cholesterol 7β-OOH in comparison to cholesterol 7α-OOH. Cholesterol 7β-OOH did not undergo Hock fragmentation in 0.001 M HCl at a noticeable rate (Figure 3.15).

Cholesterol 7α-OOH upon protonation fragments to form the corresponding α-epoxy carbenium ion while cholesterol 7β-OOH upon protonation fragments to form the corresponding β-epoxy carbenium ion. The α-epoxy carbenium ion is 4.2 kcal/mol lower in enthalpy than the β-epoxy carbenium ion.[§] This is likely due to the diaxial interaction between the epoxide and the C10-methyl group (which would also be present, though maybe to a lesser extent, in the transition state) (Scheme 3.8). Also, the α-epoxy carbenium ion has the A ring in a chair conformation and the B ring in a twist-boat conformation. The less stable β-epoxy carbenium ion has both the A and B rings in half-chair conformations. Interestingly, in both cases, you can see the H_2O prefers to be near C7, where it would attack to perform the Hock fragmentation (Scheme 3.24).

[§]All the DFT calculations were carried out by Zosia Zielinski, a doctoral candidate in the Pratt group.

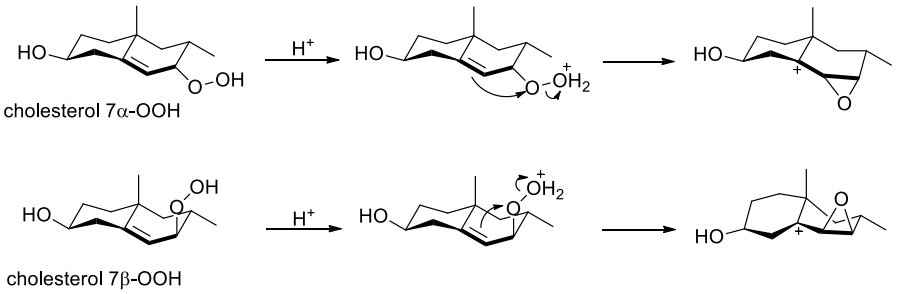

Scheme 3.8. Proposed mechanism of α-epoxy and β-epoxy carbenium ion intermediates via the Hock fragmentation of cholesterol 7α- and 7β-OOH respectively.

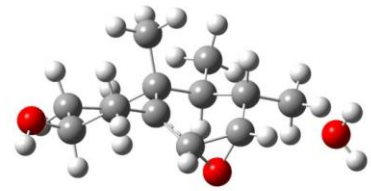

α-epoxy carbenium ion (side)

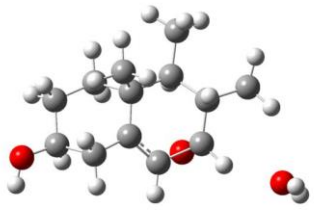

α-epoxy carbenium ion (top)

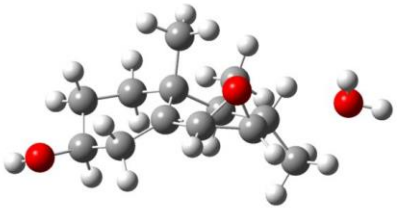

β-epoxy carbenium ion (side)

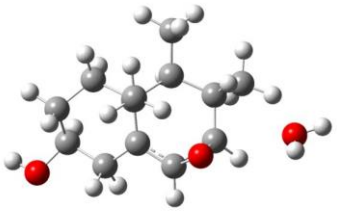

β-epoxy carbenium ion (top)

Figure 3.24. Conformations adapted by cholesterol 7-OOH-derived epoxy carbenium ions. α-epoxy carbenium ion obtained from cholesterol 7α-OOH is 4.2 kcal/mol lower in energy than β-epoxy carbenium ion generated from cholesterol 7β-OOH. Water molecule near the C7 is also shown.

Cholesterol 7α and 7β-OOH in acidic conditions can not only undergo Hock fragmentation, but they also can undergo dehydration to form 7-ketocholesterol. In our kinetic studies (in the absence of DNPH) we only observed a small growth of the vinyl peak corresponding to 7-ketocholesterol. We speculated that the acid concentration in our kinetic study might have been too low to catalyze cholesterol 7α-OOH dehydration. This, however, might be in contradiction to the reported abundance of 7-ketocholesterol amongst other oxysterols in biological systems. Firstly, in neutral pH of biological systems, 7-ketocholesterol can also be formed via enzymatic reactions of cholesterol with 11β-hydroxysteriod dehydrogenase type 1. Secondly, 7-ketocholesterol is relatively more stable and can accumulate in biological systems for a longer time, resulting in their higher concentration *in vivo*.

In the presence of DNPH, the hydrazone derived from 7-ketocholesterol seemed to be one of the major products (Peak-C, cf. Figure 3.5). However, a close examination of our spectra revealed that during the Hock fragmentation of cholesterol 7-OOH in methanol, the amount of aldehyde generated did not correspond to the disappearance of the vinyl peak of cholesterol 7-OOH. Therefore, misleadingly, the amount of 7-ketohydrazone relative to other hydrazones (minor products) seemed to be of significance.

We also studied what effect, if any, DNPH concentration had on product distributions of hydrazones in both cholesterol 5α-OOH and cholesterol 7α-OOH Hock fragmentation. At high DNPH concentration, DNPH-derivatized secosterol-A was the major product, while at low DNPH concentration DNPH-derivatized secosterol-B was the major product. This can be justified by considering the fate of secosterol-A that can either be derivatized or aldolized. At high DNPH concentration, secosterol-A undergoes faster derivatization, which most likely can cyclise at

slower rates due to steric and electronic interactions. At low DNPH concentration the aldolization pathway likely predominates, where most of the secosterol-A undergoes aldolization first and then eventually gets derivatized (Scheme 3.9).

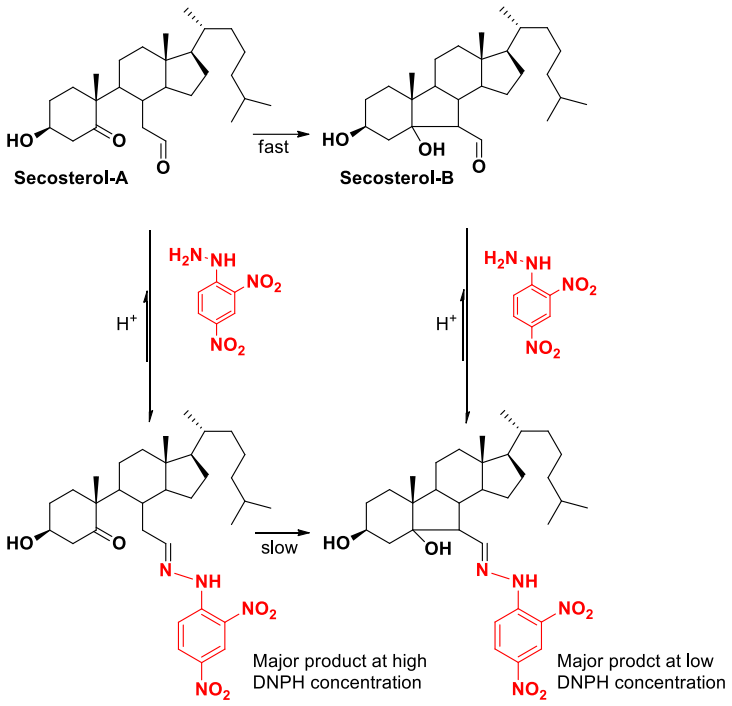

Scheme 3.9. Acid dependence on the formation and hydrolysis of secosterol-A and secosterol-B.

DNPH concentration also affected the distribution of hydrazones derived from the Hock fragmentation of cholesterol 7α-OOH. This again can be explained by the availability of DNPH to derivatize structures and stabilize them to slow down any side reactions and formation of secondary products. At high DNPH concentration we observed three dominant peaks which are presumably primary products. Under high DNPH concentration, the initially formed Hock products get derivatized immediately upon their formation, hence they have less chance to undergo intra- and intermolecular reactions to form any secondary products. We also showed

that the Hock fragmentation of cholesterol 5α-OOH and cholesterol 7α-OOH under DNPH conditions are acid catalyzed as by increasing the acid concentration the amount of corresponding Hock products increased.

We observed a greater amount of DNPH starting material in cholesterol 7α-OOH chromatograms than cholesterol 5α-OOH. At first glance, we predicted that this could be due to the faster rate of the Hock fragmentation of cholesterol 5α-OOH compared to cholesterol 7α-OOH. However, given the acid concentration involved (1 M HCl) and the length of the reaction (2 hours) this is probably not the case, since the half-life of cholesterol 7α-OOH in a less acidic solution (0.01 M HCl) is less than 5 minutes. Instead, it might suggest that hydrazone-hydrazine equilibrium might be relevant here. However, looking back at our spectra, it seems that although Hock fragmentation of cholesterol 7α-OOH proceeds readily, aldehydes are not major products. Therefore, it is unlikely that inefficiency of Hock fragmentation or derivatization caused higher unreacted DNPH concentration and overall lower yield of collected hydrazones. We believe that during acid-catalyzed Hock fragmentation of cholesterol 7-OOH in methanol the mass was going elsewhere, which will be discussed in more detail in chapter 4.

At last our results highlighted the experimental design flaws in Wentworth and co-worker's studies. By derivatizing the specimen, they eliminated a wide range of products from their sample. They only were able to detect hydrazones, while other oxysterols which lacked an aldehyde group were left undetected. Those undetected structures could have been the key to understanding the formation of secosterols.

3.4 Experimental

Materials and methods: All chemicals and solvents were purchased from Sigma Aldrich Co. LLC and used as received, unless otherwise stated. 2,6-di-tert-4-methylphenyl (BHT) was purified by recrystallization from hexane prior to use. 2,4-dinitrophenylhydrazine (DNPH) was purified by recrystallization from n-butane prior to use. ^{1}H-NMR spectra were collected on a Bruker AVANCE -500, -400 and -300 spectrometers. Reverse-phase HPLC was carried out on Waters XBridge Semi-preparative C18, 5 µm (10 × 150 mm) and Atiantis C18, 5 µm (4.6 × 150mm) columns. Normal-phase HPLC was carried out on XTerra, 5 µm (4.6 × 150mm) and SunFire, 5µm(4.6 × 250mm). HPLC graded solvents were used for mobile phases. LC/MS data were obtained on a Water Alliance equipped with TQD operating in the negative ion mode.

cholesterol 5α-OOH: Rose bengal (14 mg) was added to a mixture of cholesterol (1.0 g) in pyridine (15 mL) and the mixture was irradiated by an HPS 400 W sodium lamp while oxygen was bubbled though at 0 °C for 6 hours. BHT (0.6 g) was added to the resulting mixture and stirred for another 20 minutes at room temperature. The reaction mixture was concentrated under vacuum to give a completely dry red solid residue. The residue was dissolved in chloroform and adsorbed on silica (1.0 g). Chloroform was removed under vacuum and the product-coated silica was added on top of the preparative silica column (ether: hexane, 1:1) to give pure cholesterol 5α-OOH as white powder-like crystals (60% yield). ^{1}H-NMR (400 MHz, $CDCl_3$) δ 5.81 (dd, *J*=2.4, 10.1 Hz, 1H), 5.58 (dd, *J*= 2.7, 10.1 Hz, 1H), 4.10 (m, 1H), 2.5-0.95 (Comp, 28H), 0.93 (s, 3H), 0.89 (d, *J*=6.4 Hz, 3H), 0.85 (dd, *J*= 1.7, 6.4 Hz, 6H), 0.64 (s, 3H). Analytical data were in accordance with those reported in the literature.[30]

Cholesterol 7α-OOH and cholesterol 7β-OOH: A solution of cholesterol 5α-OOH (170 mg) in chloroform (10 mL) was stirred for 12 hours at room temperature. The product mixture was concentrated under vacuum. A preparative silica column (ether: hexane, 1:1) was used to give pure cholesterol 7α-OOH as white crystals (80% yield). To obtain cholesterol 7β-OOH the reaction mixture was stirred for 2 days, but the same work up and purification was employed to give a mixture of cholesterol 7α-OOH and cholesterol 7β-OOH. Cholesterol 7α-OOH: ^{1}H-NMR (500 MHz, $CDCl_3$) δ 5.70 (dd, *J*=1.8, 5.0 Hz, 1H), 4.14 (td, *J*= 1.7, 4.7 Hz, 1H), 3.60 (m, 1H), 2.50-0.98 (Comp, 28H), 0.97 (s, 3H), 0.89 (d, *J*=6.7 Hz, 3H), 0.85 (dd, *J*= 2.7, 7.0 Hz, 6H), 0.64 (s, 3H). Cholesterol 7β-OOH: ^{1}H-NMR (300 MHz, CD_3OD) δ 5.50 (t, *J*=1.9, 1H), 3.90 (m, 1H), 3.40 (m, 1H), 2.50-0.98 (Comp, 28H), 0.90 (s, 3H), 0.85 (d, *J*=6.7 Hz, 3H), 0.85 (dd, *J*= 2.7, 7.0 Hz, 6H), 0.65 (s, 3H). Analytical data were in accordance with those reported in the literature.[26]

Hock fragmentation of cholesterol 7α-OOH by Trifluoroacetic acid in acetonitrile: To a solution of cholesterol 7α-OOH (16 mg) in acetonitrile (8 mL), trifluoroacetic acid (29 µL) was added and stirred at room temperature for 4 hours. The resulting mixture was immediately diluted by chloroform and was washed with water multiple times. The organic layer was concentrated under high vacuum. The product mixture was analyzed by ^{1}H-NMR without any further purification.

Hock fragmentation of cholesterol 7α-OOH by p-toluenesolphonic acid in chloroform*:* To a solution of cholesterol 7α-OOH (16 mg) in chloroform (8 mL), *p*-toluenesolphonic acid (70 mg) was added and stirred at room temperature for 4 hours. The resulting mixture was immediately diluted by chloroform and was washed with water multiple times. The organic layer was concentrated under high vacuum. The product mixture was analyzed by ^{1}H-NMR without any further purification.

Hock fragmentation of cholesterol 7α-OOH by hydrochloric acid in iso-Propanol*:* Cholesterol 7α-OOH (10 mg) was dissolved in 1M HCl solution in *iso*-propanol and was stirred at room temperature for 1 hour. The resulting mixture was immediately diluted by chloroform and was washed with water multiple times. The organic layer was concentrated under high vacuum. The product mixture was analyzed by ^{1}H-NMR without any further purification.

Hock fragmentation of cholesterol 7α-OOH under DNPH derivatization condition**:** A solution of DNPH (47 mg) in 0.1 M HCl in methanol (50 mL) was stirred at room temperature to obtain a homogenous solution. Cholesterol 7α-OOH (1.0 g) was added to the mixture and the reaction was stirred at room temperature for another 3 hours. The resulting mixture was immediately diluted by chloroform and was washed with water multiple times. The organic layer was concentrated under high vacuum for several days. Various combination of preparative silica column (ethyl acetate: Hexane, 1:7), preparative TLC (ethyl acetate: hexane, 1:3) and preparative HPLC column (2% isopropanol in hexane with 4 mL/min flow rate) were used to separate and isolate the products. Isolated products and fractions were analyzed by 1D and 2D ^{1}H-NMR's and UPLC-MS.

Hock fragmentation of cholesterol 7α-OOH vs. cholesterol 5α-OOH with HCl in d_4-methanol: Benzyl alcohol (0.2 µl) as an internal standard and BHT (20 mg) were added to a 0.01M HCl solution in d_4-methanol (500 µl). Cholesterol 7α-OOH (4.8 mM) or cholesterol 5α-OOH (4.8 mM) was added to the mixture and was transferred to an NMR tube. The Hock fragmentation of cholesterol 7α-OOH was monitored by ^{1}H-NMR every 5 minutes for 100 minutes. The Hock fragmentation of cholesterol 5α-OOH was monitored by ^{1}H-NMR every 80 seconds for 20 minutes. Conversion was determined by the relative integration of the benzyl alcohol peak to the vinyl peak of cholesterol 7α-OOH or cholesterol 5α-OOH.

***Hock fragmentation of cholesterol 7α-OOH in the absence and presence of BHT with HCl in d_4-methanol*:** Cholesterol 7α-OOH (4.8 mM) was added to a mixture of benzyl alcohol (0.2 µl) and 0.01M HCl solution in d_4-methanol (500 µl). BHT (20 mg) was added to the mixture and the resulting mixture was transferred to an NMR tube. Identical reaction conditions and analysis was used when monitoring the Hock fragmentation of cholesterol 7α-OOH in the absence of BHT where no BHT was added to the mixture. The Hock fragmentation of cholesterol 7α-OOH was monitored by ^{1}H-NMR every 5 minutes for 100 minutes. Conversion was determined by the relative integration of the benzyl alcohol peak to the alkene peak of cholesterol 7α-OOH.

Hock fragmentation of cholesterol 7α-OOH vs. cholesterol 7β-OOH with HCl in d_4-methanol: To a mixture of cholesterol 7α-OOH and cholesterol 7β-OOH (3.2 mM) in d_4-methanol was added benzyl alcohol (0.2 µl) and BHT (20 mg). An HCl solution in d_4-methanol was then added to give the final acid concentration of 0.01M. The mixture was transferred to an NMR tube and was monitored by ^{1}H-NMR every 5 minutes for 60 minutes. Conversion was determined by the relative integration of the benzyl alcohol peak to the alkene peak of cholesterol 7α-OOH.

Hock fragmentation of cholesterol 7α-OOH with HCl in d_4-methanol at different acid concentrations: To a solution of cholesterol 7α-OOH (4.8 mM) in d_4-methanol was added benzyl alcohol (0.2 µl) and BHT (20 mg). An HCl solution in d_4-methanol was then added to give the desired final acid concentration (0.1M, 0.01M and 0.001M) for the final volume of 500 µl. The final mixture was transferred to an NMR tube and was monitored by ^{1}H-NMR. Conversion was determined by the relative integration of the benzyl alcohol peak to the alkene peak of cholesterol 7α-OOH.

Hock fragmentation of cholesterol 7α-OOH vs. cholesterol 5α-OOH under DNPH derivatization condition at different acid concentrations: To a solution of DNPH (6.0 mg) in methanol was added an HCl solution in methanol to give the desired final acid concentration of 1.0 M, 0.1M, 0.01M and 0.001M HCl for the final volume of 2 ml. To the stirring DNPH solution, cholesterol 7α-OOH (4.0 mg) or cholesterol 5α-OOH (4.0 mg) wad added and the mixture was stirred at room temperature for another 3 hours. The internal standard (cholest-5-en-3-ol,4-nitrobenzoate) (1.25 mM) was added to the product mixture and after a quick vortex was immediately injected (10 µl) to a C18 column on an HPLC-UV. Mobile phase of 75% CAN, 19% MeOH, 6% H_2O with 0.5 ml/min flow rate was employed for analysis.

Hock fragmentation of cholesterol 7α-OOH vs. cholesterol 5α-OOH under DNPH derivatization condition at different DNPH concentrations: DNPH was added to 0.1M HCl solution in methanol (5 ml) to give the desired final concentration of DNPH (0.47 mM, 1.2mM, 2.4 mM, 9.5 mM). To the stirring DNPH solution, cholesterol 7α-OOH (5.0 mg) or cholesterol 5α-OOH (5.0 mg) was added and the mixture was stirred at room temperature for another 2 hours. The internal standard (cholest-5-en-3-ol,4-nitrobenzoate) (1.25 mM) was added to the product

mixture and after a quick vortex was immediately injected (10 µl) to a C18 column on an HPLC-UV. Mobile phase of 75% CAN, 19% MeOH, 6% H_2O with 0.5 ml/min flow rate was employed for analysis.

3.5 References

[1] Beckwith, A. L. J.; Davies, A. G.; Davison, I. G. E.; Maccoll, A.; Mruzek, M. H. *J. Chem. Soc. Perkin Trans. II* **1989**, 815.

[2] Zielinski, Z. A. M.; Pratt, D. A. *J. Am. Chem. Soc.* **2016**, 138, 6932.

[3] Brinkhorst, J.; Nara, S. J.; Pratt, D. A. *J. Am. Chem. Soc*. **2008**, 130, 12224.

[4] Brown, A. J.; Jessup, W. *Atherosclerosis* **1999**, 142,1.

[5] Wentworth, P.; Nieva, J.; Takeuchi, C.; Galve, R.; Wentworth, A. D.; Dilley, R. B.; DeLaria, G. A.; Saven, A.; Babior, B. M.; Janda, K. D.; Eschenmoser, A.; Lerner, R. A. *Science* **2003**, 302, 1053.

[6] Deno, N. C.; Billups, W. E.; Kramer, K. E.; Lastomirsky, R. R. *J. Org. Chem.* **1970**, 35, 3080.

[7] Smith, L. L. *Chem. Phys. Lipids*. **1987**, 44, 87.

[8] Kulig, M. J.; Smith, L. L. *J. Org. Chem.* **1973**, 38, 3639.

[9] Korytowski, W.; Girotti, A. W. *Photochemistry and photobiology* **1999**, 70, 484.

[10] Beckwith, A. L.; Davies, A. G.; Davison, I. G. E.; Maccoll, A.; Mruzek, M. H. *J. Chem. Soc., Perkin. Trans. 2* **1989**, 7, 815.

[11] Ronsein, G. E.; Prado, F. M.; Mansano, F. V.; Oliveira, M. C. B.; Medeiros, M. H. G.; Miyamoto, S.; Di Mascio, P. *Anal. Chem.* **2010**, 82, 7293.

[12] Li, Y.; Wu, X.; Bum Lee, T.; Isbell, E. K.; Parish, E. J.; Gorden, A. E. V. *J. Org. Chem*. **2010**, 75, 1807.

[13] Carvalho João, F. S.; Cruz Silva, M. M.; Moreira, J. N.; Simões, S.; Luisa Sá e Melo, M. *J. Med. Chem.* **2009**, 52, 4007.

[14] Uchiyama, S.; Inaba, Y.; Kunugita, N. *J. Chromatogr. B* **2011**, 879, 1282.

[15] Wentworth, P.; Nieva, J.; Takeuchi, C.; Galve, R.; Wentworth, A. D.; Dilley, R. B.; DeLaria, G. A.; Saven, A.; Babior, B. M.; Janda, K. D.; Eschenmoser, A.; Lerner, R. A. *Science* **2003**, 302, 1053.

[16] Yamazaki, S.; Ozama, N.; Hiratsuka, A.; Watanabe, T. *Free Radical Biol. Med*. **1999**, 27, 110.

[17] Lynett, P. T.; Pratt, D. A. unpublished results.

[18] Uemi, M.; Ronsein, G. E.; Fernando, M.; Prado, M.; Motto, F. D.; Miyamoto, S.; Medeiros, M. H. G.; DiMasico, P. *Chem. Res. Toxicol*. **2011**, 24, 887.

[19] Brooks, C. J. W.; Harland, W. A.; Steel, G. *Biochim. Biophys. Acta*. **1966**, 125, 623.

[20] Van Lier, J. E.; Smith, L. L. *Biochemistry* **1967**, 6, 3269.

[21] Carpenter, K. L.; Taylor, S. E.; Ballantine, J. A.; Fussell, B.; Halliwell, B.; Mitchinson, M. J. *Biochim. Biophys. Acta.* **1993**, 1167, 121.

[22] Björkhem, I.; Andersson, O.; Diczfalusy, U.; Sevastik, B.; Xiu, R-J.; Duan, C.; Lund, E. *Proc. Natl. Acad. Sci*. **1994**, 91, 8582.

[23] Smith, L. L.; Teng, J. I.; Lin, Y. Y.; Seitz, P. K.; McGehee, M. F. *Steroid Biochem*. **1987**, 14, 889.

[24] Brown, A, J.; Leong, S-I.; Dean, R. T.; Jessup, W. J. Lipid. Res. 1997, 38, 1730.

[25] Boyd, S. L.; Boyd, R. J.; Shi, Z.; Barclay, L. R. C.; Porter, N. A. *J. Am. Chem. Soc.* **1993**, 115, 687.

[26] Hu, D.; Pratt, D. A. *Chem. Commun.* **2010**, 46, 3711.

[27] Porter, N. In Organic Peroxides. J. Ando, editor. Wiley & Sons, Chichester. 102-155.

[28] Dzeletovic, S.; Babiker, A.; Lund, E.; Diczfalusy, U. *Chem. Phys. Lipids.* **1995**, 78, 119.

[29] Colles, S. M.; Irwin, K. C.; Chisolm, G. M. *J. Lipid Res.* **1996**, 37, 2018.

[30] Ronsein, G. E.; Prado, F. M.; Mansano, F. V.; Oliveira, M. C. B.; Medeiros, M. H. G.; Miyamoto, S.; Mascio, P. D. *Anal. Chem*. **2010**, 82, 7293.

Appendix I

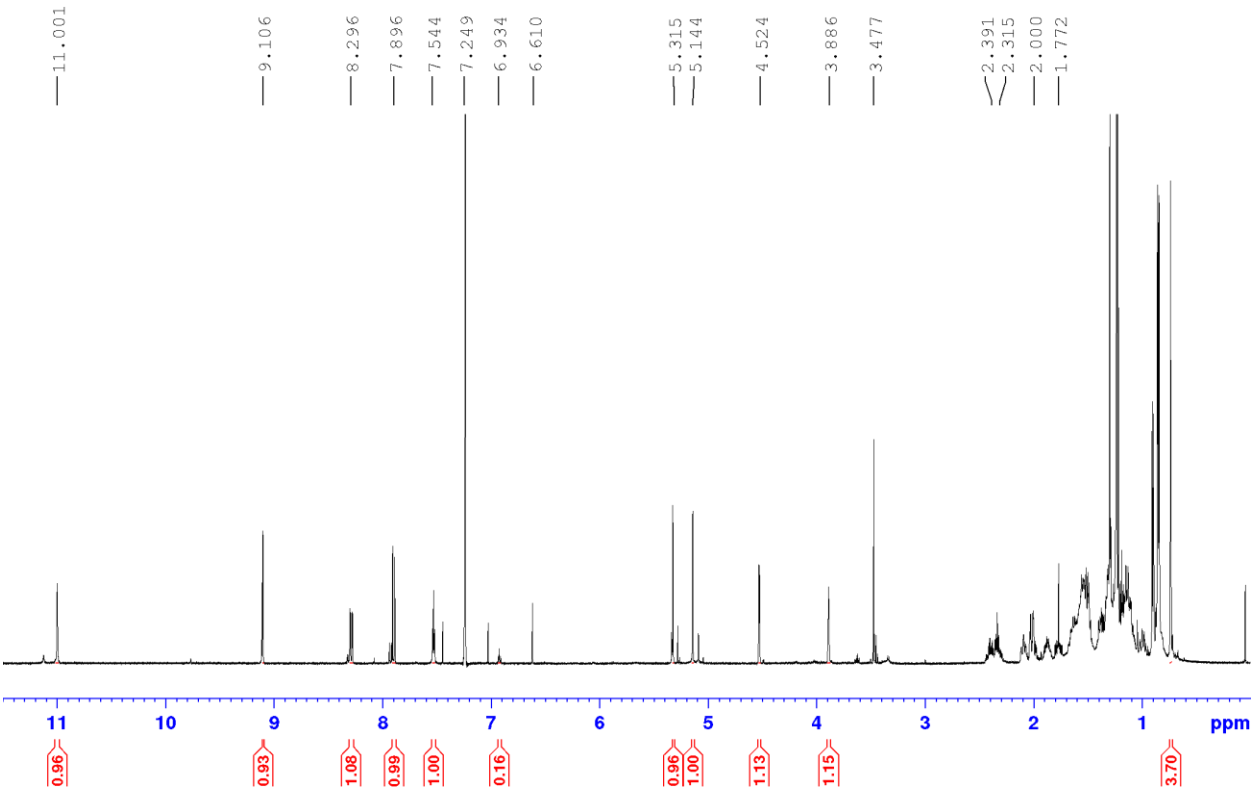

Figure 1. ^{1}H-NMR spectrum of Unknown-A. The spectrum was recorded at 400 MHz with chemical shifts reported in ppm relative to $CDCl_3$.

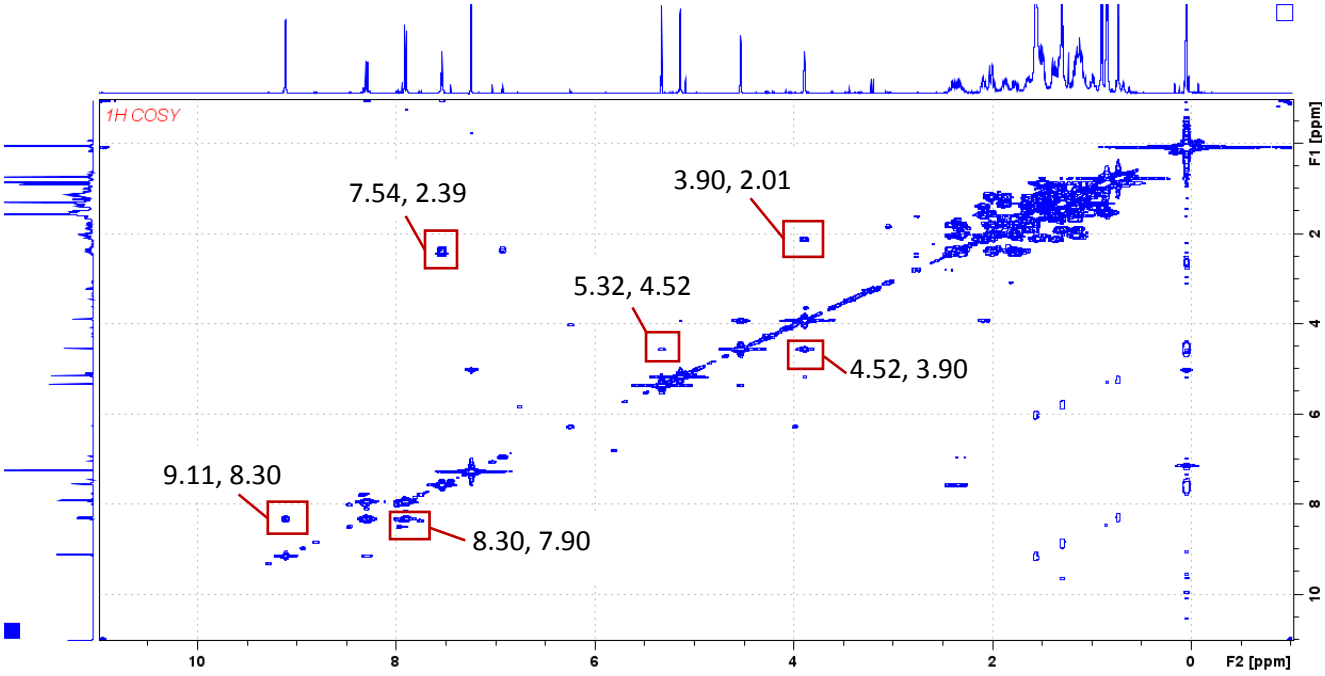

Figure 2. COSY NMR spectrum of Unknown-A. The spectrum was recorded at 400 MHz with chemical shifts reported in ppm relative to $CDCl_3$

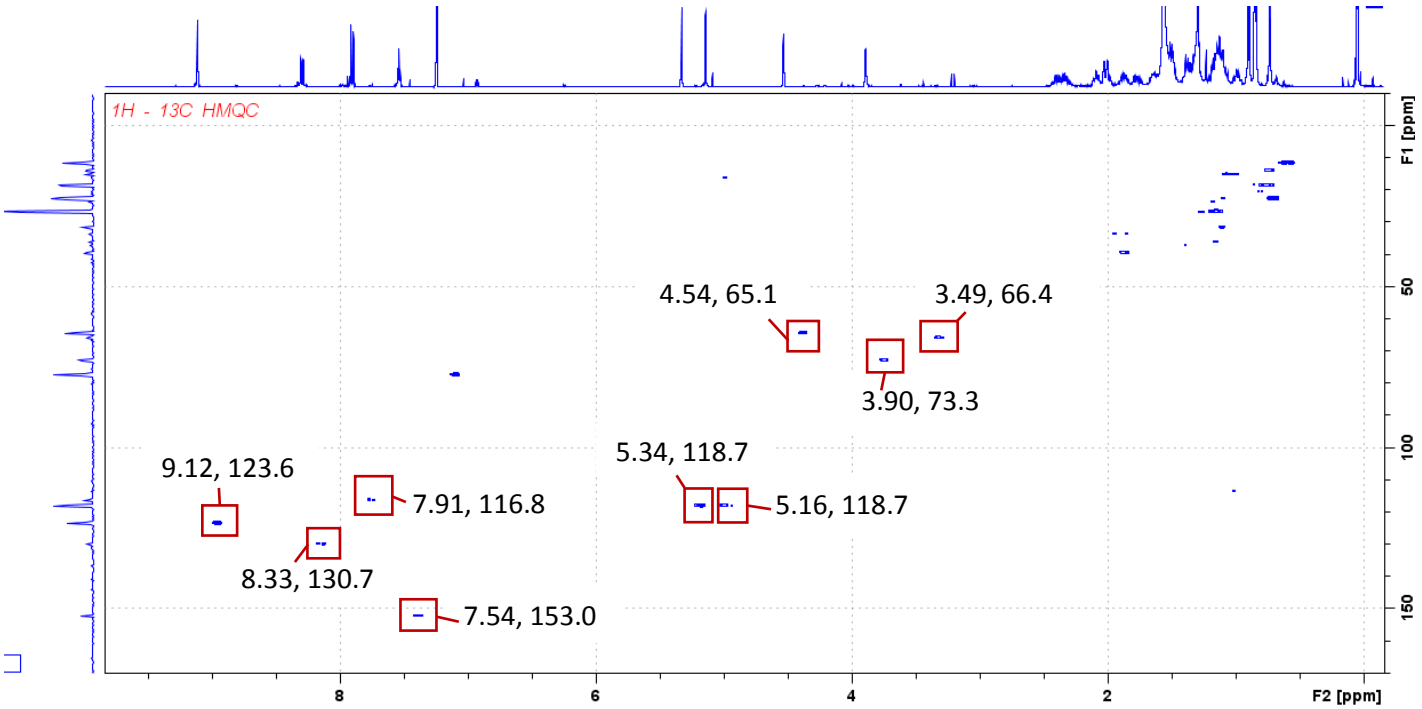

Figure 3. ^{1}H-13C HMQC NMR spectrum of Unknown-A. The spectrum was recorded at 400 MHz with chemical shifts reported in ppm relative to $CDCl_3$.

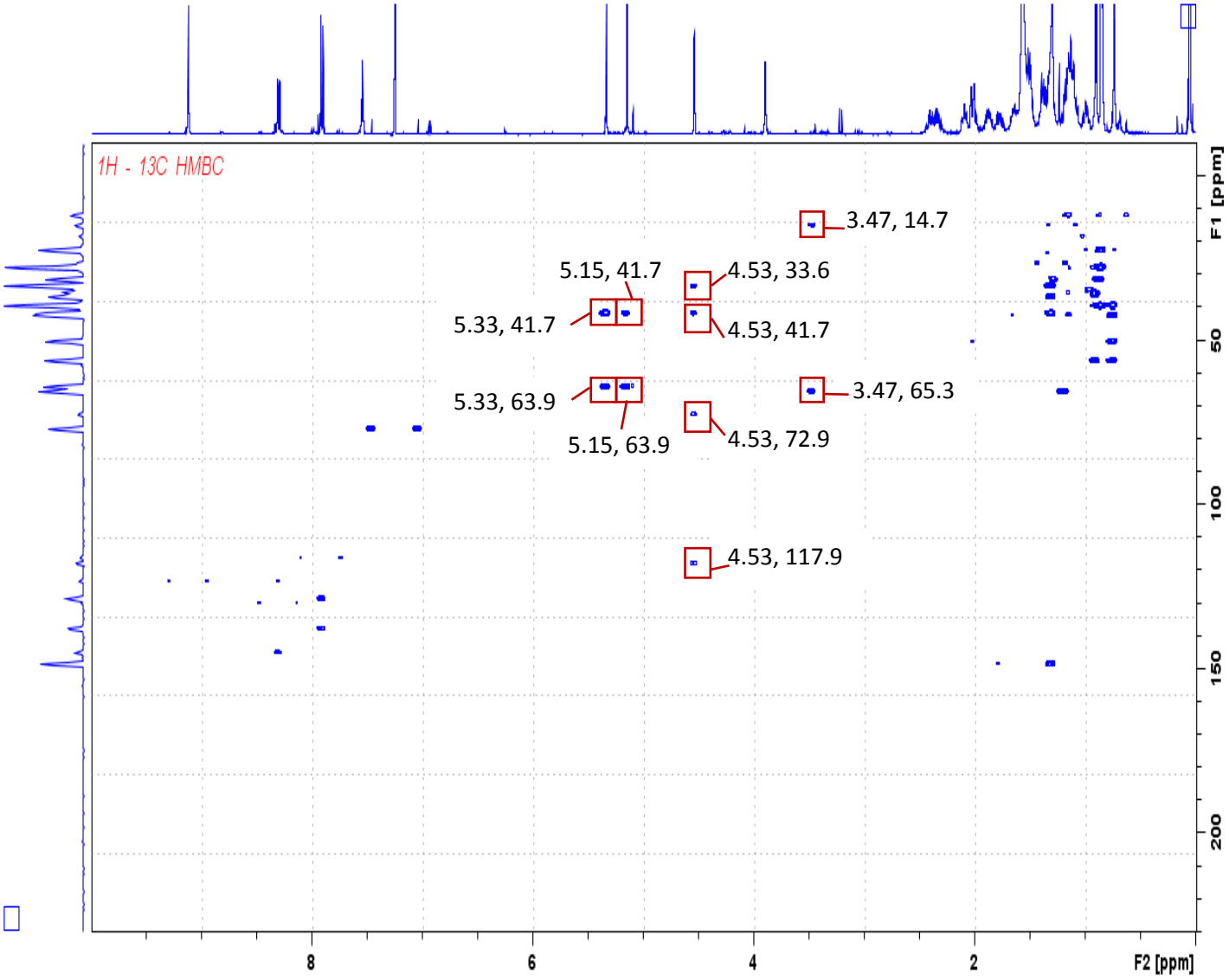

Figure 4. ^{1}H-13C HMBC NMR spectrum of Unknown-A. The spectrum was recorded at 400 MHz with chemical shifts reported in ppm relative to $CDCl_3$.

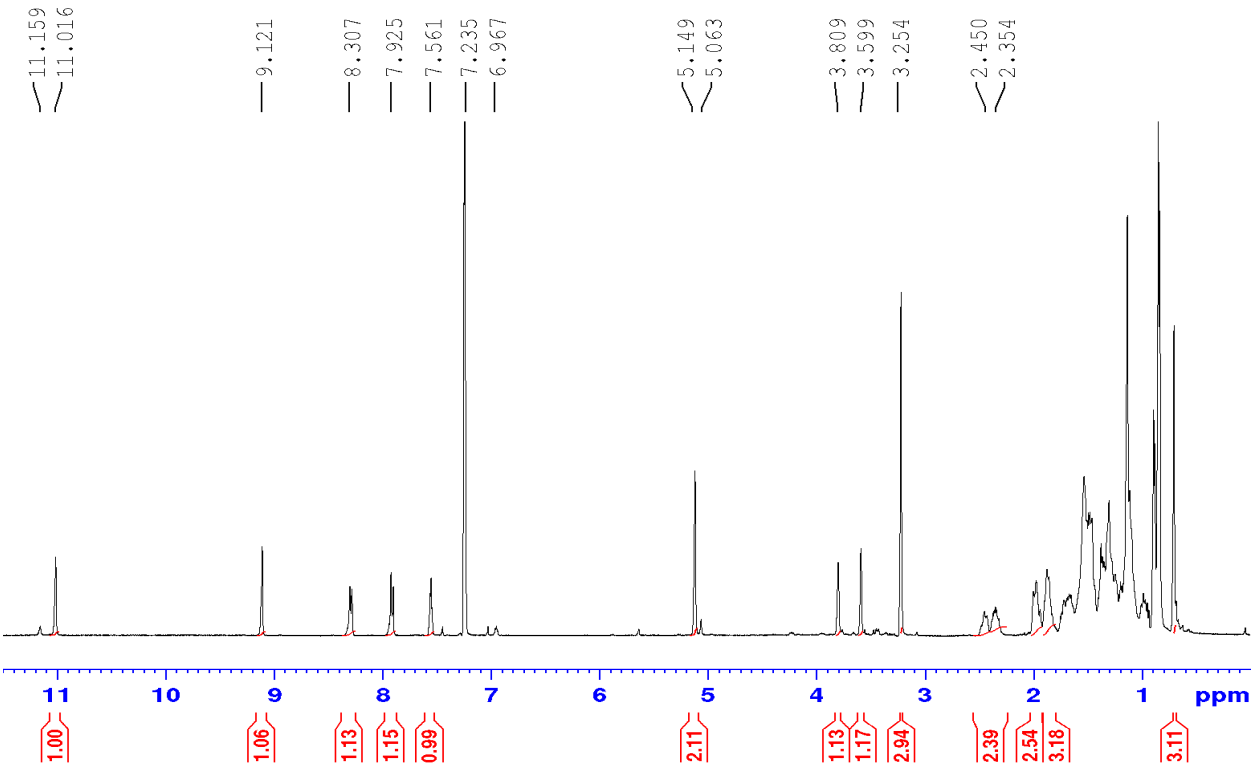

Figure 5. ^{1}H-NMR spectrum of Unknown-B. The spectrum was recorded at 400 MHz with chemical shifts reported in ppm relative to $CDCl_3$.

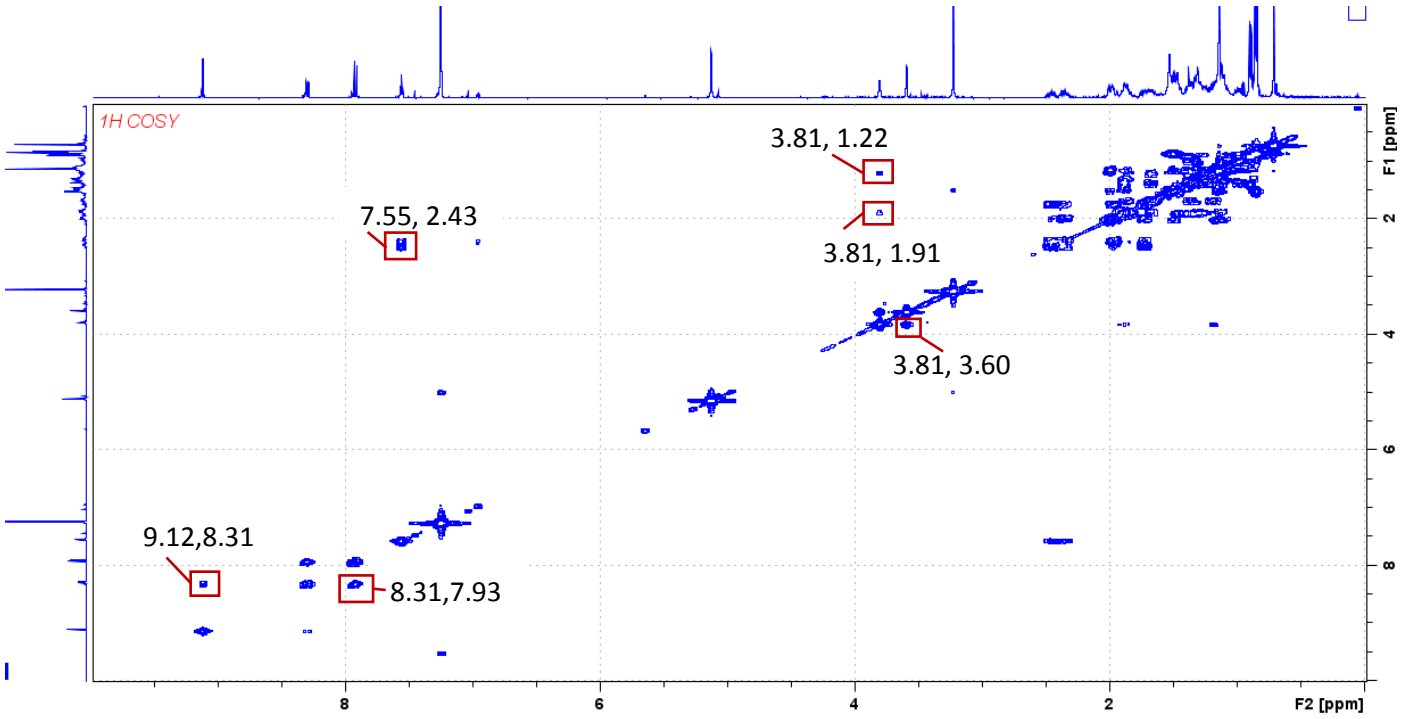

Figure 6. COSY NMR spectrum of Unknown-B. The spectrum was recorded at 400 MHz with chemical shifts reported in ppm relative to $CDCl_3$.

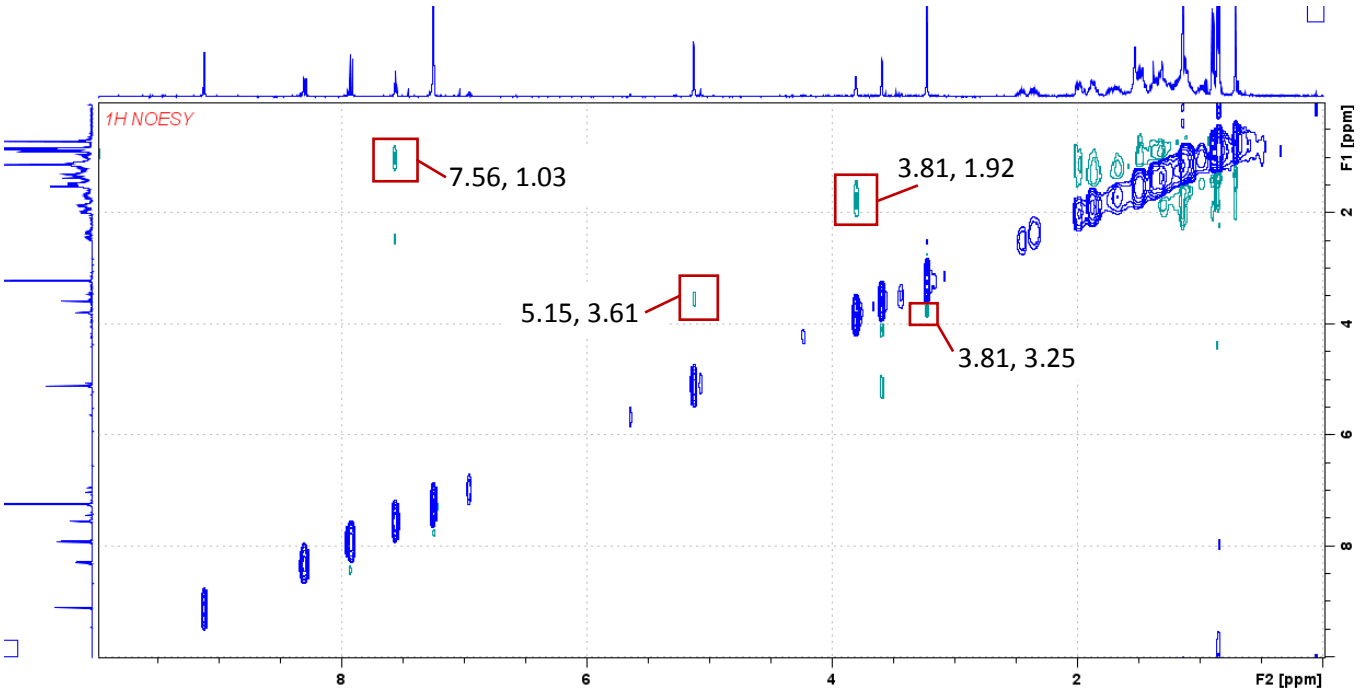

Figure 7. NOESY NMR spectrum of Unknown-B. The spectrum was recorded at 400 MHz with chemical shifts reported in ppm relative to $CDCl_3$.

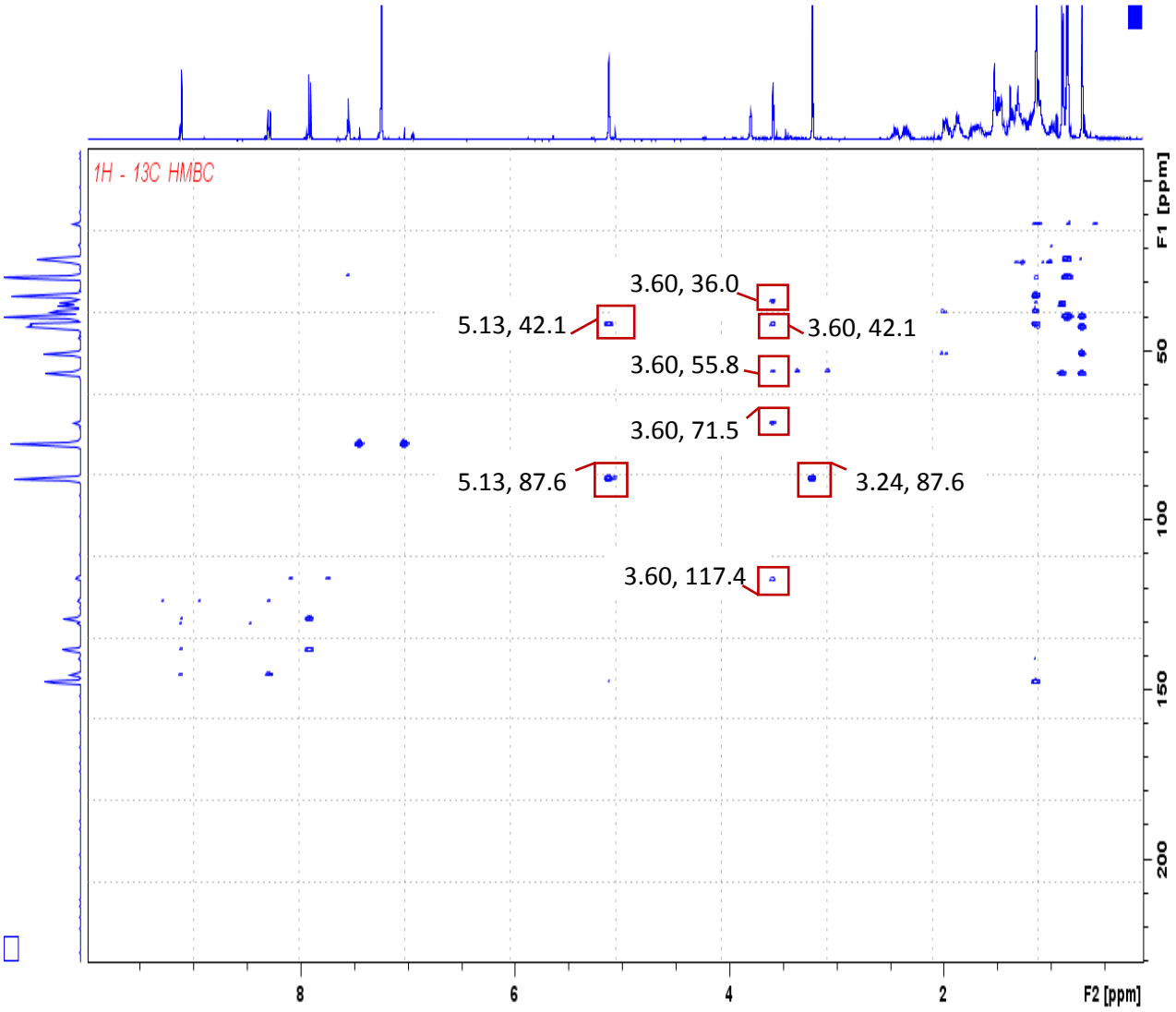

Figure 8. ^{1}H-13C HMBC NMR spectrum of Unknown-B. The spectrum was recorded at 400 MHz with chemical shifts reported in ppm relative to $CDCl_3$.

-4-

An Unexpected Product of Hock Fragmentation of Cholesterol 7-Hydroperoxide

4.1 Introduction

The acid-catalyzed decomposition of peroxides, commonly known as Hock fragmentation, is a very important synthetic process. The reaction starts with the protonation of the β-oxygen which leads to irreversible O-O cleavage, followed by carbon to oxygen rearrangement. Vinyl and aryl groups, especially those with electron donating substituents have greater migratory aptitude, similar to the Baeyer-Villiger oxidation, for this kind of rearrangement.[1, 2]

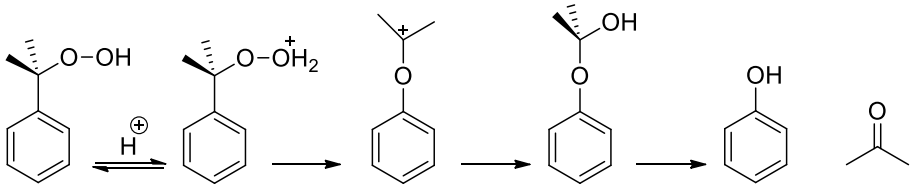

Scheme 4.1. Proposed mechanism for the Hock fragmentation of cumene hydroperoxide to generate phenol and acetone.

The Hock fragmentation of lipid hydroperoxides is widely believed to be involved in the formation of reactive carbonyl compounds in biological systems. For example, 4-hydroxynonenal (4-HNE), an α,β-unsaturated hydroxyalkenal, is generated via the Hock fragmentation of arachidonic or linoleic hydroperoxides. 4-HNE has been linked in the pathophysiology of atherosclerosis, Alzheimer disease and cancer.[3, 4]

In our studies of the acid-catalyzed Hock fragmentation of cholesterol 7α-OOH, we showed that cholesterol 7α-OOH can successfully undergo Hock fragmentation under acidic conditions. For easier detection and isolation, we derivatized the product mixture by 2,4-dinitrophenylhydrazine (DNPH). We were able to isolate two of the hydrazones, which were

analyzed by ^{1}H-NMR, ^{13}C-NMR, DEPT-90, DEPT-135, COSY, HMQC and ESI-MS. Unexpectedly, the obtained data did not correspond to any of our anticipated products (Scheme 4.2) and due to their complex structure we were not able to fully characterize them. Additionally, the yield of the hydrazones was consistently low, which made the attempts to obtain crystals for X-ray structural determination difficult.

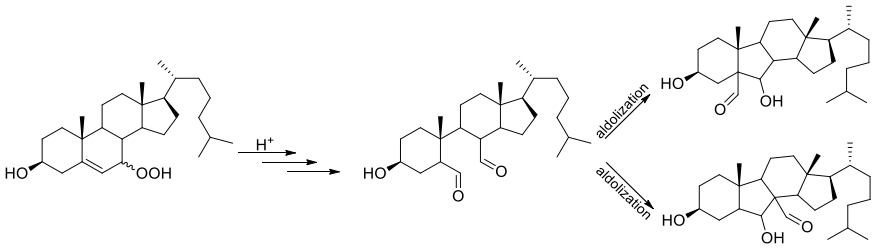

Scheme 4.2. Anticipated products of the acid-catalyzed Hock fragmentation of cholesterol 7-OOH.

At last we were able to crystalize the major product of the Hock fragmentation of cholesterol 7α-OOH which was not a hydrazone. It was an epoxide structure that could potentially be the first evidence for an intermediate in the Hock fragmentation reaction.

4.2 Results

Cholesterol 7α-OOH was prepared by radical rearrangement of cholesterol 5α-OOH and was subjected to acid catalyzed Hock fragmentation under typical DNPH derivatization conditions (see Chapter 3).[5] The crude product mixture was concentrated under vacuum. The concentrated crude product was then dissolved in a mixture of benzene and methanol which yielded crystals when left overnight at room temperature. The corresponding ^{1}H-NMR spectra of the crystals showed that the compound is not a hydrazone (Figure 4.1).

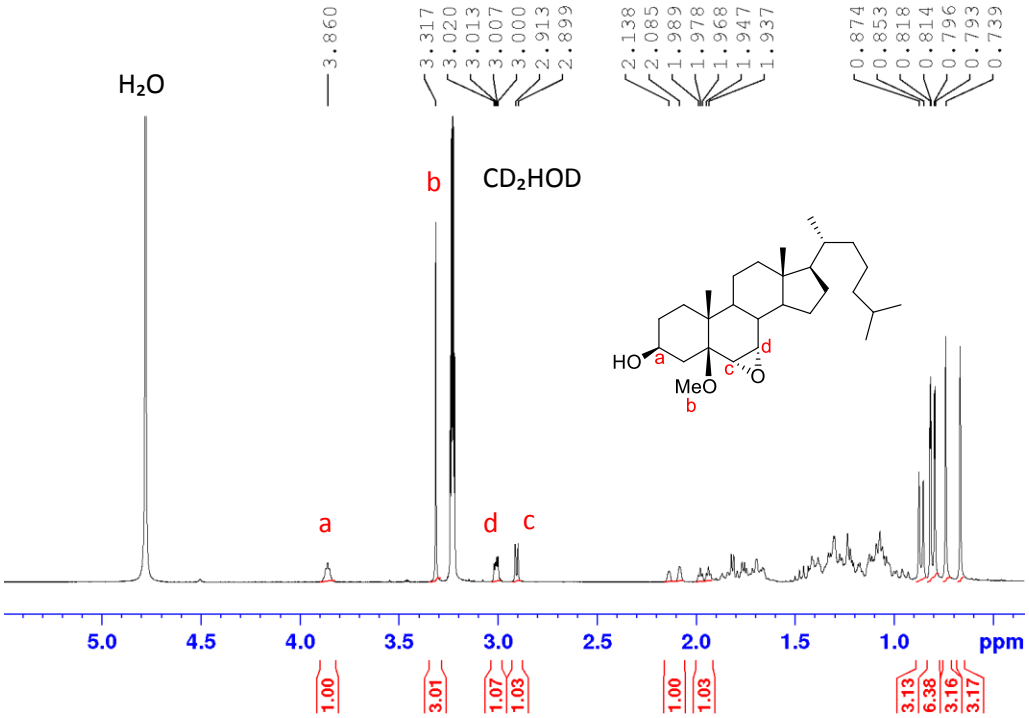

Figure 4.1. ^{1}H-NMR spectrum of 6,7-epoxy-5β-methoxycholesterol, the major product of the Hock fragmentation of cholesterol 7α-OOH in MeOH. The spectrum was collected at 400 MHz with chemical shifts reported in ppm relative to CD_3OD.

We also carried out x-ray crystallographic analysis. According to the X-ray data, the structure lacked any aldehyde or ketone moiety to be derivatized with DNPH; however, it had an epoxide moiety attached to C6 and C7 and a β-methoxy group attached to C5 corresponding to 6,7-epoxy-5β-methoxycholesterol (Figure 4.2).

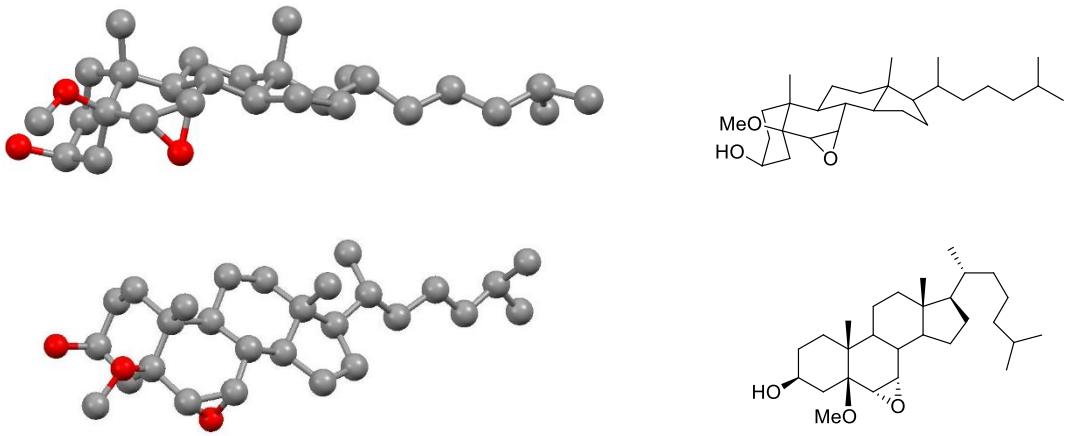

Figure 4.2. 3D structure of the 6,7-epoxy-5β-methoxycholesterol. For simplicity hydrogens are not shown, gray represents carbon and red represents oxygen. Analysis was done at 200 k with wavelength of 0.71073 Å and Orthohombic crystal system.

Since epoxides are, in general, electrophilic species, we wondered whether DNPH could still be incorporated under the derivatization conditions. Hence, we dissolved 6,7-epoxy-5β-methoxycholesterol in methanol with 0.1 M HCl and 3 equivalents of DNPH and monitored the reaction by ^{1}H-NMR for 12 hours. Although the epoxide peaks gradually disappeared, we did not observe signals associated with incorporation of the DNPH moiety. However, we observed the growth of two peaks as the epoxide peaks were disappearing which we speculated to correspond to the hydrolysis of epoxide (Figure 4.3).

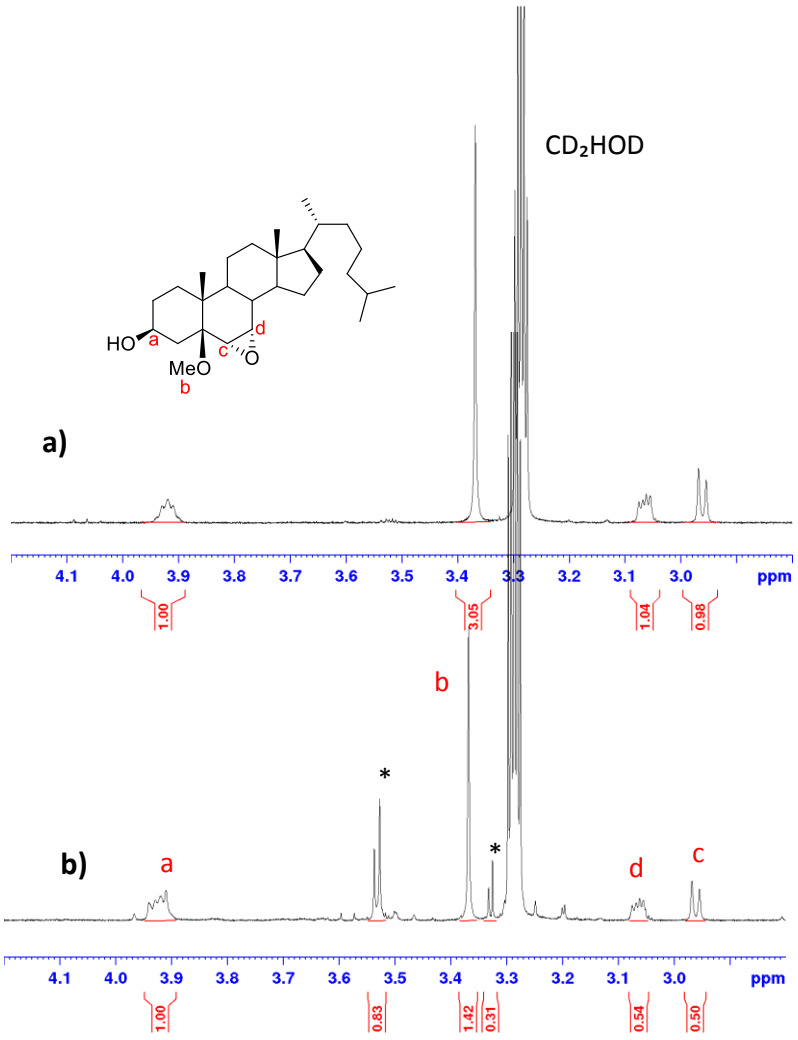

Figure 4.3. ^{1}H-NMR spectrum of 6,7-epoxy-5β-methoxycholesterol dissolved in 0.1 M HCl in d_4-methanol and DNPH solution. a) Immediately after addition of acid, b) 12 hours after addition of acid. The spectrum was collected at 400 MHz with chemical shifts reported in ppm relative to CD_3OD. * Proposed hydrolysis products.

We were also curious to know if the epoxide was only an artifact of our reaction conditions. Therefore, we looked at the product mixture of the Hock fragmentation of cholesterol 7α-OOH in the absence of DNPH and at 100-fold lower acid concentration (0.001 M HCl) (Figure

4.4). We monitored the epoxide peaks corresponding to 6,7-epoxy-5β-methoxycholesterol and its isomer (6,7-epoxy-5α-methoxycholesterol).** After 100 minutes in a 0.001 M HCl solution, more than 50% of the products consisted of 6,7-epoxy-5-methoxycholesterol.

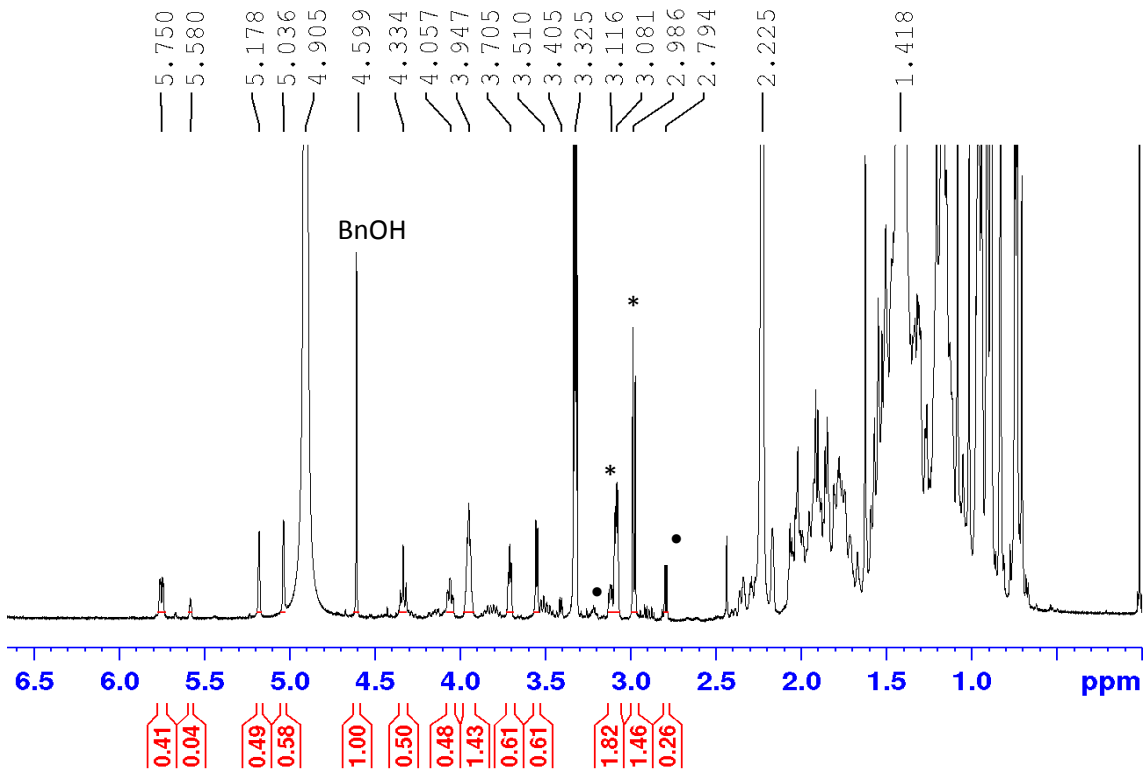

Figure 4.4. ^{1}H-NMR spectrum of crude product mixture of the Hock fragmentation of cholesterol 7α-OOH in 0.001 M HCl solution after 100 minutes. The spectrum was collected at 400 MHz with chemical shifts reported in ppm relative to CD_3OD. * 6,7-epoxy-5β-methoxycholesterol, • 6,7-epoxy-5α-methoxycholesterol. Benzyl alcohol was added as an internal standard.

**Obtained by consecutive work carried out by a colleague, Emily Schaefer, in the Pratt group.

We also studied the relative rate of formation of isomers of 6,7-epoxy-5-methoxycholesterol compared to other Hock products under different acid concentrations (Figure 4.5). 6,7-epoxy-5-methoxy cholesterol consisted of 35%, 55% and 70 % of the total Hock fragmentation products at 0.0001M, 0.001M and 0.01 M HCl in methanol, respectively.

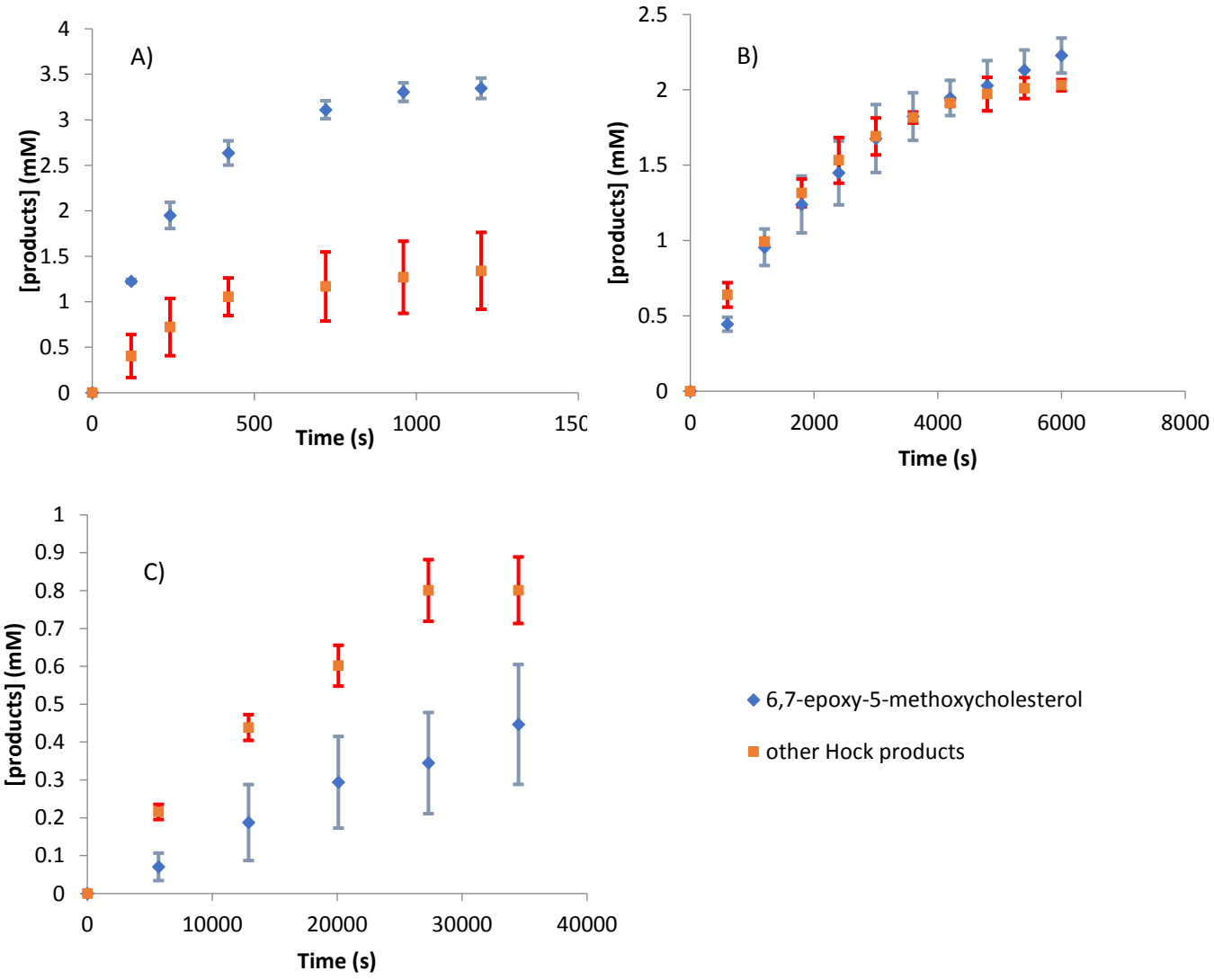

Figure 4.5. Conversion of 4.8 mM cholesterol 7α-OOH to Hock products with different acid concentration in d_4-methanol as a function of time in the presence of BHT. A) 0.01 M HCl, B) 0.001 M HCl, C) 0.0001 M HCl.

4.3 Discussion

The crystal structure obtained for the epoxide products of the Hock fragmentation of cholesterol 7α-OOH provided some insight as to the course of the reaction. In principle, the mechanism of Hock fragmentation can go through either α-epoxy carbenium ion or O-vinyl oxocarbenium ion but no evidence has yet been reported in favour of one pathway over the other (Scheme 4.3).[6, 7, 8] Herein, an obtained epoxide structure suggests that the Hock fragmentation of cholesterol 7α-OOH goes through epoxide formation. This is the first recorded evidence for an intermediate in the Hock fragmentation reaction.

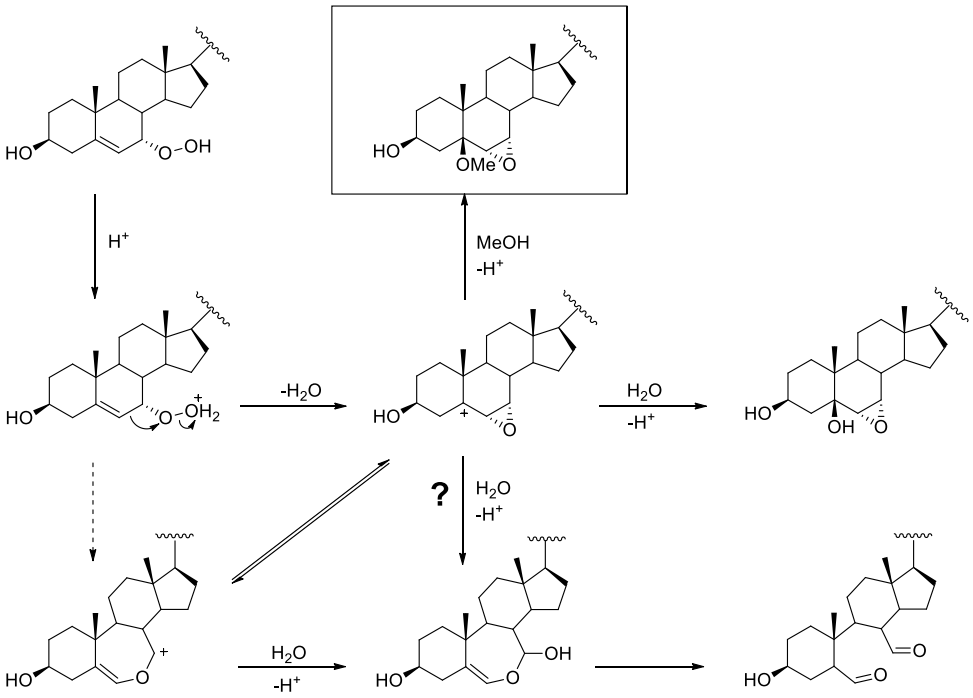

Scheme 4.3. Proposed mechanism for the acid catalyzed Hock fragmentation of cholesterol 7α-OOH.

The acid-catalyzed Hock fragmentation of cholesterol 7α-OOH starts with the protonation of the hydroperoxide followed by dehydration which results in an epoxide structure juxtaposed to a carbocation centre. Water can either attack the carbocation centre and form the corresponding 6,7-epoxy-5-hydroxycholesterol or directly attack C6 or C7 on either side of the epoxide which upon ring opening can form the anticipated dialdehyde product. In our reaction conditions, the carbocation centre was attacked by methanol, forming the corresponding 6,7-epoxy-5β-methoxycholesterol.

Alkoxylation not only adds to the diversity and complexity of the products but it also prevents the reaction from reaching completion. Upon alkoxylation, the corresponding product can not undergo proper fragmentation to yield the expected Hock fragmentation products. This is evident in our experiment where we dissolved the 6,7-epoxy-5β-methoxycholesterol in 0.1 M HCl solution in methanol in the presence of DNPH. After 12 hours no hydrazone was formed when we monitored the reaction by ^{1}H-NMR (Figure 4.3). We also did not observe any aldehyde peaks in the spectrum which demonstrates the incapability of 6,7-epoxy-5β-methoxycholesterol to fragment to form carbonyl groups. However, the hydrolysis of the epoxide did take place as new peaks started to appear at the expense of epoxide peaks (Figure 4.3).

In biological systems, water may intercept the intermediate epoxy carbenium ion to generate 6,7-epoxy-5-hydroxycholesterol. Second nucleophilic attack of water can hydrolyze the epoxide to generate the 5,6,7-trihydroxycholesterol. This structure can fragment from either direction to form either the dialdehyde structure and/or the keto-aldehyde structure-secosterol-A (Scheme 4.4).

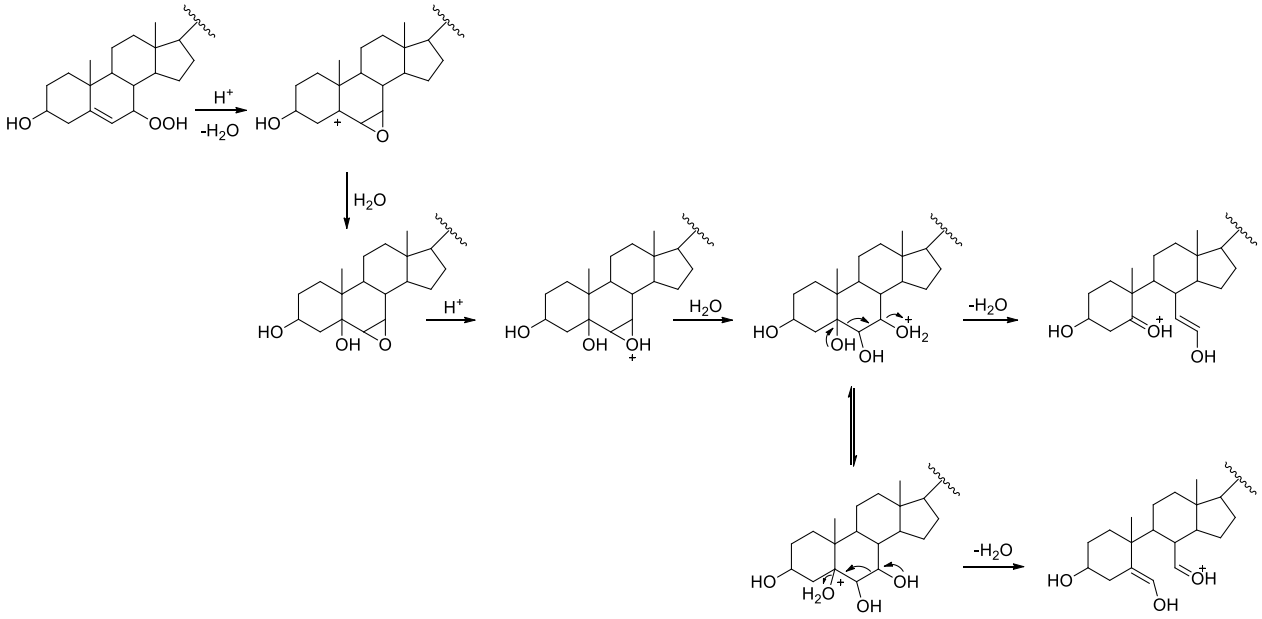

Scheme 4.4. Proposed mechanism for epoxide opening of 6,7-epoxy-5-hydroxycholesterol via hydroxyl nucleophilic attack.

Water can also attack the α-epoxy carbenium ion directly at C6 or C7 to cleave the epoxide structure. Due to the adjacent carbocation centre the C6 and C7 bond breaks instead of C-O bond to eventually generate the anticipated dialdehyde product. As a matter of fact, when the reaction was done in acetone/water aldehydes were formed.[††] Furthermore, according to our DFT analysis,[‡‡] water molecule prefers to be near the C7 of the cholesterol-derived epoxy carbenium ion, where it would attack the epoxide to perform the Hock fragmentation to generate the anticipated dialdehyde product.

[††] Observed by consecutive work carried out by a colleague, Emily Schaefer, in the Pratt group.
[‡‡] DFT calculations were carried out by Zosia Zielinski, a doctoral candidate in the Pratt group.

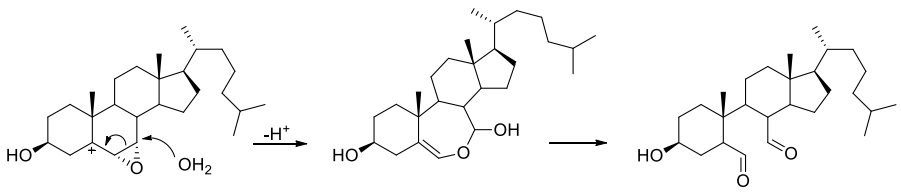

Scheme 4.5. Proposed mechanism of nucleophilic attack of water to open epoxide of the cholesterol-derived α-epoxy carbenium ion.

Nevertheless, we did not observe the corresponding epoxide structure in our previous studies of the Hock fragmentation of cholesterol 5α-OOH. This may be because an equilibrium between the two carbenium ions may favour the epoxide structure for that derived from cholesterol 7α-OOH and the O-vinyl structure for that derived from cholesterol 5α-OOH. The α-epoxy carbenium ion derived from cholesterol 5α-OOH contains a secondary carbocation center while that derived from cholesterol 7α-OOH contains a more stable tertiary carbocation center. In contrary, the O-vinyl oxocarbenium ion derived from cholesterol 5α-OOH contains tertiary carbocation center and is more stable than that derived from cholesterol 7α-OOH (Scheme 4.6).

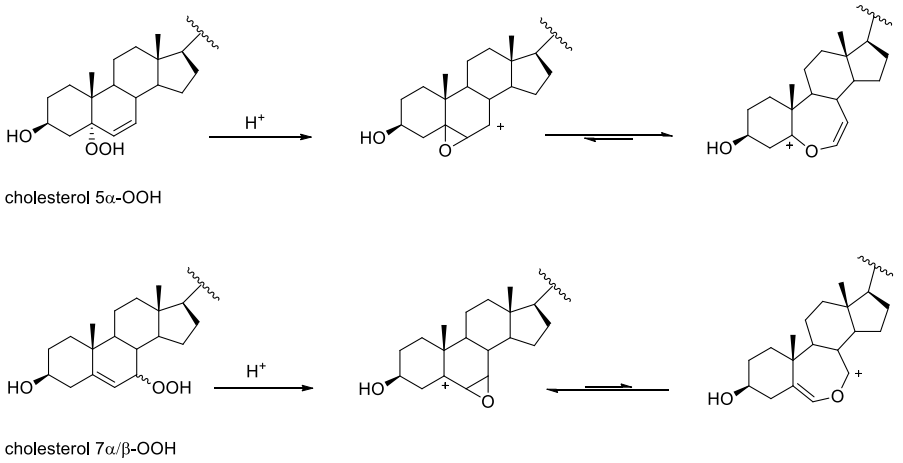

Scheme 4.6. Putative epoxide intermediates generated from cholesterol 5α-OOH and cholesterol 7α- and 7β-OOH under acidic conditions.

Under acidic conditions, 0.001 M and 0.01 M HCl, 55% and 70 % of the total Hock products were isomers of 6,7-epoxy-5-methoxycholesterol. Nonetheless, if this trend would continue, we expect to have mainly isomers of 6,7-epoxy-5-methoxycholesterol and trace amount of other Hock products at higher acid concentration (n.b. majority of our experiments were done in 0.1 and 1 M HCl) This explains why the yield of hydrazones was consistently low as the majority of the products lacked the carbonyl group to be derivatized. However, in a more biologically relevant acidic conditions, 0.0001 M HCl, only 35 % of the total Hock products are isomers of 6,7-epoxy-5-methoxycholesterol. Regardless of the origin of the difference, which is not clear, this proposes that in biological systems the Hock fragmentation of the cholesterol 7-OOH generates more of the carbonyl products not only due to the presence of water but also due to the lower acidity of the biological media.

In summary, we provided the first evidence for an α-epoxy carbenium ion in the mechanism of the Hock fragmentation of hydroperoxides. Carrying out the reactions in methanol enabled trapping of this intermediate, which could be isolated and its structure determined by x-ray crystallography. This can not exclusively deny the formation of an oxocarbenium ion intermediate but may account for the complexity and diversity of the products.

Going forward, we would like to study the biological characteristics of the isomers of 6,7-epoxy-5-methoxycholesterol in order to understand their *in vivo* formation, their effect on biological systems and their distribution across the membranes. More importantly, the chromatographic conditions had been optimized such that the direct analysis of the tissue samples should reveal the actual characteristics of the secosterols. Furthermore, more studies are underway to characterize the other two major hydrazones (derived from acid-catalyzed Hock fragmentation of cholesterol 7-OOH) where other derivatizing agents had been used to aid in their purification and crystallization.

4.4 Experimental

Materials and methods: All chemicals and solvents were purchased from Sigma Aldrich Co. LLC and used as received, unless otherwise stated. 2,6-di-tert-4-methylphenyl (BHT) was purified by recrystallization from hexane prior to use. 2,4-dinitrophenylhydrazine (DNPH) was purified by recrystallization from n-butane prior to use. ^{1}H-NMR spectra were collected on a Bruker AVANCE -500, -400 and -300 spectrometer.

Cholesterol 7α-OOH: Rose bengal (14 mg) was added to a mixture of cholesterol (1.0 g) in pyridine (15 mL) and the mixture was irradiated by an HPS 400 W sodium lamp while oxygen was bubbled though at 0°C for 6 hours. BHT (0.6 g) was added to the resulting mixture and let to stir for another 20 minutes at room temperature. The reaction mixture was concentrated under vacuum to give a red solid residue. The residue was dissolved in chloroform and adsorbed on silica (1.0 g). Chloroform was removed under the vacuum and the product coated silica was added on top of the preparative silica column (ether: hexane, 1:1) to give pure cholesterol 5α-OOH as white powder-like crystals. A solution of cholesterol 5α-OOH (170 mg) in chloroform (10 mL) was stirred for 10 hours at room temperature. Product mixture was concentrated to dryness under the vacuum. Preparative silica column (ether: hexane, 1:1) was used to give pure cholesterol 7α-OOH as white crystals (80% yield). ^{1}H-NMR (500 MHz, $CDCl_3$) δ 5.70 (dd, *J*=1.8, 5.0 Hz, 1H), 4.14 (td, *J*= 1.7, 4.7 Hz, 1H), 3.60 (m, 1H), 2.50-0.98 (Comp, 28H), 0.97 (s, 3H), 0.89 (d, *J*=6.7 Hz, 3H), 0.85 (dd, *J*= 2.7, 7.0 Hz, 6H), 0.64 (s, 3H) .Analytical data were in accordance with those reported in the literature.[9]

***6,7-Epoxy-5β-methoxycholesterol*:** Cholesterol 7α-OOH (1.0 g) was added to the mixture of DNPH (3 equivalent) in 0.1 M HCl -methanol solution (50 mL). Reaction mixture was stirred at room temperature for another 2 hours. The resulted mixture was immediately diluted by chloroform and was washed with water multiple times. The organic layer was concentrated moderately under the high vacuum and was re-crystalized from benzene and methanol over night. Crystals were rinsed by distilled ethanol and were dried under the high vacuum. ^{1}H-NMR (500 MHz, CD_3OD) δ 3.97 (m, 1H), 3.42 (s, 3H) 3.12 (dd, *J*= 2.1, 4.0 Hz, 1H), 3.01 (d, *J*= 4.0 Hz, 1H), 2.22 (d, *J*= 16.1 Hz, 1H), 2.07 (dt, *J*=3.1, 12.5 Hz, 1H), 1.97-1.78 (Comp, 5H), 1.57 (m, 1H), 1.52-1.03 (Comp, 20H), 0.86 (d, *J*=6.5 Hz, 1H), 0.80 (dd, *J*= 1.2, 6.6 Hz, 6H), 0.74 (s, 1H), 0.67 (s, 1H). ^{13}C-NMR (300 MHz, CD_3OD) δ 77.29, 66.70, 57.34, 56.37, 54.98, 53.23, 50.22, 44.30, 41.22, 40.69, 39.95, 37.54, 37.40, 37.20, 36.72, 30.14, 29.57, 29.15, 28.36, 26.06, 25.03, 24.47, 23.23, 22.94, 21.60, 19.12, 18.81, 12.33.

Table 4.1. Crystal data and structure refinement for 6,7-epoxy-5β-methoxy cholesterol obtained at 200 k, at wavelength of 0.71073Å with Orthorhombic crystal system.

Identification code	shelx	
Empirical formula	C28 H48 O3	
Formula weight	432.66	
Temperature	200(2) K	
Wavelength	0.71073 Å	
Crystal system	Orthorhombic	
Space group	P 21 21 2	
Unit cell dimensions	a = 10.229(6) Å	α= 90°.
	b = 21.774(12) Å	β= 90°.
	c = 23.825(13) Å	γ = 90°.
Volume	5307(5) $Å^3$	
Z	8	
Density (calculated)	1.083 Mg/m^3	
Absorption coefficient	0.068 mm^{-1}	
F(000)	1920	
Crystal size	0.955 x 0.338 x 0.102 mm^3	
Theta range for data collection	1.709 to 28.259°.	
Index ranges	-13<=h<=13, -27<=k<=28, -25<=l<=30	
Reflections collected	37631	
Independent reflections	12660 [R(int) = 0.0709]	
Completeness to theta = 25.242°	99.9 %	
Refinement method	Full-matrix least-squares on F^2	
Data / restraints / parameters	12660 / 16 / 622	
Goodness-of-fit on F^2	0.953	
Final R indices [I>2sigma(I)]	R1 = 0.0546, wR2 = 0.1148	
R indices (all data)	R1 = 0.1412, wR2 = 0.1491	
Absolute structure parameter	-1.9(8)	
Extinction coefficient	n/a	
Largest diff. peak and hole	0.208 and -0.167 $e.Å^{-3}$	

4.5 References

[1] Krow, G. R.; *Org. React.* **1993**, 43, 251.

[2] Crudden, C. M.; Chen, A. C.; Calhoun, L. A. *Angew. Chem. Int. Ed* **2000**, 39, 2851.

[3] Negre-Salvayre, A.; Auge, N.; Ayala, V.; Basaga, H.; Boada, J.; Brenke, R.; Chapple, S.; Cohen, G.; Feher, J.; Grune, T.; Lengyel, G.; Mann, G. E.; Pamplona, R.; Poli, G.; Portero-Otin, M.; Riahi, Y.; Salvayre, R.; Sasson, S.; Serrano, J.; Shamni, O.; Siems, W.; Siow, R. C. M.; Wisewedel, I.; Zarkovic, K.; Zarkovic, N. *Free Radical Res*. **2010**, 44, 1125.

[4] Zhong, H.; Yin, H. *Redox Biol.* **2015**, 4, 193.

[5] Wentworth, Jr. P.; Wentworth, A. D.; Zhu, X.; Wilson, I. A; Janda, K. D.; Eschenmoser, A.; Lerner, R. A. *Proc. Natl. Acad. Sci. USA.* **2003**, 100, 1490.

[6] Frimer, A. A. *Chem. Rev.* **1979**, 79, 359.

[7] Tanigawa, S.; Kajiware, T.; Hatanaka, A. *Phytochemistry* **1984**, 23, 2439.

[8] Gardner, H.; Planter, R. D. *Lipids* **1984**, 119, 294.

[9] Ronsein, G. E.; Prado, F. M.; Mansano, F. V.; Oliveira, M. C. B.; Medeiros, M. H. G.; Miyamoto, S.; Mascio, P. D. *Anal. Chem*. **2010**, 82, 7293.